Atmos. Chem. Phys., 6, 4175–4214, 2006
www.atmos-chem-phys.net/6/4175/2006/

Atmospheric Chemistry and Physics

Columnar modelling of nucleation burst evolution in the convective boundary layer – first results from a feasibility study Part I: Modelling approach

O. Hellmuth

Leibniz Institute for Tropospheric Research, Modelling Department, Permoserstrasse 15, 04318 Leipzig, Germany

Received: 1 August 2005 – Published in Atmos. Chem. Phys. Discuss.: 10 November 2005
Revised: 14 February 2006 – Accepted: 11 May 2006 – Published: 21 September 2006

Abstract. A high-order modelling approach to interpret "continental-type" particle formation bursts in the anthropogenically influenced convective boundary layer (CBL) is proposed. The model considers third-order closure for planetary boundary layer turbulence, sulphur and ammonia chemistry as well as aerosol dynamics. In Paper I of four papers, previous observations of ultrafine particle evolution are reviewed, model equations are derived, the model setup for a conceptual study on binary and ternary homogeneous nucleation is defined and shortcomings of process parameterisation are discussed. In the subsequent Papers II, III and IV simulation results, obtained within the framework of a conceptual study on the CBL evolution and new particle formation (NPF), will be presented and compared with observational findings.

1 Introduction

At the end of the 1960's, James Lovelock came up with an influential theory of homeostasis of a fictive planet Gaia, represented by the conceptual "daisyworld" model (Lovelock, 1993). Lovelock proposed a negative feedback mechanism to explain the relative stability of Earth's climate over geological times, which became generally known as "Gaia hypothesis"[1]. At the end of the 1980's, the Gaia theory was essentially extended by Charlson, Lovelock, Andrea and Warren[2] (Charlson et al., 1987). In their postulated negative feedback mechanism, abundant atmospheric sulphate aerosols are hypothesised to play a key role in stabilising Earth's climate. An assumed global warming, caused by radiative forcing of greenhouse gases, would lead to an increase of the sea surface temperature and, consequently, to an increase of dimethyl sulphide emissions (DMS, $(CH_3)_2S$) from marine phytoplankton (e.g., macroalgae) into the atmosphere. The gas phase oxidation of DMS produces sulphur dioxide (SO_2), which further oxidises with the hydroxyl radical (OH) to form sulphuric acid (H_2SO_4). According to the present level of process understanding, H_2SO_4 vapour and water (H_2O) vapour are key precursor gases for the homogeneous heteromolecular (binary) nucleation of sulphate aerosols over the ocean. Due to condensation and coagulation processes, these microscopic particles can grow via intermediate, not yet fully understood stages from so-called thermodynamically stable clusters (TSCs) (Kulmala et al., 2000; Kulmala, 2003) via ultrafine condensation nuclei (UCNs) to non-sea-salt (nss) sulphate aerosols and, finally, to cloud condensation nuclei (CCNs). An increase of the CCN concentration leads to an enhancement of the number concentration of cloud droplets. According to an effect proposed by Twomey (1974), a higher cloud droplet concentration causes an enhancement of the cloud reflectivity for a given liquid water content. An increased reflectivity of solar radiation by clouds cools the atmosphere and counteracts the initial warming. Via this route, a thermal stabilisation of Earth's climate is accomplished. For the illustration of this theory the reader is referred, e.g., to Easter and Peters (1994) and Brasseur et al. (2003, pp. 142–143, Fig. 4.10). Apart from their climate impact, aerosol particles are also affecting human health, visibility etc.

Correspondence to: O. Hellmuth
(olaf@tropos.de)

[1] In the Hellenistic mythology, "Gaia" is the name of the godhood of Earth. James Lovelock and the Nobel prize winner William Golding used this name as a synonym for a self-regulating geophysical and biophysical mechanism on a global scale. According to the Gaia hypothesis, temperature, oxidation state, acidity as well as different physicochemical parameters of rocks and waters remain constant at each time due to homeostatic interactions, maintained by massive feedback processes. These feedback processes are initiated by the "living world", whereas the equilibrium conditions are changing dynamically with the evolution of Earth's live (not of single creatures).

[2] According to the initials of the authors, this theory became known as CLAW hypothesis.

Published by Copernicus GmbH on behalf of the European Geosciences Union.

Recently, Kulmala et al. (2004c, Fig. 1) proposed a possible connection between the carbon balance of ecosystems and aerosol-cloud-climate interactions, also suspected to play a significant role in climate stabilisation. Increasing carbon dioxide (CO_2) concentrations accelerate photosynthesis, which in turn consumes more CO_2. But forest ecosystems also act as significant sources of atmospheric aerosols via enhanced photosynthesis-induced emissions of non-methane biogenic volatile organic compounds (BVOCs) from vegetation[3]. Owing to the capability of BVOCs to get activated into CCNs, biogenic aerosol formation may also serve as negative feedback mechanism in the climate system, slowing down the global warming similar as proposed in the CLAW hypothesis.

2 Key mechanisms of new particle formation in the atmosphere

Atmospheric NPF is known to widely and frequently occur in Earth's atmosphere. It is generally accepted to be an essential process, which must be better understood and included in global and regional climate models (Kulmala, 2003). So far, the most comprehensive review of observations and phenomenological studies of NPF, atmospheric conditions under which NPF has been observed, and empirical nucleation rates etc. over the past decade, from a global retrospective and from different sensor platforms was performed by Kulmala et al. (2004d). The authors reviewed altogether 149 studies and collected 124 observational references of NPF events in the atmosphere.

The elucidation of the mechanism, by which new particles nucleate and grow in the atmosphere, is of key importance to better understand these effects, especially the role of aerosols in climate control (Kulmala et al., 2000; Kulmala, 2003). Kulmala et al. (2000) pointed out, that in some cases observed NPF rates can be adequately explained by binary nucleation involving H_2O and H_2SO_4. But in certain locations, e.g., within the marine boundary layer (MBL) and at continental sites, the observed nucleation rates exceed those predicted by the binary scheme. In such cases, ambient H_2SO_4 concentrations are typically lower than those required for binary nucleation, but are sufficient for ternary nucleation involving H_2O, H_2SO_4 and ammonia (NH_3). The authors presented a hypothesis, *"which – in principle – enables us to explain all observed particle production bursts in the atmosphere: (1) In the atmosphere, nucleation is occurring almost everywhere, at least in the daytime. The conditions in the free troposphere (cooler temperature, fewer pre-existing aerosols) will favour nucleation. (2) Nucleation maintains a reservoir of thermodynamically stable clusters (TSCs), which are too small to be detected. (3) Under certain conditions TSCs grow to detectable sizes and further to cloud condensation nuclei"*[4] (Kulmala et al., 2000, p. 66). Depending on the availability of pre-existing particles and/or condensable vapours, Kulmala et al. (2000) hypothesised two possibilities for the growth of TSC particles to detectable size: (a) When the concentration of pre-existing particles is low, TSCs can effectively grow by self-coagulation. (b) In the presence of a high source of available condensable vapours (e.g., organics, inorganics, NH_3) TSCs can effectively grow to detectable size and even to Aitken mode size by condensation. By means of the advanced sectional aerosol dynamical model AEROFOR the authors concluded, that ternary nucleation is able to produce a high enough reservoir of TSCs, which can grow to detectable size and subsequently being able to explain observed particle formation bursts in the atmosphere. The occurrence of bursts was demonstrated to be connected to the activation of TSCs with extra condensable vapours (e.g., after advection over sources or mixing). Ion-induced nucleation was ruled out as a TSC formation pathway because of the typically low ionisation rate in the troposphere. Later on, this concept has been advanced by Kulmala (2003). The author refers to four main nucleation mechanisms, which are suspected to be relevant for NPF in the atmosphere:

1. Homogeneous nucleation involving binary mixtures of H_2O and H_2SO_4 (occurrence, e.g., in industrial plumes);

2. Homogeneous ternary $H_2O/H_2SO_4/NH_3$ nucleation (occurrence in the CBL);

3. Ion-induced nucleation of binary, ternary or organic vapours (occurrence in the upper troposphere (UT) and lower stratosphere);

4. Homogeneous nucleation involving iodide species (occurrence in coastal environments).

The effectiveness of these mechanisms has been confirmed in laboratory studies. However, the concentrations considered in these studies were typically far above those observed in the atmosphere. Moreover, the concentrations of the nucleating vapours in laboratory experiments are regularly so high, that these vapours are also responsible for condensation growth. In opposite to this, the nucleation of atmospheric particles can be kinetically limited by TSCs, which are formed during intermediate steps of particle nucleation (Kulmala, 2003). As the author pointed out, homogeneous or ion-induced ternary nucleation mechanisms can explain the nucleation of new atmospheric particles (diameter <2 nm) in many circumstances, but the observed particle growth can not be explained by condensation of H_2SO_4 alone. Kulmala (2003, see references therein) concluded, that nucle-

[3] BVOCs are important precursors for atmospheric NPF, e.g., in forest regions.

[4] TSCs are newly formed particles, whose sizes are greater than a critical cluster (about 1 nm), but are smaller than the detectable size of $\sim$3 nm.

ation and growth are probably decoupled under most atmospheric conditions and other vapours, such as organic acids, are involved in the growth process. According to this concept, non-soluble organic vapour (*n*-nonane) starts to condense on newly nucleated water clusters. After formation, the particles can grow, e.g., by heterogeneous nucleation of organic insoluble vapours on ternary clusters, activation of the clusters for condensation of soluble organic vapours and chemical reactions at the surfaces of small clusters. Following these initial steps, multicomponent condensation of organic and inorganic vapours is suspected to occur. Condensation growth and coagulation loss are competing processes, i.e., the more effective the condensation growth, the larger the fraction of nucleated particles, that can survive. Among the serious problems, which are deserved to be solved in future, the author stated the need for an interdisciplinary approach involving laboratory studies, continuous field observations, new theoretical approaches and dynamical models.

Based on the traditional Köhler theory to describe the formation of cloud droplets due to spontaneous condensation of water vapour (Köhler, 1936), Kulmala et al. (2004a) proposed an analogous attempt to describe the activation of inorganic stable nanoclusters into aerosol particles in a supersaturated organic vapour, which initiates spontaneous and rapid growth of clusters[5]. The authors pointed out, that the existing evidences, supporting the prevalence of condensed organic species in new 3–5 nm particles, can not be explained by homogeneous nucleation of organic vapours under atmospheric conditions. The supersaturation of organic vapours was estimated to be well below that required for homogeneous nucleation to occur. The Nano-Köhler theory *"describes a thermodynamic equilibrium between a nanometer-size cluster, water and an organic compound, which is fully soluble in water, i.e., it does not form a separate solid phase, but is totally dissolved into the solution. Furthermore, organic and inorganic compounds present together in growing clusters form a single aqueous solution. It is also assumed, that gaseous sulphuric acid condenses irreversibly into the cluster along with ammonia, so that a molar ratio of 1:1 is maintained between the concentrations of these two compounds in the solution"*(Kulmala et al., 2004a, pp. 2–3 of 7). Using an advanced sectional aerosol dynamics box model, the authors evaluated the new theory in order to predict the yield of aerosol particles as a function of organic vapour density. It was demonstrated, that for a pseudo-constant reservoir of TSCs the proposed mechanism leads to a rapid activation of the clusters by organic vapours. The model simulations of Kulmala et al. (2004a) show, that prior to the activation, the cluster growth is driven by H_2SO_4 condensation. The authors proposed the following dual step process to interpret their modelling results: One process considers the condensation growth of nuclei by H_2SO_4 and organic vapour to a threshold size. The second, subsequent process involves organic condensation during activation. For organic aerosol formation to occur, two preconditions must be fulfilled: (1) The H_2SO_4 vapour concentrations must be $\geq 2.5\times10^6\,cm^{-3}$, otherwise the clusters are scavenged before they can be activated. (2) The condensable organic vapour concentration must be greater than $\sim10^7\,cm^{-3}$. Higher concentrations of H_2SO_4 will result in activation at lower organic vapour concentrations. The proposed mechanism of cluster activation by organic vapours suggests, that small increases in the availability or production of organic vapours will lead to large increases in the aerosol population. The authors refer to an increase in the production of condensable organic vapours, e.g., resulting from increasing oxidant concentration (e.g., ozone) associated with globally increasing pollution levels.

A description of state-of-the-art growth hypotheses and their theoretical background is given in Kulmala et al. (2004b). Based on measurements of particle size distributions and air ion size distributions, the authors provided observational evidences, that organic substances soluble into TSCs (either ion clusters or neutral clusters) are mainly responsible for the growth of clusters and nanometer-size aerosol particles. Although no observational evidences were found, that support the dominance of charged-enhanced particle growth associated with ion-mediated nucleation, initial growth (around 1–1.5 nm) may be dominated by ion-mediated condensation. It is hypothesised, that later those charged clusters are neutralised by recombination and that they continue their growth by vapour condensation on neutral clusters. The observations revealed a remarkably steady ion distribution between about 0.5 and 1.5 nm, which appears to be present all the time during both NPF event and non-event days. This finding supports the hypothesis of Kulmala et al. (2000) on the frequent abundance of nanometer-size thermodynamically stable neutral clusters, which can grow to detectable size at sufficient high concentrations of condensable vapours. The study of Kulmala et al. (2004b) strongly supports the idea, that vapours responsible for the main growth of small clusters/particles are different from those driving the nucleation, i.e., nucleation and subsequent growth of nucleated clusters are likely to be uncoupled from each other. The suggested abundance of TSCs in connection with less frequent occurrence of NPF events indicates, that atmospheric NPF may be limited by initial steps of growth rather than by nucleation.

More recently, Kulmala et al. (2005) confirmed the hypothesis on the existence of neutral TSCs both experimentally and theoretically. With respect to their modelling approach, the best agreement with the observations was obtained by using a barrierless (kinetic) ternary nucleation mechanism together with a size dependent growth rate, supporting the Nano-Köhler theory. The model was able to predict both the existence of nucleation events and, with reasonable accuracy, the concentrations of neutral and charged particles of all sizes.

[5]The authors introduced the annotation "Nano-Köhler theory" to emphasise the analogy to Köhler's traditional approach.

3 On the role of multiscale transport processes in new particle formation

Among others, the question how multiscale transport processes influence NPF is not yet answered and a subject of ongoing research. A review of scales and the potential of atmospheric mixing processes to enhance the binary nucleation rate was performed by Nilsson and Kulmala (1998). On the base of the classical concept of mixing-induced supersaturation – to our knowledge at first proposed by James Hutton in 1784 (Bohren and Albrecht, 1998, see p. 322–324) – Nilsson and Kulmala (1998) proposed a parameterisation for the mixing-enhanced nucleation rate. The influence of atmospheric waves, such as Kelvin-Helmholtz instabilities, on NPF was investigated by Bigg (1997), Nyeki et al. (1999) and Nilsson et al. (2000a). The effects of synoptic weather, planetary boundary layer (PBL) evolution, e.g., adiabatic cooling, turbulence, entrainment and convection, respectively, on aerosol formation were analysed:

- In the MBL by Russell et al. (1998), Coe et al. (2000), Pirjola et al. (2000) and O'Dowd et al. (2002);
- In the CBL by Nilsson et al. (2000b), Aalto et al. (2001), Buzorius et al. (2001), Nilsson et al. (2001a,b), Boy and Kulmala (2002), Buzorius et al. (2003), Stratmann et al. (2003), Uhrner et al. (2003), Boy et al. (2004) and Siebert et al. (2004);
- In the free troposphere (FT) and UT by Schröder and Ström (1997), Clarke et al. (1999), de Reus et al. (1999), Hermann et al. (2003) and Khosrawi and Konopka (2003).

The influence of small-scale and subgridscale (abbreviated as SGS) fluctuations, respectively, on the mean-state nucleation rate and the parameterisation of turbulence-enhanced nucleation was subject of investigations performed by Easter and Peters (1994), Lesniewski and Friedlander (1995), Andronache et al. (1997), Jaenisch et al. (1998a,b), Clement and Ford (1999b), Elperin et al. (2000), Hellmuth and Helmert (2002), Schröder et al. (2002), Buzorius et al. (2003), Housiadas et al. (2004), Lauros et al. (2004), Shaw (2004) and Lauros et al. (2006).

Summing up previous works, further investigations are deserved to answer the following questions:

1. How strong can SGS fluctuations enhance the nucleation rate during intensive mixing periods?
2. Can NPF be triggered by upward moving air parcels across atmospheric layers with large temperature gradients?
3. Where does NPF occur in the PBL (within the surface layer or at levels above, followed by downward transport after breakup of the nocturnal residual layer and mixing of vapour and aerosol loaded surface layer with clean residual layer air)?

Previous eddy co-variance particle flux measurements above forests, such as performed by Buzorius et al. (2001, Figs. 4, 6, 8), Nilsson et al. (2001b, Fig. 9) and Held et al. (2004, Fig. 3), yield net deposition of particles, i.e., downward directed particle fluxes, but these measurements were restricted to altitudes nearby the canopy layer. To date, the net effect of forest stands on particle mass is not yet determined (Held et al., 2004).

Turbulence-related investigations of NPF are subject of ongoing research, e.g., on the European as well as on the process scale within the framework of the QUEST project (Quantification of Aerosol Nucleation in the European Boundary Layer, http://venda.uku.fi/quest/, http://www.itm.su.se/research/project.php?id=84). A comprehensive compilation of previous and current results of the QUEST project can be found in an ACP Special Issue edited by Hämeri and Laaksonen (2004) (http://www.copernicus.org/EGU/acp/acp/special_issue9.html).

Present day modelling studies to explain NPF events are often based on box models, e.g., applied within a Lagrangian framework:

1. Analytical and semi-analytical burst models, intended to be used for the parameterisation of SGS bursts in large-scale global transport models (Clement and Ford, 1999a,b; Katoshevski et al., 1999; Clement et al., 2001; Dal Maso et al., 2002; Kerminen and Kulmala, 2002);
2. Multimodal moment models (Kulmala et al., 1995; Whitby and McMurry, 1997; Wilck and Stratmann, 1997; Pirjola and Kulmala, 1998; Wilck, 1998);
3. Sectional models (Raes and Janssens, 1986; Kerminen and Wexler, 1997; Pirjola, 1999; Birmili et al., 2000; Korhonen et al., 2004; Gaydos et al., 2005).

Such models were demonstrated to successfully describe NPF events, when transport processes can be neglected. However, from in situ measurements Stratmann et al. (2003) and Siebert et al. (2004) provided evidences for a direct link between turbulence intensity near the CBL inversion and ground-observed NPF bursts on event days. When CBL turbulence is suspected to be important, occurrence and evolution of NPF bursts are not yet satisfying modelled (Birmili et al., 2003; Stratmann et al., 2003; Uhrner et al., 2003; Wehner and Wiedensohler, 2003). Independent from the degree of sophistication, zero-dimensional models are a priori not able to explicitly describe transport processes, neither gridscale nor SGS ones. At most, such models can implicitly consider transport effects by more or less sophisticated artificial tendency terms (e.g., for entrainment) or by empirically adjusted tuning parameters. For example, Uhrner et al. (2003, Figs. 1 and 5) derived a semi-empirical prefactor for

the binary nucleation rate to correct for the influence of vertical exchange processes in their box model study. The logarithm of that prefactor varied from −3 to 17.2 depending on the local temperature gradient in the Prandtl layer, whereas largest values were obtained for very unstable conditions.

To overcome present shortcomings in NPF burst modelling, Boy et al. (2003a) proposed an one-dimensional boundary layer model with aerosol dynamics and a second-order turbulence closure (BLMARC, Boundary, layer, mixing, aerosols, radiation and clouds) including binary and ternary nucleation. The underlying assumption of horizontal homogeneity is justified by the fact, that NPF often quasi-simultaneously occurs over distances ranging from approximately 50 km to the synoptic scale with a horizontal extension of more than 1000 km (Nilsson et al., 2001a; Birmili et al., 2003; Komppula et al., 2003a; Plauskaite et al., 2003; Stratmann et al., 2003; Wehner et al., 2003; Vana et al., 2004; Gaydos et al., 2005).

As a contribution to the ongoing discussion on the role of turbulence during the evolution of "continental-type" NPF bursts in anthropogenically influenced regions, a columnar modelling approach is proposed here. Compared to former studies, CBL dynamics, chemistry reactions and aerosol dynamics will be treated in a self-consistent manner by applying a high-order closure to PBL dynamics, appropriate sulphur and ammonia chemistry as well as aerosol dynamics.

A comprehensive explanation of the annotation applied in turbulence closure techniques can be found, e.g., in Stull (1997, Chapter 6, p. 197–250). In general, the closure problem is a direct consequence of Reynolds' flow decomposition and averaging approach (Stull, 1997, p. 33–42). The closure problem results from the fact, that *"the number of unknowns in the set of equations for turbulent flow is larger than the number of equations"* (Stull, 1997, p. 197). The introduction of additional diagnostic or prognostic equations to determine these unknown variables results in the appearance of even more new unknowns. Consequently, the total statistical description of a turbulent flow requires an infinite set of equations. In opposite to this, for a finite set of governing equations the description of turbulence is not closed. This fact is commonly known as the "closure problem". As demonstrated by Stull (1997, Tables 6–1, p. 198), the prognostic equation for any mean variable $\overline{\alpha}$ (first statistical moment) includes at least one double correlation term $\overline{\alpha'\beta'}$ (second statistical moment). The forecast equation for this second-moment turbulence term contains additional triple correlations terms $\overline{\alpha'\beta'\gamma'}$ (third statistical moments). Subsequently, the governing equations for the triple correlations contain fourth-moment quantities $\overline{\alpha'\beta'\gamma'\delta'}$ and so on. For practical reasons only a finite number of equations can be solved, and the remaining unknowns have to be parameterised in terms of known variables: *"Such closure approximations or closure assumptions are named by the highest order prognostic equations that are retained"* (Stull, 1997, p. 199). For example, in a first-order closure scheme only first-moment variables are predictive, and second-order moments are parameterised. In a second-order closure scheme first-moment and second-moment variables are predictive, and third-moment variables are parameterised. Finally, in a third-order closure scheme all first-moment, second-moment and third-moment variables are determined via prognostic equations, while the fourth-moment variables are parameterised in terms of lower-moment variables. With respect to the treatment of the "parameterisation problem", the reader is also referred to Stull's ostensive perception of this tricky subject, which culminates in a quotation of Donaldson (1973): *"There are more models for closure of the equations of the motion at the second-order correlation level than there are principal investigators working on the problem"* (Stull, 1997, p. 201). Considering the important role of human interpretation and creativity in the construction of approximations, the parameterisation can be to some degree located at an intermediate stage between science and art. Hence, "[. . .] *parameterisation will rarely be perfect. The hope is that it will be adequate"* (Stull, 1997, p. 201).

So far, previous attempts to extend third-order closure to aerosol dynamics in the PBL are not known. In this paper, the approach is motivated, model formalism and assumptions are described. In subsequent papers, a conceptual study on meteorological and physicochemical conditions, that favour NPF in the anthropogenically influenced CBL, will be performed.

4 Characterisation of "continental-type" NPF bursts

In each case over a period of 1.5 years, Birmili and Wiedensohler (2000) observed NPF events in the CBL on approximately 20% of all days, Stanier et al. (2003, Pittsburgh region, Pennsylvania) on over 30% of the days, most frequent in fall and spring and least frequent in winter. NPF was observed to be favoured on sunny days with below average $PM_{2.5}$ concentrations. NPF events were found to be fairly correlated with the product of ultraviolet (UV) intensity and SO_2 dioxide concentration and to be dependent on the effective area available for condensation, indicating that H_2SO_4 is a component of new particles.

Mäkelä et al. (1997) performed an early study on NPF occurring in boreal forests. Evaluating number size distributions of ambient submicron and ultrafine aerosol particles for three quarters of the year 1996, measured at the Hyytiälä station in Southern Finland, the authors clearly demonstrated the existence of a well-defined mode of ultrafine particles. With reference to the literature, the authors noted: *"The origin of the particles observed in this study may be connected with biogenic activity* [. . .]. *On the other hand, since the formation events are observed as early as February, we can not directly explain all the events by photosynthesis or related activity. There should be no photosynthesis going on in February–March in Finland. However, the role of the biogenic sources, whether from plant processes or soil microbial*

processes, or reactions on the surfaces of the plants deserve further research" (Mäkelä et al., 1997, p. 1222).

Kulmala et al. (1998b) analysed the growth of nucleation mode particles observed at a boreal forest site in Southern Finland. During an one-year period the authors observed significant NPF at the Hyytiälä measurement site on more than 50 days. Using an integral aerosol dynamics model, the authors selected 10 days of the data, representing NPF event days with a clear subsequent growth, for a closer examination. Among others, the model predicts the gas phase concentration of the condensing species as a function of time. From a sensitivity study the authors concluded, that the molecular properties of the condensing compound have only a small effect on the daily maximum concentration of the condensing species. Investigating the sensitivity of the model results against variations in the source term of the condensable species and against variations in temperature and relative humidity, the authors concluded, *"that the maximum concentration of the condensing molecules is in the order of* 10^7-10^9 cm^{-3}, *while their saturation vapour density is below* 10^5 cm^{-3}*"* (Kulmala et al., 1998b, p. 461). However, the condensable vapour causing the observed growth could not yet be identified in the study of Kulmala et al. (1998b).

In their overview of the EU funded project BIOFOR (Biogenic aerosol formation in the boreal forest), performed at the measurement site Hyytiälä in Southern Finland, Kulmala et al. (2001b) stated, that the exact formation route for 3 nm particles remains unclear. However, the main results could be summarised as follows:

- NPF was always connected with arctic and polar air advecting over the site, leading to the formation of a stable nocturnal boundary layer, followed by a rapid formation and growth of a turbulent convective mixed layer, closely followed by NPF.
- NPF seems to occur in the mixed layer or entrainment zone.
- Certain thresholds of high enough H_2SO_4 and NH_3 concentrations are probably needed, as the number of newly formed particles was correlated with the product of the H_2SO_4 production and the NH_3 concentration. A corresponding correlation with the oxidation products of terpenes was not found.
- The condensation sink, i.e., the effective area of pre-existing particles, is probably of importance, as no nucleation was observed at high values of the condensation sink.
- Inorganic compounds and hygroscopic organic compounds were found to contribute both to the particle growth during daytime, while at night-time organic compounds dominated.
- The authors concluded: *"The most probable formation mechanism is ternary nucleation (water–sulphuric acid–ammonia). After nucleation, growth into observable sizes (≥3 nm) is required before new particles appear. The major part of this growth is probably due to condensation of organic vapours"* (Kulmala et al., 2001b, p. 325).

Anyway, Kulmala et al. (2001b) emphasised the preliminary character of their conclusions, i.e., the lack of direct proof of this phenomenon because the composition of 1–5 nm size particles is extremely difficult to determine using the present state-of-the-art instrumentation.

In a forest region Boy et al. (2003b) found, that SO_2 is not correlated or even anti-correlated with the number concentration of small particles. As SO_2 is mainly of anthropogenic origin, it is mostly associated with high number concentrations of pre-existing aerosols, representing polluted conditions. Previous findings from laboratory studies revealed a direct correlation between increasing SO_2 concentrations and measured number concentrations of newly formed particles in an ozone/α-pinene reaction system (Boy et al., 2003b).

Held et al. (2004, BEWA field campaign in summer 2001 and 2002) observed NPF on approximately 22% of all days at an ecosystem research site in the Bavarian Fichtelgebirge. During a 15 month field campaign Gaydos et al. (2005, Pittsburgh Air Quality Study (PAQS)) observed regional NPF on approximately 33% of all days.

During 21 months (April 2000–December 2001) of continuous measurements of aerosol particle number size distributions in a subarctic area in Northern Finland Komppula et al. (2003a, Pallas station in Western Lapland and Värriö station in Eastern Lapland, distance 250 km) observed over 90 NPF events, corresponding to >14% of all days. All events were associated with marine/polar air masses originating from the Northern Atlantic or the Arctic Ocean. 55% of NPF events were observed on the same day at both sites, while 45% were observed at only one of the stations. Most of the differences could be related to the influence of air masses of different origin or rain/fog at the respective other station. Among the NPF events observed only in Eastern Lapland, experiencing air masses from Kola Peninsula industrial area, about 80% were associated with high SO_2 concentrations. In Western Lapland, no increase in SO_2 concentrations was observed in connection with NPF events. The authors concluded, that in plumes originating from the Kola industrial area, new particles are formed by nucleation involving H_2SO_4 from SO_2 oxidation. About one third of the NPF events, observed in Eastern Lapland, was found to be affected or caused by the Kola Peninsula industry.

Evaluating continuous measurements, performed at the Pallas Global Atmosphere Watch (GAW) station area, which started on 13 April 2000 and ended on 16 February 2002, Komppula et al. (2003b) identified in total 65 NPF events, corresponding to 10% of all days, i.e., not as frequent and not as intense as seen in the measurements in Southern Finland (>50 events per year in Hyytiälä, see references therein). The

largest number of events occurred in April and May. The synoptic analysis revealed NPF events favourably occurring in polar or arctic air masses. Solar radiation was observed to be one key factor needed for NPF. Additionally, a link between NPF and vertical movement of air masses caused by turbulence was observed.

From the analysis of an eight-year dataset of aerosol size distributions observed at the boreal forest measurement site in Hyytiälä (30 January 1996–31 December 2003, total of 2892 days) Dal Maso et al. (2005) found, that NPF events happened in the boreal forest boundary layer on at least 24% of all days. The average formation rate of particles larger than 3 nm was $0.8\,\mathrm{cm}^{-3}\,\mathrm{s}^{-1}$, with enhanced rates during spring and autumn. The created event database is valuable for the elucidation of the mechanism leading to atmospheric NPF.

Recently, Hyvönen et al. (2005, see references therein) reported on an occurrence of NPF events in boreal forest environments of around 50–100 times a year, corresponding to 14–27% of all days. A detailed evaluation of their findings will be given in Paper IV.

In general, NPF events are characterised by a strong increase in the concentration of nucleation mode particles (diameter <10 nm, particle number concentration $>10^4\,\mathrm{cm}^{-3}$), a subsequent shift in the mean size of the nucleated particles and the gradual disappearance of particles over several hours (Birmili and Wiedensohler, 2000; Birmili, 2001). Figure 1 shows a generalised pattern of the diurnal evolution of the UCN number concentration during a typical NPF event, observable in the convective surface layer (CSL). The typical UCN evolution, shown in that figure, is derived from a number of previous observations, published, e. g., by Kulmala et al. (1998b, Figs. 3 and 4), Clement and Ford (1999a, Fig. 2), Birmili and Wiedensohler (2000, Fig. 1), Birmili et al. (2000, Figs. 1 and 2), Coe et al. (2000, Fig. 1), Aalto et al. (2001, Figs. 8, 11 and 13), Buzorius et al. (2001, Fig. 6), Clement et al. (2001, Fig. 1), Kulmala et al. (2001a, Fig. 1), Kulmala et al. (2001b, Fig. 4), Nilsson et al. (2001a, Fig. 4), Boy and Kulmala (2002, Fig. 1), Birmili et al. (2003, Figs. 1, 2, 4, 5 and 14), Boy et al. (2003b, Fig. 1), Buzorius et al. (2003, Fig. 6), Stratmann et al. (2003, Figs. 10, 11 and 17), Boy et al. (2004, Figs. 1 and 2), Held et al. (2004, Figs. 1, 2 and 3), Kulmala et al. (2004b, Fig. 1), Kulmala et al. (2004d, Fig. 2), O'Dowd et al. (2004, Fig. 3), Siebert et al. (2004, Fig. 3), Steinbrecher and BEWA2000-Team (2004, Fig. 5), Dal Maso et al. (2005, Figs. 2 and 4), Gaydos et al. (2005, Figs. 1, 3 and 4) and Kulmala et al. (2005, Fig. 1).

The aim of the present approach is twofold:

1. Reproduction of the typical UCN evolution during a NPF event as represented in Fig. 1;

2. Proposition of a suitable method for the estimation of chemical composition fluxes of the particulate phase, which is suggested to be a major task for future PBL research (Held et al., 2004).

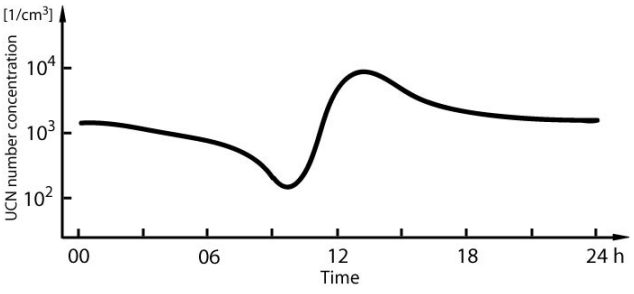

Fig. 1. Typical UCN evolution in the CSL during a NPF burst.

5 Modelling approach

5.1 Rationale of non-local and high-order modelling

The modelling approach is motivated by the following facts:

1. Local closure (known, e.g., as K-, small-eddy, or downgradient theory) is generally accepted to be only valid, if the characteristic scale of turbulent motions is very small compared to the scale of the mean flow. This is ensured for stable and neutral conditions.

2. During convective conditions, the dominant eddy length scale often exceeds the CBL depth, hence:

   (a) Turbulent motions are not completely SGS ones in grid layers.

   (b) Vertical gradients in the well-mixed layer are usually very weak.

   (c) Entrainment fluxes can significantly alter the CBL dynamics.

   (d) Countergradient transports can take place in nearly the entire upper part of the CBL (Sorbjan, 1996; Sullivan et al., 1998). Such transports are relevant for turbulent heat, momentum and concentration fluxes (Holtslag and Moeng, 1991; Frech and Mahrt, 1995; Brown, 1996; Brown and Grant, 1997).

   Consequently, for unstable conditions non-local closure techniques are required even for horizontally homogeneous turbulence over a flat surface and zero mean wind (Ebert et al., 1989; Pleim and Chang, 1992). Nevertheless, even most of state-of-the-art non-local mixing schemes have difficulties to represent the entrainment processes at the top of even the cloudless boundary layer (Ayotte et al., 1996; Siebesma and Holtslag, 1996; Abdella and McFarlane, 1997, 1999; Mironov et al., 1999).

3. Turbulent non-local transport was demonstrated to be important not only in convective turbulence but also in neutral conditions, hence deserving to be accounted for in PBL modelling (Ferrero and Racca, 2004).

4. As gradients of chemical concentrations are often more severe than gradients of heat, moisture and momentum, non-local closure is much more stringent for atmospheric chemistry models than for meteorological ones (Pleim and Chang, 1992). In addition, in the CBL reactants were found to be normally segregated. Under such conditions, chemical transformations depend on turbulent mixing, especially when the time scale of the chemical transformations is in the order of the turbulent characteristic time scale. Then, the mean transformation rate of multimolecular reactions can be strongly affected by co-variances of concentration fluctuations, which deserves, e.g., an adjustment of the eddy diffusivity or a parameterisation of effective reaction rates, accounting for inefficient mixing due to SGS turbulence in terms of large-scale grid length (Galmarini et al., 1997; Thuburn and Tan, 1997; Verver et al., 1997; Vinuesa and Vilà-Guerau de Arellano, 2005). Thuburn and Tan (1997, see references therein) demonstrated, that the negligence of co-variance terms in chemical reaction rates can cause significant errors in predicted chemical rates. Vinuesa and Vilà-Guerau de Arellano (2005) demonstrated, that heterogeneous mixing due to convective turbulence importantly impacts chemical transformations by slowing down or increasing the reaction rate, depending on whether reactants are transported in opposite direction or not.

5. High-order closure becomes more and more common in modelling physical climate processes and their feedbacks (IPCC, 2001, Section 7.2.2.3). A comprehensive review and discussion of state-of-the-art parameterisations of triple correlations and SGS condensation can be found in Zilitinkevich et al. (1999) and Abdella and McFarlane (2001). Recent high-order modelling studies were performed, e.g., by Cheng et al. (2004), Ferrero and Racca (2004), Larson (2004), Lewellen and Lewellen (2004) and Vinuesa and Vilà-Guerau de Arellano (2005).

5.2 Model description

The closure approach adapted here, inclusive approximations (e.g., Rotta's return-to-isotropy hypothesis for pressure covariance terms, quasi-normal approximation for the quadruple correlations, clipping approximation for ad hoc damping of excessive growing triple correlations), parameterisation of turbulence-length scale, numerical model (discretisation, time integration scheme, filtering of spurious oscillations), initial and boundary conditions and stability analysis are based on the third-order modelling studies of André et al. (1976a,b, 1978, 1981) and on the second-order ones of Wichmann and Schaller (1985, 1986) and Verver et al. (1997), in each case for the cloudless PBL.

To ensure traceability, the final equations are given in Appendix A–E. The appendices are organised as follows:

– Appendix A contains the list of symbols (A1), the list of constants (A2), the list of parameters (A3), the list of annotations (A4), the used abbreviations (A5), the definition of the scaling properties (A6) and the definition of the turbulence-dissipation length scale (A7).

– In Appendix B, the basic model equations are given, including the description of the meteorological model (B1), the description of the chemical model (B2), the description of the aerosoldynamical model (B3), the determination of the condensation coefficient and Fuchs–Sutugin correction for the transition regime (B4), the determination of the Brownian coagulation coefficient (B5), the determination of the humidity–growth factor (B6), the semi-empirical expression for the determination of the time-height cross-section of the hydroxyl radical (B7) and the expression for the large-scale subsidence velocity (B8).

– Appendix C includes the Reynolds averaged model equations including the first-order moment equations (C1), the second-order moment equations (C2) (i.e., the velocity correlations (C2.1), the scalar fluxes (C2.2), the scalar correlations (C2.3), the interaction of a reactive tracer with a passive scalar (C2.4), the interaction of reactive tracers (C2.5)), the third-order moment equations (C3) (i.e., the turbulent transport of momentum fluxes (C3.1), the turbulent transport of scalar fluxes (C3.2), the turbulent transport of scalar correlations (C3.3–C3.4)) and the buoyancy fluxes (C4).

– In Appendix D, the initial and boundary conditions are given, for the first-order moments (D1) (i.e., the initial conditions (D1.1), the lower boundary conditions (D1.2), the similarity functions (D1.3), the skin properties (D1.4), the stability functions (D1.5), the upper boundary conditions (D1.6)), for the second-order moments (D2) (i.e., the initial conditions (D2.1), the lower boundary conditions (D2.2), the upper boundary conditions (D2.3)) and for the third-order moments (D3) (i.e., the initial conditions (D3.1), the upper boundary conditions (D3.2)).

– Appendix E contains a brief description of the numerical realisation of the model, including the Adams–Bashforth time differencing scheme (E1), the vertical finite-differencing scheme (E2) (i.e., the grid structure (E2.1), the standard differencing scheme (E2.2), the derivatives of the mean variables in the third-order moment equations (E2.3)).

5.2.1 PBL model

The PBL model includes predictive equations for the horizontal wind components, the potential temperature and the

water vapour mixing ratio (Appendix B1).

To calculate the surface fluxes of momentum, heat and humidity a semi-empirical flux-partitioning scheme proposed by Holtslag (1987) is used. It solves the surface energy budget by a simplified Penman–Monteith approach. This scheme was originally developed for daytime estimates of the surface fluxes from routine weather data. The scheme is designed for grass surfaces, but it contains parameters, which take variable surface properties into account. In the scheme, both the surface radiation budget (incoming solar radiation, reflected solar radiation from the surface, incoming longwave radiation from the atmosphere, outgoing longwave radiation from the surface) (Holtslag, 1987, p. 31–39, Section 3) and the surface energy budget (sensible heat flux, latent heat flux, soil heat flux, surface radiation budget) (Holtslag, 1987, p. 39–47, Section 4) are employed. The soil heat flux is parameterised in terms of the net radiation. The partitioning of the surface energy flux (minus soil heat flux) between the sensible and latent heat flux is based on the Penman–Monteith approach (Monteith, 1981). Both fluxes are parameterised in terms of net radiation and soil flux using semi-empirical parameters, which are adapted from observations (Holtslag, 1987, p. 40–41). Knowing the heat flux, the Monin–Obukhov length scale and the surface momentum flux or shear stress, respectively, is determined (Holtslag, 1987, p. 47–50). This way, the Prandtl layer parameterisation is closed, i.e., the required fluxes can be calculated from gridscale variables. Although this scheme is highly parameterised, it was found to be suitable for the present purpose. Alternatively, the model can be forced using prescribed lower boundary conditions from observations.

The diabatic heating/cooling rate due to longwave and shortwave radiation, i.e., $(\partial\overline{\theta}/\partial t)_{\mathrm{rad}}=\overline{\theta}/\overline{T})\times(\partial\overline{T}/\partial t)_{\mathrm{rad}}$, is calculated according to Krishnamurti and Bounoua (1996, p. 194–207). For the longwave radiation an emissivity tabulation method is used. In this method, the emissivity is expressed as a function of the path length, which in turn depends on temperature, pressure and relative humidity. The basic emissivity values are given in a look-up-table, from which the actual value of emissivity is then interpolated for a given path length. Only absorption and emission by water vapour are considered. The calculation of shortwave radiation is based on an empirical absorptivity function of water vapour. Aerosols are not considered in the radiation model. The radiative transfer calculations are performed at each time step.

Vertical advection due to large-scale subsidence is considered by an empirically prescribed subsidence velocity. For fair-weather conditions, anticyclones etc., associated with clear skies and strong nocturnal radiative cooling, Carlson and Stull (1986) found vertical velocities of $-0.1\,\mathrm{ms}^{-1}$ to $-0.5\,\mathrm{ms}^{-1}$ near the top of the stable boundary layer.

As a consequence of the quasi-normal approximation, the third-order moment equations were demonstrated to be of hyperbolic type (wave equation) containing non-physical solutions, which are called "spurious oscillations" (Moeng and Randall, 1984). Wichmann and Schaller (1985) argued, that spurious oscillation solutions are neither typical for nor restricted to third-order closure models and arise from the use of explicit time differencing schemes. Using a second-order turbulence closure, the authors showed, that spurious oscillations can be suppressed by use of an implicit time differencing scheme. In the present version, an explicit time differencing scheme is retained. To damp spurious oscillations, artificial diffusion terms are added to the right-hand sides of the third-order moment equations as recommended by Moeng and Randall (1984). The treatment of spurious oscillations are discussed in more detail in Section 6.

5.2.2 Chemical model

The chemical model consists of three predictive equations for NH_3, SO_2 and H_2SO_4, in which emission, gas phase oxidation, condensation loss on nucleation mode, Aitken mode and accumulation mode particles, molecule loss due to homogeneous nucleation and dry deposition are considered (Appendix B2). To reduce the chemical mechanism, the OH evolution is diagnostically prescribed (Liu et al., 2001) (see Appendix B7, Eq. (B20) and Appendix D1.1, Eq. (D2)). For the pseudo-second order rate coefficient k_1 of the OH–SO_2 reaction to produce H_2SO_4, a value of $k_1=1.5\times10^{-12}$ $\mathrm{cm}^3\,\mathrm{molecules}^{-1}\,\mathrm{s}^{-1}$ according to DeMore et al. (1994) is used (see Eq. (B7), Appendix B2). This value was also used in Liu et al. (2001). In her study, Ervens (2001) used a higher value of $k_1=2\times10^{-12}\,\mathrm{cm}^3\,\mathrm{molecules}^{-1}\,\mathrm{s}^{-1}$ taken from Atkinson et al. (1997). In their pseudo-steady state approximation of the H_2SO_4 mass balance equation Birmili et al. (2000) used a lower value of $k_1=8.5\times10^{-13}\,\mathrm{cm}^3\,\mathrm{molecules}^{-1}\,\mathrm{s}^{-1}$ proposed by DeMore et al. (1997). This value is close to that employed in the H_2SO_4 closure study of Boy et al. (2005, Table 2, Reaction 14, parameter k_{14}, see references therein), who used $k_1=9.82\times10^{-13}\,\mathrm{cm}^3\,\mathrm{molecules}^{-1}\,\mathrm{s}^{-1}$. With respect to the reaction constants reported here, the maximum is by a factor of $\approx$2.35 higher than the minimum. Hence, the choice of the higher value of k_1 in the present study moves the predicted H_2SO_4 vapour toward higher concentrations. The consequences for the interpretation of the model results will be discussed in more detail in Paper IV.

5.2.3 Aerosoldynamical model

As in a third-order turbulence closure the total number of equations exponentially increases with the number of predictive variables (Stull, 1997, p. 198–199, Table 6-1 and 6-2), an aerosoldynamical model with a low number of predictive variables is applied. The aerosol model is based on a monodisperse approach of Kulmala et al. (1995, 1998b)[6],

[6]The authors used the annotation *integral aerosol dynamics model*.

Pirjola and Kulmala (1998) and Pirjola et al. (1999, 2003). It consists of predictive equations for two moments (number and mass concentration) in three modes (nucleation mode, Aitken mode, accumulation mode) and considers homogeneous nucleation, condensation onto particle surfaces, intra- and inter-mode coagulation as well as dry particle deposition (Appendix B3).

5.2.4 Nucleation model

The calculation of the nucleation rate is based on the classical theory of homogeneous nucleation. Thereafter, the rate of homogeneous nucleation $J_{\mathrm{nuc}}=K_{\mathrm{kin}}\exp(-G_{\mathrm{sp}}/(k_BT))$, i.e., the number of newly formed critical embryos or nuclei per volume and time unit is a product of both a kinetic and a thermodynamical part. The prefactor K_{kin} is mainly based on nucleation kinetics, and the thermodynamical part is proportional to the Gibbs free energy G_{sp}, required to form the critical cluster (Kulmala et al., 2003). Owing to limited solvation, small clusters are less stable then the bulk, which leads for moderate supersaturation to the formation of a barrier on the Gibbs free energy surface for cluster growth (Lovejoy et al., 2004). Nucleation according to the classical nucleation theory (CNT) is limited by barrierless nucleation, where the formation energy is zero and only kinetic contribution is included. The kinetic part itself is smaller, the lower the vapour concentration is (Kulmala et al., 2003). Corresponding to the number of participating species, the applicability of the classical binary nucleation theory (CBNT) and the classical ternary nucleation theory (CTNT) is a subject of a controversial discussion.

The CBNT is known for its large uncertainties in explaining observed nucleation rates. The difference between predicted and observed nucleation rates can exceed several orders of magnitude (Pandis et al., 1995; Kulmala et al., 1998a). NPF often occurs at H_2SO_4 concentrations, which are lower than those predicted by the CBNT. The observed nucleation frequencies are often higher than those predicted by the CBNT (de Reus et al., 1998; Stanier et al., 2003). On the other side, binary nucleation is supported by the fact, that many observed NPF events are associated with elevated SO_2 levels and photochemically induced production of H_2SO_4 vapour (e.g., Marti et al., 1997) and by the dominating contribution of sulphate to the total aerosol mass, as shown, e.g., by Müller (1999) for a rural continental test site influenced by power plants. Strong arguments for kinetically controlled binary nucleation were provided by Weber et al. (1996) and Yu (2003). The nucleation rate can be enhanced due to the higher stability of embryonic H_2O/H_2SO_4 clusters, which increases the cluster lifetime and hence, the chance of such a cluster to grow into a particle of detectable size (de Reus et al., 1998).

Compared to the CBNT, the CTNT of $H_2O/H_2SO_4/NH_3$ predicts significantly higher nucleation rates and more frequent nucleation under typical tropospheric concentrations of H_2SO_4 and NH_3 (Korhonen et al., 1999). This is due to the effect, that NH_3 is able to stabilise the critical embryo, i.e., to reduce its size leading to enhanced nucleation rates (Yu, 2003; Weber et al., 1996).

Recently, Berndt et al. (2005) performed laboratory experiments on NPF in an atmospheric pressure flow tube. Under irradiation with UV light, H_2SO_4 was in situ produced from the reaction of OH with SO_2. NPF was observed for $[H_2SO_4] \geq 7\times10^6\,\mathrm{cm}^{-3}$. For a temperature of 293 K, a relative humidity ranging from 28–49.5%, a NH_3 mixing ratio below 0.5 pptv and a H_2SO_4 concentration of $\sim10^7\,\mathrm{cm}^{-3}$, the authors observed a nucleation rate of $0.3-0.4\,\mathrm{cm}^{-3}\,\mathrm{s}^{-1}$ (particle size $\geq$3 nm). This nucleation rate was found to be in line with the lower limit of the nucleation rates observed in the atmosphere. Because of the very low NH_3 concentration of $\leq$0.5 pptv in the flow tube compared to 100 to 10 000 pptv occurring in the CBL, the authors called the substantial role of NH_3 in the nucleation process into question. Berndt et al. (2005) compared their experimental nucleation rates with theoretical ones of Napari et al. (2002a) and Vehkamäki et al. (2002). The authors concluded: *"The* H_2SO_4 *concentration needed for substantial binary nucleation is* $\sim10^{10}cm^{-3}$*, i.e., far too high compared to the experimental values*[7]*. Ternary* NH_3*-influenced nucleation does not explain the observed particle numbers if* NH_3 *mixing ratios below 0.5 pptv are assumed* [...]*. Furthermore, the nucleation rate seems to behave like* H_2SO_4 *concentration to a power of smaller than 3 to 5, indicating that the nucleation mechanism depends clearly on* H_2SO_4 *concentration, and suggesting a very close to trimer or dimer (kinetically controlled) nucleation mechanism* [...]*"* (Berndt et al., 2005, p. 700, see references therein).

Weber et al. (1996) derived a semi-empirical expression for the collision-controlled nucleation rate with consideration of cluster evaporation, non-accommodation for H_2SO_4 collision and the reaction of a stabilising species such as NH_3 with clusters containing one or more H_2SO_4 molecules and H_2O. The steady-state rate of particle formation in the absence of cluster scavenging by pre-existing particles reads

$$J_{\mathrm{obs}} \approx \beta\gamma^2[H_2SO_4]^2 \quad (1)$$

with $[H_2SO_4]$ being the sulphuric acid concentration in $[\mathrm{cm}^{-3}]$, $\beta=3\times10^{-10}\,\mathrm{cm}^3\,\mathrm{s}^{-1}$ being the collision frequency function for the molecular cluster, that contain the stabilised H_2SO_4 molecule, and γ being the thermodynamically determined NH_3-stabilised fraction of the H_2SO_4 monomer (γ=0.001 for Hawaii, γ=0.003 for Colorado).

In the literature, the so-called ion-mediated nucleation has attracted growing attention, because atmospheric gaseous ions were found to can effectively induce NPF in two steps (Eichkorn et al., 2002):

1. Ion-induced nucleation:

[7] This statement refers to predictions from the theoretical approaches of Napari et al. (2002a) and Vehkamäki et al. (2002).

(a) Formation of a stable neutral molecular cluster;

(b) Attachment of low-volatility trace gas molecules to small ions leading to large cluster ions;

(c) Ion-ion recombination of positive and negative cluster ions leading to an electrically neutral molecular cluster, which may be sufficiently large to experience spontaneous growth by condensation of low-volatility trace gas molecules;

2. Subsequent growth of the freshly nucleated cluster to a small volatile aerosol particle of detectable size ($D_p \geq 3$ nm).

There are two major effects of the net electric charge of an ion:

– Large stabilisation of a cluster ion compared to an electrically neutral cluster of the same size and composition;

– Much faster growth of a cluster ion due to the large ion-molecule collision cross-section resulting from the long range of the charge-dipole interaction.

Favoured conditions for the occurrence of ion-induced nucleation are low temperatures and large concentrations of low-volatility gases. The UT is suspected to be a favoured place for ion-mediated nucleation under certain conditions (Eichkorn et al., 2002; Lovejoy et al., 2004). A strong argument supporting ion-mediated NPF also results from the fact, that in both the homogeneous binary and ternary nucleation, the growth rate of newly formed nanoparticles from condensation of H_2O, H_2SO_4 and NH_3 was found to be often far too low to explain the rapid appearance of fresh ultrafine particles during midday (Weber et al., 1997; Yu and Turco, 2000). Consequently, Yu and Turco (2000) hypothesised, that some of present day discrepancies between theory and observation may be due to the intervention of background ionisation in NPF. For details the reader is referred, e.g., to Weber et al. (1997), Hõrrak et al. (1998), Yu and Turco (2000, 2001a,b), Eichkorn et al. (2002), Laakso et al. (2002), Hermann et al. (2003), Laakso et al. (2003), Nadykto and Yu (2003), Yu (2003), Lovejoy et al. (2004) and Wilhelm et al. (2004).

Apart from the question, which species contribute to nucleation, the CNT suffers from two essential shortcomings:

1. Molecular clusters are represented by droplets up to and including the critical size, characterised by bulk properties of the condensed phase, such as surface tension, density, vapour pressure (Yu and Turco, 2001b). This so-called "capillarity approximation" is known to be inappropriate for small molecular clusters with ∼1 nm diameter. It causes large uncertainties in nucleation rates predicted by the CNT (Lovejoy et al., 2004).

2. According to the CNT, NPF performs instantaneously, i.e., the time scale of the growth kinetics of the subcritical embryos is neglected compared to other relevant time scales in aerosol evolution (Yu and Turco, 2001b).

To overcome these shortcomings, self-consistent kinetic theory is desired. In the kinetic theory, the cluster formation is described as a sequence of basic collision steps beginning with the vapour phase (Yu and Turco, 2001b). Afterwards, molecular-scale coagulation and dissociation act as the driving processes of aerosol evolution. Condensation and coagulation are treated analogously, i.e., condensation (evaporation) is equivalent to coagulation (dissociation) of a molecule or small molecular cluster with (from) a particle (Yu and Turco, 2001b). Kinetic theory can explicitly describe interacting systems of vapours, ions, charged and neutral clusters and pre-existing particles at all sizes in a straightforward and self-consistent manner. Being physically more realistic and flexible, it is considered to be superior to the classical approach (Yu and Turco, 2001b). However, compared to new theoretical approaches based, e.g., on ab initio molecular dynamics and Monte-Carlo simulations, the CNT is still the only one, which can be used in atmospheric modelling, even if molecular approaches are needed to confirm results obtained by the CNT (Noppel et al., 2002). At least, the time scale of the growth kinetics of critical embryos can be a posteriori considered within the framework of the CNT by adapting the concept of the "apparent nucleation rate" (Kerminen and Kulmala, 2002). The apparent nucleation rate is the rate, at which newly formed particles appear in the sensor detection range. When new embryos, i.e., critical clusters with ∼1 nm diameter, grow in size by condensation and intramode coagulation, their number concentration decreases. As a result, the apparent nucleation rate is lower than the real one derived from nucleation theory. Kerminen and Kulmala (2002) derived an analytical formula to relate the apparent to the real nucleation rate to cut off the lowest desirable scale for the evolution of the aerosol size distribution in explicit nucleation schemes of atmospheric models. However, this formula is not applicable to very intensive nucleation bursts, to potential nucleation events associated with cloud outflows or to nucleation occurring in plumes, which undergo strong mixing with ambient air.

Based on a critical analysis of the advantages and shortcomings of the classical Gibbs approach to determine the parameters of the critical cluster and the work of critical cluster formation in heterogeneous systems, a generalised Gibbs approach has been proposed and applied to describe phase formation processes in multicomponent solutions by Schmelzer et al. (1999, 2002, 2003, 2004a,b, 2005), Schmelzer and Schmelzer Jr. (2002) and Schmelzer and Abyzov (2005). This approach delivers a theoretically well-founded description not only of thermodynamic equilibrium but also of thermodynamic non-equilibrium states of a cluster or ensembles of clusters of arbitrary sizes and composi-

tions. The new method allows the consideration of a dependence of the surface tension of the clusters of arbitrary sizes on the state parameters of both coexisting macrophases. The generalised Gibbs approach results in relations for the parameters of the critical cluster, which are different, in general, from the mechanical, thermodynamical and chemical equilibrium conditions derived by Gibbs. Most importantly, for clusters of nanometric sizes, the generalised Gibbs approach leads to different results for the determination of the state parameters of the critical clusters and the work of critical cluster formation in comparison with the classical Gibbs method. Schmelzer et al. (2005) found, that the results of the generalised Gibbs approach are in qualitative and partly even quantitative agreement with the van der Waals square gradient method and more advanced density functional computations of the parameters of the critical clusters and the work of critical cluster formation.

Kuni et al. (1999) investigated the kinetics of non-steady condensation on macroscopic solid wettable nuclei. The authors determined kinetic characteristics, such as the number of supercritical drops formed, the time of start and the time of duration of the stage of effective nucleation of supercritical drops as well as the width of the size spectrum of the supercritical drops in dependence (i) on initial parameters specifying the properties of condensing liquid, the vapour-gas surroundings and the kind of matter of solid wettable nucleus, (ii) on sizes of condensation nuclei and their initial number in the vapour-gas medium as well as (iii) on the rate of externally determined establishment of the vapour supersaturation.

Shchekin et al. (1999) investigated the thermodynamic conditions of the process of heterogeneous nucleation through the formation of thin, uniform and non-uniform, wetting films on solid insoluble macroscopic nuclei, which allows, e.g., the determination of the work of wetting using a relatively small number of, in general, quantifiable parameters. The obtained expressions can be easily incorporated into an analytical theory, which describes the possibility of barrierless heterogeneous nucleation, developed for thermodynamics and kinetics of heterogeneous nucleation occurring via formation of films of uniform thickness. Recently, Shchekin and Shabaev (2005) presented a thermodynamic theory of deliquescence of small soluble solid particles in an undersaturated vapour, which allows, e.g., the determination of the work of droplet formation under different assumptions regarding the size dependence and chemical state of the soluble solid core[8].

[8]The authors defined deliquescence as follows: *"The stage of nucleation by soluble particles in the atmosphere of solvent vapour, when arising droplets consist of a liquid film around incompletely dissolved particles, is called deliquescence stage. In a supersaturated vapour, this stage is the initial one in the whole condensation process, and the particles inside the droplets will completely dissolve in the growing droplets with time. In an undersaturated vapour, this stage finishes by establishing the aggregative equilibrium between droplets of different sizes, with residues of the particles (solid cores within the droplets) varying in size down to complete dissolution"*(Shchekin and Shabaev, 2005, p. 268).

Recently, Kulmala et al. (2006) proposed a cluster activation theory to explain the linear dependence between the formation rate of 3 nm particles and the H_2SO_4 concentration. While existing nucleation theories predict a dependence of the nucleation rate on the H_2SO_4 concentration to the power of ≥ 2, atmospheric observations suggest a power between one and two. The activation theory is able to explain the observed slope. According to the new approach, the cluster containing one H_2SO_4 molecule will activate for further growth due to heterogeneous nucleation, heterogeneous chemical reactions including polymerisation or activation of soluble clusters. In the activation process organic vapours are typically needed as condensing agents. This concept is in general agreement with the theory of TSCs proposed by Kulmala et al. (2000).

A detailed evaluation of the most recent nucleation concepts is beyond the scope of the present paper. The intention of the present paper is to discuss mechanistic ways, how CBL turbulence can affect atmospheric NPF. Therefore, the present approach is restricted to the evaluation of classical concepts of homogeneous binary and ternary nucleation. For the calculation of the homogeneous binary H_2O/H_2SO_4 nucleation rate and the critical cluster composition the so-called "exact" model with consideration of cluster hydration effects is implemented (Stauffer, 1976; Jaecker-Voirol et al., 1987; Jaecker-Voirol and Mirabel, 1988, 1989; Kulmala and Laaksonen, 1990; Laaksonen and Kulmala, 1991; Kulmala et al., 1998a; Seinfeld and Pandis, 1998, Chapter 10). For the ternary $H_2O/H_2SO_4/NH_3$ nucleation rate and the critical cluster composition a state-of-the-art parameterisation of Napari et al. (2002a,b) is used. The limits of the validity of the ternary nucleation parameterisation are T=240−300 K, RH=5−90%, $[H_2SO_4]=10^4-10^9$ cm^{-3}, $[NH_3]$=0.1−100 ppt and $J_{ter}=10^{-5}-10^6$ cm^{-3} s^{-1}. The parameterisation can not be used to obtain the binary H_2O/H_2SO_4 or H_2O/NH_3 limit (Napari et al., 2002b). When the vapour concentrations fall below their lower parameterisation limits, they were kept at their corresponding minimum concentrations.

5.2.5 Condensation flux model

(a) Treatment of H_2SO_4 *vapour*

The condensation flux represents the vapour molecular deposition rate onto spherical droplets of a certain radius. It results from the solution of the mass transport equation in the continuum regime, i.e., when the particle is sufficiently large compared to the mean free path of the diffusing vapour molecules. The solution obtained by Maxwell (1877) describes the total flow of vapour molecules toward an aerosol particle by diffusion on a molecular scale (Seinfeld and Pan-

dis, 1998, p. 596–597, Maxwellian flux). When the mean free path length of diffusing vapour becomes comparable to the particle diameter, i.e., when the Knudsen number is Kn≈1, the phenomena are said to lie in the transition regime (Seinfeld and Pandis, 1998, p. 601). Then, the Maxwellian flux needs to be adjusted by a transitional correction factor. This correction factor extends the growth rate from the continuum regime into the transition regime. To match the continuum and free molecule fluxes, several approaches have been proposed, known, e.g., as Fuchs theory, Fuchs and Sutugin approach, Dahneke approach, Loyalka approach, Sitarski and Nowakowski approach. For a description and additional references the reader is referred to Seinfeld and Pandis (1998, p. 601–605). Following previous attempts, e.g., that of Liu et al. (2001), here the so-called Fuchs–Sutugin factor in terms of Knudsen number has been applied (Fuchs and Sutugin, 1971).

In the present approach, the condensation flux parameterisation is applied to nucleation mode, Aitken mode and accumulation mode particles. The Maxwellian flux is proportional to the driving force, i.e., the difference between the partial pressure of the condensable vapour far from the particle (ambient conditions) and the vapour pressure at the droplet surface, the latter being a product of the equilibrium partial pressure at ambient temperature and the acid activity in the condensed phase. If the driving force is positive, the flow of vapour molecules is directed toward the particle surface and if negative vice versa. In the present approach, maximum Maxwellian flux is considered, i.e., the ratio of the vapour pressure at the droplet surface to the ambient partial pressure is assumed to be much lower than 1. This means, that the diffusive flux is always directed to the particle surface. This assumption is accepted to be valid for low-volatile vapours, such as sulphuric acid (Clement and Ford, 1999a,b; Liu et al., 2001; Boy et al., 2003b; Krejci et al., 2003; Held et al., 2004; Gaydos et al., 2005) and for organic molecules, such as dicarboxylic acids and for pinon aldehyde as the main product of α-pinene oxidation (Boy et al., 2003b; Held et al., 2004).

(b) H_2SO_4 *mass accommodation coefficient (or sticking probability)*

The Fuchs–Sutugin transitional correction factor depends on, among others, the so-called mass accommodation coefficient α_{gas} (or sticking probability S_p) (see Eq. (B16) in Appendix B4). In their box modelling study Kulmala et al. (1998b) investigated the sensitivity of the model results against the sticking probability. Varying this parameter between 0.001 and 1.0, the authors concluded, that the change of the sticking probability on accumulation mode particles does not change the growth properties of nucleation mode particles significantly.

In opposite to this, Clement and Ford (1999a) considered the uncertainty in the sticking probability as the main problem in defining the growth rate. The authors argued: *"There appeared recently to be a theoretical and experimental consensus that sticking probabilities for water and sulphuric acid on liquid droplets are small (Itoh, 1990; Van Dingenen and Raes, 1991). Values quoted for sulphuric acid ranged between 0.02 and 0.09, and, in their model of the relationship between DMS flux and CCN concentration in remote marine regions, Pandis et al. (1994) used a base case value of 0.02 with a test value of 0.05. However, experimental and theoretical evidence from a wide field of surface science, including molecular beam experiments and molecular dynamics simulations, suggests that such small values are extremely unlikely at normal atmospheric temperatures (Clement et al., 1996). Direct experiments on growing droplets of n-propanol/water mixtures give results consistent with* S_p=1*, the theoretically most likely value for all except very light atoms or molecules on dense materials at normal temperatures. Recent measurements of the growth rates of ultrafine particles at remote marine and continental sites (Weber et al., 1996, 1997) are consistent with* S_p=1 *for sulphuric acid. Since the evidence for* S_p *that is much less than unity is generally reliant on complex modelling subject to alternative interpretations, we much prefer values close to unity"* (Clement and Ford, 1999a, p. 478). Clement and Ford (1999a, Fig. 1) investigated the influence of the sticking probability of H_2SO_4 onto the droplet growth rate in the range of droplet size radii R_p=0.001−10 µm. The Fuchs–Sutugin transitional correction factor (and therewith the growth rate of droplets with radius R_p) for R_p=10 nm is by approximately two orders of magnitude lower at S_p=0.02 than at S_p=1. At the smaller sizes, the Fuchs–Sutugin transitional correction factor is proportional to S_p. For droplets with R_p=1 µm the respective correction factors differ by one order of magnitude. As the most of the atmospheric aerosol is in the size range 0.01−1 µm, growth rates have an uncertainty of over a factor of 10 for nearly all the aerosol if S_p is undetermined (Clement and Ford, 1999a). The authors emphasised, that the change in the slope of the S_p=1 and S_p=0.1 curves in the accumulation mode region R_p=0.1−1 µm, depicted in Clement and Ford (1999a, Fig. 1), has an influence on the acid condensation on the aerosol in this mode relative to that on smaller sized aerosols. From their modelling study on sulphate particle growth in the MBL, Kerminen and Wexler (1995) concluded the necessity to use high values of S_p for smaller particles. The choice of the sticking probability is highly important for the determination of the molecular removal onto aerosol, which often specifies the molecular concentration in the atmosphere. Clement and Ford (1999a, p. 485) concluded: *"For sulphuric acid molecules there is a large difference in removal rates used at present arising from differing values for the molecular sticking probability. For theoretical reasons we favour a value of unity, which is the value supported by experiments on other molecules such as water."* For barrierless nucleation Clement

and Ford (1999b) found a strong influence of the sticking probability on the characteristic time scale for a homogeneous nucleation process to affect the vapour concentration (time scale for burst). This time scale will be reduced by a factor of 0.074, when S_p is reduced from 1 to 0.02. Correspondingly, an increase of the characteristic time scale for removal on pre-existing aerosols is expected as a result of this change. Hence, low values of the sticking probability favour the occurrence of NPF events.

Evaluating the pseudo-steady state approximation of the H_2SO_4 mass balance to calculate the H_2SO_4 concentration, Birmili et al. (2000) assumed a sticking probability of unity to estimate the condensation sink.

In their mesoscale aerosol modelling study Liu et al. (2001) used a sticking probability of 0.3 for H_2SO_4 according to Worsnop et al. (1989). Liu et al. (2001, p. 9700) commented this value as follows: "*Our value for the accommodation coefficient is an intermediate value in the range which extends from ∼0.1 to 1.0 (Jefferson et al., 1997). More extreme values could significantly modify the magnitude of nucleation rates although spatial patterns are unlikely to be altered.*"

In their analytical tool to derive formation and growth properties of nucleation mode aerosols (diameter growth rate, aerosol condensation and coagulation sinks, concentration of condensable vapours and their source rate, 1 nm particle nucleation rates) from measured aerosol particle spectral evolution, Kulmala et al. (2001a, Fig. 3a) used a sticking probability of unity. Performing a sensitivity study with varying sticking probabilities the authors demonstrated, that for S_p=0.01 the total sink is significantly smaller than that for S_p=1. Not only the magnitude of the condensation was shown to be significantly affected by the choice of the sticking probability, but also the influence of supermicron particles was demonstrated to contribute more significantly to the total removal of condensable vapours and a bimodal sink results. The sticking probability also significantly affects the calculated vapour concentration. Dividing the sticking probability by a factor of 100 (S_p=0.01) requires 100 times more vapour to reproduce the observed aerosol growth.

In their tropospheric multiphase chemistry mechanism CAPRAM2.4 Ervens (2001) and Ervens et al. (2003) (see also http://projects.tropos.de:8088/capram/capram24.pdf, Table 3b: Mass accommodation coefficients and gas phase diffusion coefficients) used a H_2SO_4 sticking probability of S_p=0.12 according to Schwartz (1986). For comparison the authors also referred to S_p=0.07 proposed by Davidovits et al. (1995).

The low H_2SO_4 sticking probability used in the present study is expected to lead to a quite low condensation loss of nucleating vapours onto newly formed and pre-existing particles, hence resulting in high amounts of H_2SO_4 vapour, that will favour NPF. This fact will be discussed in more detail in Paper IV, where the model results are compared with observed NPF events.

(c) Treatment of NH_3

With respect to atmospheric NH_3, the assumption of maximum Maxwellian flux is questionable. As demonstrated by Nenes et al. (2000), the vapour pressure at the droplet surface strongly depends, e.g., on droplet composition. In their NPF modelling study, Gaydos et al. (2005) argued, that H_2SO_4 condensation alone produces growth, that is similar to observations, hence NH_3 condensation by molecular diffusion was not considered explicitly. Therefore, the NH_3 gas phase concentration was diagnostically determined from the assumption, that total ammonia, total nitrate and total sulphate, taken from measurements, are always in thermodynamic equilibrium with gas phase and particulate phase concentrations (Ansari and Pandis, 1999, model GFEMN). Here, a similar approach is applied. The gas phase NH_3 concentration is diagnostically determined for given total ammonium and total sulphate concentration (gas phase plus particle phase) using the inorganic aerosol thermodynamic equilibrium model ISORROPIA (meaning "equilibrium" in Greek) of Nenes et al. (2000). The total ammonium and total sulphate concentrations are prognostically determined.

5.2.6 Humidity growth

The water uptake of dry aerosol is considered by applying the empirical humidity–growth factor of Birmili and Wiedensohler (2004, personal communication, see Appendix B6, Eq. (B19)).

5.2.7 Particle deposition model

The size-segregated particle dry deposition velocity is parameterised according to Zhang et al. (2001).

5.2.8 Alternative approaches

Alternatively to the third-order closure approach presented here, a "mixed closure model" can be realised, e.g., running the third-order closure for PBL dynamics and the first-order closure for chemistry and aerosol dynamics, respectively. Then, a higher number of predictive physicochemical variables can be considered, such as organic compounds and size bins of a sectional aerosoldynamical model. Doing so, special care has to be taken to appropriately parameterise the turbulent fluxes. First-order closure is based on diagnostic flux gradient relations, i.e., the fluxes are represented by the downgradient approach, eventually semi-empirically corrected for countergradient flows. For the eddy diffusivity of scalars one can either use an ad hoc approach (e.g., O'Brien, 1970), diagnostic relations based on diagnostic flux equations (Holtslag and Moeng, 1991; Holtslag et al., 1995) or semi-empirical expressions based on the turbulence spectrum, such as proposed and evaluated, e.g., by Degrazia et al. (1997a,b, 1998, 2001). Generally, the closure type depends mainly on the question and scale of interest as well as on

the flow characteristics, e.g., on atmospheric stability (see Subsection 5.1). However, the present approach opens a suitable way to investigate turbulence-related NPF. But when focussing on "organic" NPF scenarios, e.g., occurring in boreal forests, where a large number of organic compounds and, perhaps, size bins must be considered, then either a pure first-order closure or even a mixed third/first-order closure is recommended to use.

6 Numerical realisation and basic tests

The partial differential equations (PDEs) of the present model represent a mixed class of two types of initial-value problems. The advection terms in the governing equations belong to the class of flux-conservative initial-value problems (Press et al., 1996, p. 824–838, Chapter 19.1, Eq. (19.1.6)), and the diffusion terms in the parabolic parts belong to the class of diffusive initial-value problems (Press et al., 1996, p. 838–844, Chapter 19.2, Eq. (19.2.1)). The PDEs can be numerically solved simplest by means of the Forward Time Centred Space (FTCS) representation (Press et al., 1996, p. 825–827, Eqs. (19.1.1), (19.1.11)). Thereafter, the time derivative is numerically represented by the forward Euler differencing[9], which is only first-order accurate in Δt (Press et al., 1996, p. 826, Eq. (19.1.9)). For the space derivative a centred space differencing[10] of second-order accuracy in Δz is applied (Press et al., 1996, p. 827, Eq. (19.1.10)). The FTCS scheme is an explicit scheme[11]. Regarding the requirements of a numerical scheme, Press et al. (1996, p. 830) argued, that "*the* [numerical] *inaccuracy is of a tolerable character when the scheme is stable.*" Later on the authors added an argument, "*that annoys the mathematicians: The goal of numerical simulation is not always 'accuracy' in a strictly mathematical sense, but sometimes 'fidelity' to the underlying physics in a sense that is looser and more pragmatic. In such contexts, some kinds of error are much more tolerable than other"* (Press et al., 1996, p. 832). The numerical realisation of the model closely follows pragmatic arguments as well as the recommendations given in the basic papers of André et al. (1976a,b, 1978, 1981), Bougeault (1981a,b), Moeng and Randall (1984), André and Lacarrère (1985), Bougeault (1985), Wichmann and Schaller (1985), Bougeault and André (1986), Wichmann and Schaller (1986), Bougeault and Lacarrère (1989) and Verver et al. (1997). However, there was no a priori guarantee, that the underlying PDEs are physically stable. In cases they would not, the search for a stable differencing scheme must fail. To ensure the physical and numerical stability and to evaluate the accuracy of the numerical scheme, a number of tests have been carried out, which are described below. An important result of the present approach is the objective evidence, that the considered modelling concept is conditionally stable[12] with respect to the treatment of the physicochemical processes.

6.1 Amplitude error

The satisfaction of the Courant–Friedrichs–Lewy stability criterion (CFL) (Press et al., 1996, p. 829) was ensured by empirical adjustment of the integration time step according to the prescribed vertical grid resolution. To investigate the sensitivity of the model results against the time integration scheme, the first-order forward Euler time differencing scheme was compared with the third-order Adams–Bashforth time differencing scheme[13], which is known to have attractive stability characteristics (Durran, 1999, p. 65–72, Table 2.1). The differences were visually inspected and found to be small and hence, being not relevant for the question of interest. This agrees with the findings of Durran (1999, p. 65), who argued: "[. . .] *A major reason for the lack of interest in higher-order time differencing is that in many applications the errors in the numerical representation of the spatial derivatives dominate the time discretisation error, and as a consequence it might appear unlikely that the accuracy of the solution could be improved through the use of higher-order time difference.*" The studies presented in Paper II and III were carried out using the third-order Adams–Bashforth scheme.

6.2 Transport error

The large-scale subsidence is considered by additional vertical-advection terms in the governing PDEs. The discretisation of these terms can cause transport errors (Press et al., 1996, p. 831). It was found, that the application of the centred-differencing scheme does work well for meteorological advection, but not for advection of physicochemical properties, where at very low mean concentrations first-order moments can become negative. To avoid this effect, an upwind differencing is generally used for the advection terms (Press et al., 1996, p. 832, Eq. (19.1.27)). This scheme is only first-order accurate in the calculation of the spatial derivatives, but it was found to be appropriate for the discretisation of advection terms.

[9] The forward Euler time scheme has the advantage, that the quantities at time step $n+1$ can be calculated in terms of only quantities known at time step n.

[10] The centred space differencing also uses quantities known at time step n only.

[11] Explicit scheme means, that the quantities at the time step $n+1$ at each level can be calculated explicitly from the quantities that are already known. The FTCS approach is also classified as a single-level scheme, since only values at time level n have to be stored to find values at time level $n+1$.

[12] To ensure physical stability, the third-order moment PDEs for the physicochemical variables must be modified. See Paper III.

[13] There exists also a second-order version of this scheme.

6.3 Phase error and non-linear instability

6.3.1 Inspection of clipping approximation

The clipping approximation was found to be both a necessary and sufficient condition to ensure the stability of the meteorological model. This is fully in accordance with André et al. (1978, p. 1881, see their conclusions), who concluded, that the realisability inequalities are absolutely necessary *"since if one ceases to enforce them at any time the model blows up very rapidly."* In opposite to this, the clipping approximation was found to be a necessary but insufficient condition to stabilise the physicochemical part of the model (see below).

6.3.2 Inspection of spurious oscillations

Moeng and Randall (1984) demonstrated, that the third-order equations proposed by André et al. (1978) are of hyperbolic type. The solution of these equations exhibits oscillations, which arise from the mean gradient and buoyancy terms of the triple-moment equations. In the present approach, the author followed the attempt of Moeng and Randall (1984, Eq. (3.5)) to damp these oscillations by introducing artificial diffusion terms into the triple-moment equations. With a reasonable choice of the diffusion coefficient, these oscillations can be additionally damped in the cloudless case considered here. This is fully in accordance with Moeng and Randall (1984). It was found, that the physical stability of the numerical model is a prerequisite to damp spurious oscillations. When the numerical model is not stable, physical stability can not be achieved by considering artificial diffusion terms. From a visual inspection of the triple moments it was found, that the amplitude of the spurious oscillations can be effectively damped by artificial diffusion terms, but not be prevented. It should be noted, that spurious oscillations – even being non-physical – are a part of the mathematical solution of the underlying hyperbolic PDEs. These parts of the solution can be traced back to an insufficient physical parameterisation of quadruple correlations. The spurious oscillations, occurring in the meteorological part of the third-order moment PDEs, could be successfully damped by the recommendations of Moeng and Randall (1984). In contrary to this, the damping of these spurious oscillations is exceptionally difficult in the physicochemical part. Apart from modelling passive tracers, for which spurious can be successfully damped, these oscillations were found to amplify themselves, when physicochemical interactions are considered (reactive tracers). This causes instability of the physicochemical part[14]. The introduction of artificial diffusion terms damps physicochemical oscillations effectively but not sufficiently.

6.3.3 Inspection of space differencing

Performing a third-order modelling study of a marine stratocumulus layer, Bougeault (1985) pointed out, that a modification of the vertical finite-differencing scheme is required to handle the strong gradients in the temperature and moisture profile at the inversion level. During the simulation of stratocumulus a very sharp inversion can develop, featuring a strong change over one grid length with negligible gradients immediately above and below. The vertical derivatives of the first-order moments appear both in second- and third-order moment equations. Bougeault (1985) argued, that owing to the staggered structure of the grid[15], the derivatives evaluated by the centred finite-difference scheme at the half levels can differ by a factor 2. This creates problems in the third-order moment equations, leading to the appearance of negative values of the variances at the half level just below the inversion. The ultimate way to solve this problem is a variable grid spacing with higher resolution near the inversion. To bypass a variable grid, the author proposed a more empirical solution. The centred differencing of the derivatives of the first-moment variables in the third-order moment equations is replaced by a geometric approximation, while all other derivatives are still evaluated by centred finite-differencing (Bougeault, 1985, p. 2827–2828, Fig. 1, Eqs. (2)–(3)). In the present study it was found, that the revised finite-differencing scheme for the mean variables in the third-order moment equations – originally designed to be applied near a stratocumulus top – is not necessary for the simulation of the meteorological fields in the cloudless case. This is plausible, as near the cloudless PBL top such large gradients of temperature and humidity, as observed near stratocumulus cloud tops, are unlikely. Anyway, for physicochemical properties the situation is completely different. In both the cloudless and the cloudy case much higher vertical gradients of physicochemical properties can be expected, compared to those appearing in the meteorological profiles. Consequently, the revised finite-differencing scheme was applied. This way, the physical stability of the physicochemical model could be effectively enhanced. To be consistently, the approach proposed by Bougeault (1985) is used both in the physicochemical and meteorological model. As for artificial diffusion, the physical stability of the numerical model is a prerequisite for the stabilising effect of the revised differencing scheme. When the model is physically unstable, instability can be damped, but full stability can not be achieved by the proposed alteration of the differencing scheme.

[14]The same numerical model and subroutines are used in both the meteorological and the physicochemical model. Self-amplifying oscillations can be hardly called "spurious". However, it seems, that the amplification directly originate from spurious oscillations, or at least are strongly related to them.

[15]In a staggered grid, first- and third-order moments are calculated at the main levels, and second-order ones are calculated at the half levels.

6.3.4 Effect of artificial retardation terms

To prevent amplifying oscillations of physicochemical third-order moments, several attempts have been made, which consider additional empirical retardation terms in the corresponding PDEs. Such terms secure an evolutionary tendency of the predicted fields toward some prescribed values, such as realised in the classical nudging concept. Runs were performed, e.g., with different retardation time scales. It was found, that such terms can prolongate the "characteristic runtime" of an executable, that exhibits amplifying oscillations. However, it was not possible to prevent the amplification of such oscillations at all.

6.3.5 Remaining stability problems

To prevent the amplification of oscillations, which destabilise the model, physical arguments must be considered for the modification of the third-order moment equations of the physicochemical model. This is explained in detail in Paper III. Finite-difference schemes for hyperbolic equations can exhibit purely numerical dispersion (phase errors) and non-linear instability (Press et al., 1996, p. 831). The questions, to what extent numerical phase errors and non-linear instability can be separated from spurious oscillations, or how they interact, could not be answered for the time being. This issue deserves a special evaluation in a separate work.

6.4 Mass conservation

The mass conservation was investigated in connection with the prevention of amplifying oscillations in the physicochemical part. Three tests using a passive tracer have been performed. Firstly, a scenario with zero-background tracer concentration and a source with a time-independent unit strength located at the ground was considered. Sinks were excluded. In the course of the day, the source continuously replenished the mixing layer with the tracer. The result was a tracer profile exponentially decreasing with height. The tracer concentration near the ground increased when the mixing layer height collapsed in the late afternoon. Secondly, a number of runs were performed with different height-dependent initial profiles without a ground source. In each case, the tracer concentration became stationary and height-independent after a couple of model hours, i.e., the tracer was fully diluted throughout the boundary layer. Thirdly, runs were performed with a height-independent initial profile. This profile was found to remain nearly constant during the runs, i.e., the fluctuations around the initial profile were found to be negligibly small with respect to the question of interest. Such kinds of tests were performed several times, e.g., when numerically relevant revisions were conducted (replacement of the time integration scheme and the discretisation scheme, modification of the clipping approximation, alteration of prescribed fine-tuning parameters etc.). A detailed re-evaluation of this issue is intended to be performed in the context of the replacement of the clipping approximation by a state-of-the-art parameterisation of third-order moments, recently proposed in the literature.

6.5 Sensitivity against changes in the turbulence parameterisation

6.5.1 Extension of PDE numbers

The model equations, proposed by André et al. (1978), are originally based on a number of simplifications, e.g., the governing equations for the kinematic humidity fluxes, inclusive the corresponding equations of the related triple correlations, are neglected. In the present model version, these simplifications were omitted to generalise the approach. Although the consideration of the additional equations is numerically more expensive compared to the base case, and although it does presently not lead to an evaluable gain of information with respect to the question of interest, the model was found to behave "well-tempered" against that important extension of the number of equations, i.e., stability remains ensured and the results are qualitatively similar.

6.5.2 Fine-tuning turbulence parameters

The fine-tuning parameters, recommended to use by André et al. (1978), should not be changed without reasonable care, especially without a physically motivated revision of the underlying parameterisation. The model was found to be noticeably sensitive against changes of these parameters. However, corresponding tests were not systematically performed, because they are ill-motivated at the present stage of work.

6.5.3 Length scale parameterisation

The mixing length effectively affects the dissipation rate. As already stated by Moeng and Randall (1984), there exists no proper way to determine the length scale. Existing formulations are more or less arbitrary, or their validity is restricted to special conditions, such as certain ranges of atmospheric stability, respectively. Tests using several commonly accepted parameterisations of the mixing length scale and the mixing layer height (used as scaling properties) were carried out. In the present case, the mixing length parameterisation was extensively evaluated in the context of the treatment of spurious oscillations. Bougeault and André (1986) argued, that the mixing length formulation of Mellor and Yamada (1974) is known to grossly overestimate the mixing length near the inversion and therefore leads to a gross underestimation of the dissipation rate. From a linear stability analysis the authors concluded, that oscillations can only develop in a region of unstable stratification, and that in this case, they can be efficiently controlled by decreasing the mixing length. These findings are very important, especially for the cloud-topped

PBL, but perhaps even though for physicochemical processes near the top of the cloudless PBL. Sensitivity tests show, that the mixing length parameterisation used in André et al. (1978) is appropriate to simulate the meteorological evolution of the cloudless PBL. But owing to the more sophisticated adjustment of their length scale parameterisation to buoyancy-induced instabilities, the approach of Bougeault and André (1986) was also evaluated. With respect to the meteorological model, the results using different schemes were found to be qualitatively very similar, but to differ quantitatively. Without a more detailed PBL verification study, no scheme could be ad hoc favoured over the other one. Considering the physicochemical model it appears, that the revised approach proposed by Bougeault and André (1986) enhances the model stability. However, as previously discussed, when the numerical model is not physically stable, than stability can also not be achieved by alteration of the mixing length parameterisation. The observed sensitivity of the model results against the length scale parameterisation shows, that its evaluation in a model like the present one remains an important task, even after years of great efforts on this subject.

7 Reference case scenarios

To select meaningful reference scenarios for the present feasibility study, both phenomenological and numerical arguments are considered. In Paper III, two scenarios will be investigated with an emission source at the ground but very low background concentrations of aerosol, henceforth called "clean air mass" scenarios. Such situations are possible to occur in anthropogenically influenced CBLs depleted from air pollutants in connection with frontal air mass change and post-frontal advection of fresh polar and subpolar air, respectively.

1. Firstly, a ground emission source is required to provide precursor gases for the production of nucleating vapours. A low background concentration of aerosol particles is required to ensure the absence of condensation sinks, which condensable vapours prevent from nucleating or TSCs prevent from growing to detectable size (see Kulmala et al., 2000). Such a scenario was hypothesised and observed as a prerequisite for NPF (Nilsson et al., 2001a; Birmili et al., 2003; Buzorius et al., 2003). For example, in a comprehensive NPF-CBL evolution study Nilsson et al. (2001a, p. 459, Subsection 4.1, item (1)) hypothesised: "*On the days when a dilution of the preexisting aerosol number and condensation sink was observed before nucleation, this may itself be enough to trigger nucleation by decreasing the sink of precursor gases at the same time that the precursor production may be increasing due to increasing photochemical activity. Such a scenario would form favorable conditions for nucleation*". The low initial Aitken mode and accumulation mode number concentrations of respective 10 an 10 cm^{-3}, used in the present study, correspond to the values, used in the rural (R1, R2), the urban (U1, U2) and the marine case scenarios (M1, M2, M3) of the modelling study performed by Pirjola and Kulmala (1998, Fig. 1). In the binary nucleation study performed by Pirjola et al. (1999, Table 1), e.g., an initial number concentration of 100 cm^{-3} was assumed for Aitken mode particles and 10 cm^{-3} for accumulation mode particles (see their cases 1 and 2).
2. As discussed in Section 6, spurious oscillations are unwanted solutions of the non-linear PDE system. They were found to be not critical in the meteorological part. In opposite to this, such oscillations can become critical in the physicochemical model. Especially near the CBL top, at very low concentrations of condensing vapours and pre-existing aerosols the physicochemical variables could cross zero owing to spurious oscillations. Hence, a scenario with low background concentration is reasonable for the evaluation of the model behaviour.

The considered scenarios will be quantitatively characterised in Paper III. They are not claimed to represent the variety of observations. A systematic evaluation of other possible NPF scenarios and the direct evaluation of a dedicated measurement campaign is beyond the scope of the present paper and deserves further studies.

8 Conclusions

Based on previous findings on high-order modelling, an attempt is made to describe gas-aerosol-turbulence interactions in the CBL. The approach can be characterised as follows:

1. A third-order closure is self-consistently applied to a system of meteorological, chemical and quasi-linearised aerosoldynamical equations under horizontally homogeneous conditions.
2. The model is designed to predict time-height profiles of meteorological, chemical and aerosoldynamical mean-state variables, variances, co-variances and triple correlations in the CBL.
3. The approach might be instrumental in interpreting observed particle fluxes from in situ measurements and/or remote sensing. In addition, it provides information about gas-aerosol-turbulence interactions, that can not be directly observed in the CBL.
4. Though highly parameterised, the model configuration considers the basic processes, which are supposed to be involved in the evolution of NPF bursts in the CBL.
5. The model provides input information required for a more sophisticated parameterisation of the effect of

SGS turbulence on the homogeneous nucleation rate, such as variances and co-variances of temperatures, humidity and the condensable vapours H_2SO_4 and NH_3 (Easter and Peters, 1994; Hellmuth and Helmert, 2002; Shaw, 2004; Lauros et al., 2006).

6. Provided, that the model is validated, it may serve as a tool, e.g., to perform conceptual studies and to verify parameterisations of SGS processes in large-scale chemistry and aerosol models (effective reaction rates, turbulence-enhanced condensation etc.).

Known shortcomings of the nucleation approach and condensation flux parameterisation are discussed. To consider turbulent density fluctuations, the governing equations for the first-, second- and third-order moments must be re-derived on the base of a scale analysis (Bernhardt, 1964, 1972; Bernhardt and Piazena, 1988; Foken, 1989; Venkatram, 1993; van Dop, 1998). In the subsequent Papers II and III, the model capability to predict the CBL evolution in terms of first-, second- and third-order moments and to simulate the evolution of UCNs during a NPF event will be demonstrated within the framework of a conceptual study. Furthermore, the model results are discussed with respect to previous observational findings.

Appendix A

List of symbols, annotations, scaling properties, constants, parameters and abbreviations

A1. Symbols

Latin letters

A	– Replacement variable
a	– Dual−use character (replacement variable and constant)
a_1, a_2	– Empirical parameters for the incoming solar radiation
B	– Replacement variable
b	– Dual−use character (replacement variable and constant)
b_1, b_2	– Empirical parameters for the incoming solar radiation
C	– Replacement variable
c	– Dual−use character (replacement variable and constant)
$C_1, C_2, C_4{-}C_{11}$	– Adjustment parameters for the turbulence closure scheme
C_{coag}	– Brownian coagulation coefficient $[\mathrm{m^3 s^{-1}}]$
$C_{\mathrm{cond,gas}}$	– Condensation coefficient $[\mathrm{m^3 s^{-1}}]$
C_{T_0}	– Parameter for the buoyancy fluxes
$c_1, \ldots, c_3$	– Empirical parameters for the surface energy budget
c_G	– Empirical parameter for the soil heat flux
c_R	– Parameter for the radiative destruction rate
c_h, c_m	– Scaling constants for the universalfunctions
c_p	– Specific heat capacity at constant pressure(dry air)
$D_{\mathrm{H_2SO_4}}$	– Diffusion coefficient of H_2SO_4
$D_{\mathrm{i}}, D_{\mathrm{j}}$	– Stokes−Einstein expression for the diffusion coefficient
D_p	– Particle diameter
$\tilde{D}_{\mathrm{down}}$	– Downward finite differencing
$\tilde{D}_{\mathrm{up}}$	– Upward finite differencing
d	– Constant
E_{scf}	– Water vapour mass flux
e	– Turbulent kinetic energy
F	– Replacement function
$\mathcal{F}$	– Modified Fuchs−Sutugin factor
f_c	– Coriolis parameter
G_{soil}	– Soil heat flux
G_{sp}	– Gibbs free energy of cluster formation
GF	– Humidity−growth factor
g	– Acceleration of gravity
$g_{\mathrm{i}}, g_{\mathrm{j}}$	– Parameter functions

H_{M_i} – Characteristic scale height of particle mass concentration M_i

H_{N_i} – Characteristic scale height of particle number concentration N_i

$H_{H_2SO_4}$ – Characteristic scale height of H_2SO_4

H_{NH_3} – Characteristic scale height of total NH_3

H_{OH} – Characteristic scale height OH

H_{SO_2} – Characteristic scale height SO_2

H_{sfc} – Sensible heat flux at the surface

H_w – Scale height of large−scale subsidence

h – Integration time step

i – Index

J_{nuc} – Nucleation rate [$m^{-3}s^{-1}$]

J_{obs} – Observed nucleation rate [$m^{-3}s^{-1}$]

J_{ter} – Ternary nucleation rate [$m^{-3}s^{-1}$]

j – Index

K_h, K_m – Eddy diffusivity coefficients for heat and momentum

$K^{\downarrow}$ – Incoming solar radiation at ground level

$K^{\downarrow}_{clear}$ – Incoming solar radiation at ground level in clear skies

K_{kin} – Kinetic prefactor in the nucleation rate expression

Kn – Knudsen number

k – Index of vertical main level

k_1, k_{14} – Pseudo−second order rate coefficient for reaction of OH with SO_2

k_B – Boltzmann constant

$\mathcal{K}^{\alpha}$, $\mathcal{K}^{\beta}$ $= (k^{\alpha}_{mn})$, (k^{β}_{mn}) "Coupling matrices" of the rate constants for the interaction between tracer χ_m and $\chi_n$in reaction equations α, β ((m, n) $= 1, \ldots, N$; $(\alpha, \beta) = 1, \ldots, N$)

L – Monin−Obukhov length scale

L_0 – Length scale (dual−use variable)

$L_{Blackadar}$ – Blackadar's length scale for neutral and unstable stratification

L_D – Turbulence−length scale for stable stratification

L_n – Length scale

L_{turb} – Turbulence−length scale

L_v – Latent heat of water vapourisation

$L_{v,0}$ – Latent heat of water vapourisation at $T = 273.15\,K$

$L_v E_{sfc}$ – Latent heat flux

$L^{\downarrow}$ – Incoming longwave radiation from the atmosphere

$L^{\uparrow}$ – Outgoing longwave radiation from the surface

l_i – Parameter function

M_{gas} – Molar mass of gas molecules

M_i – Mode i particle mass concentration [$kg\,m^{-3}$] (i $= 1, \ldots, 3$)

$M_{i,sfc}$ – Mode i particle mass concentration at the surface (i $= 1, \ldots, 3$)

m – Index

m_i – Mode i mean dry particle mass [kg] (i $= 1, \ldots, 3$)

$m_{H_2SO_4}$ – Mass of one H_2SO_4 molecule [kg]

m_{NH_3} – Mass of one NH_3 molecule [kg]

N – Total number of physicochemical variables

N_{cld} – Total cloud cover

N_i – Mode i particle number concentration [m^{-3}] (i $= 1, \ldots, 3$)

$N_{i,sfc}$ – Mode i particle number concentration at the surface (i $= 1, \ldots, 3$)

n – Index

n_{OH} – Exponent in the OH representation

n_w – Exponent in the representation of the large−scale subsidence

$n^{\star}_{NH_3}$, $n^{\star}_{H_2SO_4}$ – Number of NH_3 and H_2SO_4 molecules per newly formed embryo

$[OH]_{\{min/max\}}$ – Minimum/maximum of the OH concentration

P – Generation rate of, the eddy kinetic energy $\bar{e}$

$P_{diagonal}$ – Diagonal part of the pressure triple term

P_{ia} – Generation rate of the, scalar flux $\overline{u_i' a'}$

P_{ij} – Generation rate of the Reynolds stress $\overline{u_i' u_j'}$

P_{rapid}, P_{relax} – Rapid and relaxation part of the pressure triple term

$Pr_t = \dfrac{K_m(\zeta = 0)}{K_h(\zeta = 0)}$ Turbulent Prandtl number

p – Air pressure

Q_{α} – Source term in the governing equation of reactant α ($\alpha = 1, \ldots, N$)

$Q_{\alpha,emission}$ – Emission strength of reactant α ($\alpha = 1, \ldots, N$)

$Q^{\star}$ – Net radiation at the surface

q – Water vapour mixing ratio

q_s – Saturation specific humidity

$q_{\star}$ – Kinematic humidity scale

$\overline{R}_{A\chi_{\alpha}}$ – Rate of change of the second−order moment $\overline{A'\chi'_{\alpha}}$ due to the interaction of a reactive tracer χ_{α} with a nonreactive scalar A ($A \equiv$ replacement variable) ($\alpha = 1, \ldots, N$)

$\overline{R}_{a\chi_{\alpha}}$ – Rate of change of the second−order moment $\overline{a'\chi'_{\alpha}}$ due to the interaction of a reactive tracer χ_{α} with a nonreactive scalar a ($\alpha = 1, \ldots, N$)

R_p – Particle radius

R_u – Universal gas constant
$\overline{R}_{u_i \chi_\alpha}$ – Rate of change of the second−order moment $\overline{u_i' \chi_\alpha'}$ due to the interaction term in the governing equation of the tracer flux ($i = 1, \ldots, 3$; $\alpha = 1, \ldots, N$)
$\overline{R}_\alpha$ – Interaction term in the governing equation of the first−order moment $\overline{\chi}_\alpha$ ($\alpha = 1, \ldots, N$)
$\overline{R}_{\chi_\alpha \chi_\beta}$ – Rate of change of the second−order moment $\overline{\chi_\alpha' \chi_\beta'}$ due to the interaction of the reactive tracers χ_α and χ_β ($(\alpha, \beta) = 1, \ldots, N$)
RH – Relative humidity
$r_{0,\mathrm{dry}}$ – Reference radius of the dry particle in the humidity growth factor
$r_{i,\mathrm{dry}}$, $r_{i,\mathrm{wet}}$ – Mode i mean radius of the dry and wet particle [m] ($i = 1, \ldots, 3$)
S_p – Sticking probability, accommodation coefficient
s – Slope of curve of the saturation specific humidity curve
T – Temperature
T_0 – Reference temperature for the coefficient of thermal expansion
T_{scr} – Temperature at screening height (1−2 m)
t – Time (Local Standard Time)
t_0 – Initial time (Local Standard Time)
U – Horizontal wind velocity
u_i, u_j – Components of three−dimensional wind vector ($(i, j) = 1, \ldots, 3$)
u – x−component of horizontal wind
u_g – x−component of geostrophic wind
u_i, u_j, u_k – Components of the wind vector ($(i, j, k) = 1, \ldots, 3$)
$u_\star$ – Friction velocity
V_{χ_α} – Deposition velocity ($\alpha = 1, \ldots, N$)
v – y−component of horizontal wind
v_g – y−component of geostrophic wind
$\overline{v}_{\mathrm{gas}}$ – Mean speed of gas molecules
$\overline{v}_i$, $\overline{v}_j$ – Mean speed of particles with the respective masses m_i, m_j ($(i, j) = 1, \ldots, 3$)
w – Vertical velocity
$w_\star$ – Convective velocity scale
$\overline{w}$ – Large−scale subsidence velocity
$\overline{w}_H$ – Large−scale subsidence velocity at H_w
x – Normalised scaling height
x_j, x_j – Geometrical co−ordinates (three dimensions) ($(i, j) = 1, \ldots, 3$)
z – Geometrical height
z_0 – Surface roughness length
z_i – Mixing layer height
z_k – Geometrical height of main level k
$z_{k=1}$ – Geometrical height of the first main level
z_p – Prandtl layer height (first main level $z_{k=1}$)
z_s – Height level just above the surface (screening height)

Greek letters

α – Dual−use variable (index and replacement variable)
α_0 – $= 1/\mathrm{Pr_t}$ Reciprocal of turbulent Prandtl number
α_{gas} – Mass accommodation coefficient or sticking probability of a condensing gas
α_{PM} – Empirical parameter for Penman−Monteith approach
α_{sfc} – Surface albedo
α_T – Coefficient of thermal expansion
β – Dual−use variable (replacement variable and collision frequency function for molecular clusters
β_{buo} – $= \alpha_T \times g$ Buoyancy parameter
β_{PM} – Empirical parameter for Penman−Monteith approach
Γ_d – Dry−adiabatic lapse rate
γ – Dual−use variable (replacement variable and NH_3−stabilised fraction of the H_2SO_4 monomer
γ_{PM} – Psychrometric constant
δ – Replacement variable
δ_{ij} – Kronecker delta ($(i, j) = 1, \ldots, 3$) (Stull, 1997, p. 57)
ϵ_{ijk} – Alternating unit tensor ($(i, j, k) = 1, \ldots, 3$) (Stull, 1997, p. 57)
ε – Dissipation rate
ε_R – Radiative destruction rate
ε_{ab} – Dissipation rate in the governing equation of the scalar correlations $\overline{a'b'}$
ε_{abc} – Dissipation rate in the governing equation of the triple moments $\overline{a'b'c'}$
ε_{uab} – Dissipation rate in the governing equation of the triple moments $\overline{u_i' a' b'}$ ($i = 1, \ldots, 3$)
ε_{uua} – Dissipation rate in the governing equation of the triple moments $\overline{u_i' u_j' a'}$ ($(i, j) = 1, \ldots, 3$)
ε_{uuu} – Dissipation rate in the governing equation of the triple moments $\overline{u_i' u_j' w'}$ ($(i, j) = 1, \ldots, 3$)
$\zeta = z/L$ – Normalised height coordinate stability parameter
$\eta_1, \ldots, \eta_3$ – Fit parameter for humidity growth factor
θ – Potential temperature
θ_v – Virtual potential temperature
$\theta_\star$ – Kinematic temperature scale
$(\partial\theta/\partial t)_{\mathrm{rad}}$ – Diabatic heating/cooling rate due to radiative flux divergency
κ – Von Kármán constant

λ_{air} – Mean free path of air
λ_{gas} – Mean free path of gas
μ_{air} – Viscosity of air
ρ_0 – Standard value of density
ρ_{air} – Air density
ρ_p – Particle density
σ – Stefan−Boltzmann constant
Φ – Replacement variable
Φ_k – Replacement variable at main level k
Φ_{sun} – Solar elevation
Φ^n – Replacement variable at time step n
ϕ_{geo} – Geographical latitude
ϕ_h, ϕ_m – Similarity (universal) functions for heat and momentum
χ_m, χ_n – Reactive tracer and/or aerosol parameter ((m, n) = 1, . . . , N)
$\chi_\alpha, \chi_\beta, \chi_\gamma$ – Reactive tracer and/or aerosol parameter ((α, β, γ) = 1, . . . , N)
$\chi_{\alpha\star}$ – Characteristic scaling property of reactive tracer and/or aerosol parameter χ_α (α = 1, . . . , N)
Ξ – Parameter function for humidity growth factor
Ψ – Replacement function
Ψ_H, Ψ_M – Stability functions for heat and momentum
ω – Angular velocity of the Earth
$[H_2SO_4]$ – Sulphuric acid vapour concentration
$[NH_3]$ – Ammonia concentration
[OH] – Hydroxyl radical concentration
$[SO_2]$ – Sulphur dioxide concentration
$\mathcal{F}_{gas}$ – Correction formula for the transition regime of diffusion of gas molecules in a background gas to a particle
Υ_1 – Similarity function for kinematic heat, humidity and tracer fluxes
Υ_2 – Similarity function for variances and co−variances of temperature, humidity and tracer concentration

A2. Constants

Latin letters

$a_1 = 1041\,\mathrm{W\,m^{-2}}$
$a_2 = -69\,\mathrm{W\,m^{-2}}$
$b_1 = 0.75$
$b_2 = 3.4$
$C_2 = 2.5$
$C_4 = 4.5$
$C_5 = 0$
$C_6 = 4.85$
$C_7 = 0.4$
$C_8 = 8.0$
$C_9 = -0.67$
$C_{10} = 6.0$
$C_{11} = 0.2$
$c_1 = 5.31 \times 10^{-13}\,\mathrm{W\,m^{-2}\,K^{-6}}$
$c_2 = 60\,\mathrm{W\,m^{-2}}$
$c_3 = 0.12$
$c_g = 0.1$
$c_h = \alpha_0\,\kappa$
$c_m = \kappa$
$c_{pa} = 1006\,\mathrm{J\,kg^{-1}\,K^{-1}}$
$D_{H_2SO_4} = 1.2 \times 10^{-5}\,\mathrm{m^2\,s^{-1}}$
$f_c = 2\omega \sin\phi_{geo} \approx 1.117 \times 10^{-4}\,\mathrm{s^{-1}}$
$g = 9.80665\,\mathrm{m^2\,s^{-1}}$
$k_1 = 1.5 \times 10^{-18}\,\mathrm{m^3\,molecules^{-1}\,s^{-1}}$
$k_B = 1.381 \times 10^{-23}\,\mathrm{J\,K^{-1}}$
$L_{v,0} = 2515 \times 10^3\,\mathrm{J\,kg^{-1}}$
$M_{SO_2} = 64.06 \times 10^{-3}\,\mathrm{kg\,mol^{-1}}$
$M_{NH_3} = 17.0318 \times 10^{-3}\,\mathrm{kg\,mol^{-1}}$
$M_{H_2SO_4} = 98.08 \times 10^{-3}\,\mathrm{kg\,mol^{-1}}$
$N_A = 6.022 \times 10^{23}\,\mathrm{molecules}$
$r_{0,dry} = 59.49\,\mathrm{nm}$
$R_d = 287.955\,\mathrm{J\,kg^{-1}\,K^{-1}}$
$R_v = 462.520\,\mathrm{J\,kg^{-1}\,K^{-1}}$
$R_u = 8.314\,\mathrm{J\,mol^{-1}\,K^{-1}}$
$T_0 = 285\,\mathrm{K}$

Greek letters

$\alpha_{H_2SO_4} = 0.12$
$\alpha_T = 1/T_0 = 3.51 \times 10^{-3}\,\mathrm{K^{-1}}$
$\alpha_{PM} = 1$
$\alpha_{sfc} = 0.23$
$\beta_{PM} = 20\,\mathrm{W\,m^{-2}}$
$\eta_1 = 0.097$
$\eta_2 = 0.204$
$\eta_3 = 5.5826$
$\gamma_{PM} = c_p/L_v \approx 4 \times 10^{-4} \left(\frac{[\mathrm{gram}]_{water}}{[\mathrm{gram}]_{air}}\right)\mathrm{K^{-1}}$
$\Gamma_d = g/c_p \approx 1\,\mathrm{K/100\,m}$
$\kappa = 0.41$
$\lambda_{air} = 6.98 \times 10^{-8}\,\mathrm{m}$
$\mu_{air} = 1.83 \times 10^{-5}\,\mathrm{kg\,m^{-1}\,s^{-1}}$
$\omega = 7.27 \times 10^{-5}\,\mathrm{s^{-1}}$
$\rho_p = 1.5 \times 10^3\,\mathrm{kg\,m^{-3}}$
$\sigma = 5.67 \times 10^{-8}\,\mathrm{W\,m^{-2}\,K^{-4}}$

A3. Parameters

$H_{OH} = 6.9 \times 10^3$ m
$H_{SO_2} = 1.2 \times 10^3$ m
$H_{NH_3} = 1.2 \times 10^3$ m
$H_{H_2SO_4} = 1.2 \times 10^3$ m
$H_{N_i} = 1 \times 10^3$ m, (i = 1, . . . , 3)
$H_{M_i} = 1 \times 10^3$ m, (i = 1, . . . , 3)
$H_w = 1.2 \times 10^3$ m
$\overline{[H_2SO_4]}_{min} = 1 \times 10^{11}$ molecules m^{-3}
$\overline{[H_2SO_4]}_{max} = 1 \times 10^{12}$ molecules m^{-3}
$n_{OH} = 6$
$n_w = 2.4$
$\overline{[NH_3]}_{tot,sfc} = 1 \times 10^{-1}\,\mu$g m^{-3}
$\overline{[N_1]}_{sfc} = 1 \times 10^6$ m^{-3}
$\overline{[N_2]}_{sfc} = 10 \times 10^6$ m^{-3}
$\overline{[N_3]}_{sfc} = 10 \times 10^6$ m^{-3}
$\overline{[OH]}_{min} = 2 \times 10^{11}$ molecules m^{-3}
$\overline{[OH]}_{max} = 10 \times 10^{12}$ molecules m^{-3}
$\overline{[SO_2]}_{sfc} = 5\,\mu$g m^{-3}
$u_g = 5$ m s^{-1}
$v_g = 0$ m s^{-1}
$V_{SO_2} = 0.8 \times 10^{-2}$ m s^{-1}
$V_{NH_3} = 1 \times 10^{-2}$ m s^{-1}
$V_{H_2SO_4} = 1 \times 10^{-2}$ m s^{-1}
$\overline{w}_H = -1 \times 10^{-2}$ m s^{-1}
$z_s = 1$ m
$z_p = 10$ m

A4. Annotations

$\overline{(\,)}$ – Average over grid cell volume and integration time step
$\widetilde{(\,)}$ – Integration variable
$(\,)'$ – Turbulent deviation from the average
$(\,)^\star$ – Surface energy budget property
$(\,)_\star$ – Surface layer scaling property
$(\,)_{max}$, $(\,)_{min}$ – Maximum, minimum value
$(\,)_{dry}$ – Dry particle property
$(\,)_{rad}$ – Radiation−induced
$(\,)_{reac}$ – Chemical reaction−induced
$(\,)_{sfc}$ – Surface variable
$(\,)_{top}$ – Model top property
$(\,)_{tot}$ – Total (gas phase + particle phase) concentration of species
$(\,)_{wet}$ – Wet particle property

A5. Abbreviations

BIOFOR – Biogenic Aerosol Formation in the Boreal Forest
BLMARC – Boundary layer mixing, aerosols, radiation and clouds
BVOC – Biogenic volatile organic compound
CAPRAM – Chemical Aqueous Phase Radical Mechanism
CBL – Convective boundary layer
CBNT – Classical binary nucleation theory
CCN – Cloud condensation nucleus
CFL – Courant, Friedrichs, Lewy
CLAW – Charlson, Lovelock, Andrea, Warren
CNT – Classical nucleation theory
CSL – Convective surface layer
CTNT – Classical ternary nucleation theory
DMS – Dimethyl sulphide
EU – European Union
FT – Free troposphere
FTCS – Forward Time Centred Space
GAW – Global Atmosphere Watch
GFEMN – Gibbs Free Energy Minimization
MBL – Marine boundary layer
NPF – New particle formation
nss – non−sea−salt
PAQS – Pittsburgh Air Quality Study
PBL – Planetary boundary layer
PDE – Partial differential equation
QUEST – Quantification of Aerosol Nucleation in the European Boundary Layer
SGS – Subgridscale
TSC – Thermodynamically stable cluster
UCN – Ultrafine condensation nucleus
UT – Upper troposphere

A6. Scaling properties

$$
\begin{aligned}
u_\star &= \left[\left(\overline{w'u'}\right)_{z_s}^2 + \left(\overline{w'v'}\right)_{z_s}^2\right]^{1/4} \\
\left(\overline{w'u'}\right)_{z_s} &= -\left[\frac{\overline{u}(z_{k=1})}{\overline{U}(z_{k=1})}\right] u_\star^2 \\
\left(\overline{w'v'}\right)_{z_s} &= -\left[\frac{\overline{v}(z_{k=1})}{\overline{U}(z_{k=1})}\right] u_\star^2 \\
\overline{U}(z_{k=1}) &= \sqrt{\overline{u}(z_{k=1})^2 + \overline{v}(z_{k=1})^2} \\
w_\star &= \begin{cases} \left[\beta_{buo}\left(\overline{w'\theta'}\right)_{z_s} z_i\right]^{1/3}, & \left(\overline{w'\theta'}\right)_{z_s} > 0 \\ 0, & \left(\overline{w'\theta'}\right)_{z_s} < 0 \end{cases} \\
L &= -\frac{u_\star^3}{\kappa\beta_{buo}\left(\overline{w'\theta'}\right)_{z_s}} \\
\theta_\star &= -\left(\overline{w'\theta'}\right)_{z_s} / u_\star \\
q_\star &= -\left(\overline{w'q'}\right)_{z_s} / u_\star \\
\chi_{\alpha\star} &= -\left(\overline{w'\chi'_\alpha}\right)_{z_s} / u_\star \\
\left(\overline{w'\theta'}\right)_{z_s} &= -u_\star\theta_\star \\
\left(\overline{w'q'}\right)_{z_s} &= -u_\star q_\star
\end{aligned}
\tag{A1}
$$

A7. Turbulence-dissipation length scale

(References: André et al., 1978)

$$
\begin{aligned}
\varepsilon &= C_1(L_{turb})\frac{\overline{e}^{3/2}}{L_{turb}} \\
C_1(L_{turb}) &= 0.019 + 0.051\frac{L_{turb}}{L_{Blackadar}}
\end{aligned}
\tag{A2}
$$

$$
\begin{aligned}
L_{turb} &= \mathrm{Min}(L_{Blackadar}, L_D) \\
L_{Blackadar} &= \frac{\kappa z}{1+\kappa\frac{z}{L_0}} \\
L_0 &= 0.1\frac{\int_0^\infty \sqrt{\overline{e}}\, z\, dz}{\int_0^\infty \sqrt{\overline{e}}\, dz} \\
L_D &= 0.75\sqrt{\frac{\overline{e}}{\beta_{buo}\frac{\partial\overline{\theta}}{\partial z}}}
\end{aligned}
\tag{A3}
$$

Appendix B

Model equations

B1. Meteorological model

$$\frac{du}{dt} = f_c(v - v_g) \tag{B1}$$

$$\frac{dv}{dt} = -f_c(u - u_g) \tag{B2}$$

$$\frac{d\theta}{dt} = \left(\frac{\partial\theta}{\partial t}\right)_{rad} \tag{B3}$$

$$\frac{dq}{dt} = 0 \tag{B4}$$

B2. Chemical model

$$
\begin{aligned}
\frac{d\chi_\alpha}{dt} &= R_\alpha + Q_\alpha + Q_{\alpha,emission} \\
R_\alpha &= \sum_{m=1}^{N}\sum_{n=m}^{N} k_{mn}^{\alpha}\, \chi_m\chi_n \quad , \quad \alpha = 1,\ldots,N
\end{aligned}
\tag{B5}
$$

$$
\begin{aligned}
\frac{d\chi_1}{dt} &= \frac{d[NH_3]_{tot}}{dt} \\
&= Q_{1,emission}
\end{aligned}
\tag{B6}
$$

$$
\begin{aligned}
\frac{d\chi_2}{dt} &= \frac{d[SO_2]}{dt} \\
&= \underbrace{-\,k_1\,[OH]\,[SO_2]}_{Q_2} + Q_{2,emission}
\end{aligned}
\tag{B7}
$$

$$
\begin{aligned}
\frac{d\chi_3}{dt} &= \frac{d[H_2SO_4]}{dt} \\
&= \underbrace{\underbrace{-\,C_{cond,H_2SO_4}(r_{1,wet})}_{k_{34}^3}\ \underbrace{[H_2SO_4]}_{\chi_3}\ \underbrace{N_1}_{\chi_4}}_{} \\
&\quad \underbrace{\underbrace{-\,C_{cond,H_2SO_4}(r_{2,wet})}_{k_{35}^3}\ \underbrace{[H_2SO_4]}_{\chi_3}\ \underbrace{N_2}_{\chi_5}}_{} \\
&\quad \underbrace{\underbrace{-\,C_{cond,H_2SO_4}(r_{3,wet})}_{k_{36}^3}\ \underbrace{[H_2SO_4]}_{\chi_3}\ \underbrace{N_3}_{\chi_6}}_{} \\
&\quad \underbrace{+\,k_1\,[OH]\,[SO_2] \;-\; J_{nuc}\, n^\star_{H_2SO_4}}_{Q_3}
\end{aligned}
\tag{B8}
$$

B3. Aerosoldynamical model

(References: Pirjola et al., 1999)

$$\begin{aligned}\frac{d\chi_4}{dt} &= \frac{dN_1}{dt} \\ &= \underbrace{-\frac{1}{2}\,C_{\mathrm{coag}}(r_{1,\mathrm{wet}},r_{1,\mathrm{wet}})}_{k_{44}^4}\,\underbrace{N_1}_{\chi_4}\,\underbrace{N_1}_{\chi_4} \\ &\quad \underbrace{-\,C_{\mathrm{coag}}(r_{1,\mathrm{wet}},r_{2,\mathrm{wet}})}_{k_{45}^4}\,\underbrace{N_1}_{\chi_4}\,\underbrace{N_2}_{\chi_5} \\ &\quad \underbrace{-\,C_{\mathrm{coag}}(r_{1,\mathrm{wet}},r_{3,\mathrm{wet}})}_{k_{46}^4}\,\underbrace{N_1}_{\chi_4}\,\underbrace{N_3}_{\chi_6} \\ &\quad \underbrace{+\,J_{\mathrm{nuc}}}_{Q_4}\end{aligned} \tag{B9}$$

$$\begin{aligned}\frac{d\chi_5}{dt} &= \frac{dN_2}{dt} \\ &= \underbrace{-\frac{1}{2}\,C_{\mathrm{coag}}(r_{2,\mathrm{wet}},r_{2,\mathrm{wet}})}_{k_{55}^5}\,\underbrace{N_2}_{\chi_5}\,\underbrace{N_2}_{\chi_5} \\ &\quad \underbrace{-\,C_{\mathrm{coag}}(r_{2,\mathrm{wet}},r_{3,\mathrm{wet}})}_{k_{56}^5}\,\underbrace{N_2}_{\chi_5}\,\underbrace{N_3}_{\chi_6}\end{aligned} \tag{B10}$$

$$\begin{aligned}\frac{d\chi_6}{dt} &= \frac{dN_3}{dt} \\ &= \underbrace{-\frac{1}{2}\,C_{\mathrm{coag}}(r_{3,\mathrm{wet}},r_{3,\mathrm{wet}})}_{k_{66}^6}\,\underbrace{N_3}_{\chi_6}\,\underbrace{N_3}_{\chi_6}\end{aligned} \tag{B11}$$

$$\begin{aligned}\frac{d\chi_7}{dt} &= \frac{dM_1}{dt} \\ &= \underbrace{C_{\mathrm{cond},H_2SO_4}(r_{1,\mathrm{wet}})\,m_{H_2SO_4}}_{k_{34}^7}\,\underbrace{[H_2SO_4]}_{\chi_3}\,\underbrace{N_1}_{\chi_4} \\ &\quad \underbrace{-\,C_{\mathrm{coag}}(r_{1,\mathrm{wet}},r_{2,\mathrm{wet}})\,m_1}_{k_{45}^7}\,\underbrace{N_1}_{\chi_4}\,\underbrace{N_2}_{\chi_5} \\ &\quad \underbrace{-\,C_{\mathrm{coag}}(r_{1,\mathrm{wet}},r_{3,\mathrm{wet}})\,m_1}_{k_{46}^7}\,\underbrace{N_1}_{\chi_4}\,\underbrace{N_3}_{\chi_6} \\ &\quad \underbrace{+\,J_{\mathrm{nuc}}(n^\star_{H_2SO_4}m_{H_2SO_4}+n^\star_{NH_3}m_{NH_3})}_{Q_7}\end{aligned} \tag{B12}$$

$$\begin{aligned}\frac{d\chi_8}{dt} &= \frac{dM_2}{dt} \\ &= \underbrace{C_{\mathrm{cond},H_2SO_4}(r_{2,\mathrm{wet}})\,m_{H_2SO_4}}_{k_{35}^8}\,\underbrace{[H_2SO_4]}_{\chi_3}\,\underbrace{N_2}_{\chi_5} \\ &\quad \underbrace{+\,C_{\mathrm{coag}}(r_{1,\mathrm{wet}},r_{2,\mathrm{wet}})\,m_1}_{k_{45}^8}\,\underbrace{N_1}_{\chi_4}\,\underbrace{N_2}_{\chi_5} \\ &\quad \underbrace{-\,C_{\mathrm{coag}}(r_{2,\mathrm{wet}},r_{3,\mathrm{wet}})\,m_2}_{k_{56}^8}\,\underbrace{N_2}_{\chi_5}\,\underbrace{N_3}_{\chi_6}\end{aligned} \tag{B13}$$

$$\begin{aligned}\frac{d\chi_9}{dt} &= \frac{dM_3}{dt} \\ &= \underbrace{C_{\mathrm{cond},H_2SO_4}(r_{3,\mathrm{wet}})\,m_{H_2SO_4}}_{k_{36}^9}\,\underbrace{[H_2SO_4]}_{\chi_3}\,\underbrace{N_3}_{\chi_6} \\ &\quad \underbrace{+\,C_{\mathrm{coag}}(r_{1,\mathrm{wet}},r_{3,\mathrm{wet}})\,m_1}_{k_{46}^9}\,\underbrace{N_1}_{\chi_4}\,\underbrace{N_3}_{\chi_6} \\ &\quad \underbrace{+\,C_{\mathrm{coag}}(r_{2,\mathrm{wet}},r_{3,\mathrm{wet}})\,m_2}_{k_{56}^9}\,\underbrace{N_2}_{\chi_5}\,\underbrace{N_3}_{\chi_6}\end{aligned} \tag{B14}$$

B4. Condensation coefficient, Fuchs–Sutugin correction for transition regime

(References: Seinfeld and Pandis, 1998, pp. 452–459, 596–605; Fuchs and Sutugin, 1971; Clement and Ford, 1999b; Liu et al., 2001)

$$\begin{aligned}&C_{\mathrm{cond,gas}}(r_{\mathrm{i,wet}}) = 4\,\pi\,\mathcal{F}_{\mathrm{gas}}(r_{\mathrm{i,wet}})\,D_{\mathrm{gas}}\,r_{\mathrm{i,wet}}\,, \\ &(\text{"gas"} = H_2SO_4;\ \mathrm{i} = 1,\ldots,3)\end{aligned} \tag{B15}$$

$$\begin{aligned}&\mathcal{F}_{\mathrm{gas}}(r_{\mathrm{i,wet}}) = \\ &\frac{f(\mathrm{Kn_{gas}})}{1+1.333\,\mathrm{Kn_{gas}}\,f(\mathrm{Kn_{gas}})\left(\frac{1}{\alpha_{\mathrm{gas}}}-1\right)} \\ &f(\mathrm{Kn_{gas}}) = \\ &\frac{1+\mathrm{Kn_{gas}}}{1+1.7\,\mathrm{Kn_{gas}}+1.333\,(\mathrm{Kn_{gas}})^2} \\ &\mathrm{Kn_{gas}}(r_{\mathrm{i,wet}}) = \frac{\lambda_{\mathrm{gas}}}{r_{\mathrm{i,wet}}} \\ &\lambda_{\mathrm{gas}} = \frac{3\,D_{\mathrm{gas}}}{\overline{v}_{\mathrm{gas}}} \\ &\overline{v}_{\mathrm{gas}} = \sqrt{\frac{8R_uT}{\pi M_{\mathrm{gas}}}}\end{aligned} \tag{B16}$$

B5. Brownian coagulation coefficient

(References: Seinfeld and Pandis, 1998, p. 445–456, 474, 661, 662, Fig. 12.5)

$$
\begin{aligned}
&C_{\mathrm{coag}}(r_{\mathrm{i,wet}}, r_{\mathrm{j,wet}}) = \\
&4\pi \left(D_{\mathrm{i}} + D_{\mathrm{j}}\right)\left(r_{\mathrm{i,wet}} + r_{\mathrm{j,wet}}\right) \\
&\times\left[\frac{r_{\mathrm{i,wet}} + r_{\mathrm{j,wet}}}{r_{\mathrm{i,wet}} + r_{\mathrm{j,wet}} + (g_{\mathrm{i}}^2 + g_{\mathrm{j}}^2)^{1/2}}\right. \\
&\left.+\frac{4(D_{\mathrm{i}} + D_{\mathrm{j}})}{(\overline{v}_{\mathrm{i}}^2 + \overline{v}_{\mathrm{j}}^2)^{1/2}\,(r_{\mathrm{i,wet}} + r_{\mathrm{j,wet}})}\right]^{-1} \quad , \\
&(\mathrm{i},\mathrm{j}) = 1, \ldots, 3
\end{aligned}
\tag{B17}
$$

$$
\begin{aligned}
D_{\mathrm{i}} &= \frac{k_B T}{6\pi\,\mu_{\mathrm{air}} r_{\mathrm{i,wet}}} \\
&\quad\times\left(\frac{5 + 4\mathrm{Kn_i} + 6\mathrm{Kn_i}^2 + 18\mathrm{Kn_i}^3}{5 - \mathrm{Kn_i} + (8+\pi)\mathrm{Kn_i}^2}\right) \\
\mathrm{Kn_i} &= \frac{\lambda_{\mathrm{air}}}{r_{\mathrm{i,wet}}} \\
g_{\mathrm{i}} &= \frac{1}{6\,r_{\mathrm{i,wet}}\,l_{\mathrm{i}}}\left[(2\,r_{\mathrm{i,wet}} + l_{\mathrm{i}})^3\right. \\
&\quad\left.-(4\,r_{\mathrm{i,wet}}^2 + l_{\mathrm{i}}^2)^{3/2}\right] - 2\,r_{\mathrm{i,wet}} \\
\overline{v}_{\mathrm{i}} &= \sqrt{\frac{8k_B T}{\pi m_{\mathrm{i}}}} \\
l_{\mathrm{i}} &= \frac{8D_{\mathrm{i}}}{\pi\,\overline{v}_{\mathrm{i}}}
\end{aligned}
\tag{B18}
$$

B6. Humidity growth factor

(References: Birmili and Wiedensohler, pers. comm., 2004)

$$
\begin{aligned}
m_{\mathrm{i}} &= \frac{M_{\mathrm{i}}}{N_{\mathrm{i}}}\ , \quad \mathrm{i} = 1, \ldots, 3 \\
r_{\mathrm{i,dry}} &= \left(\frac{3m_{\mathrm{i}}}{4\pi\rho_p}\right)^{1/3} \\
r_{\mathrm{i,wet}} &= r_{\mathrm{i,dry}} \times \mathrm{GF}(r_{\mathrm{i,dry}}, \mathrm{RH}) \\
\mathrm{GF}(r_{\mathrm{i,dry}}, \mathrm{RH}) &= (1 - \mathrm{RH})^{-\Xi(r_{\mathrm{i,dry}})\,\mathrm{RH}} \\
\Xi(r_{\mathrm{i,dry}}) &= \eta_2 + \frac{\eta_1 - \eta_2}{\left(1 + \frac{r_{\mathrm{i,dry}}}{r_{0,\mathrm{dry}}}\right)^{\eta_3}}
\end{aligned}
\tag{B19}
$$

B7. Hydroxyl radical

(References: Liu et al., 2001, see references therein)

$$
\begin{aligned}
\overline{[\mathrm{OH}]} &= \overline{[\mathrm{OH}]}_{\mathrm{min}} + \overline{[\mathrm{OH}]}_{\mathrm{max}} \exp\left(-\frac{z}{H_{\mathrm{OH}}}\right) \\
&\quad\times\left[\sin\left(\frac{\pi}{24\times 3600}t\right)\right]^{n_{\mathrm{OH}}}
\end{aligned}
\tag{B20}
$$

B8. Large-scale subsidence

$$
\overline{w} = \begin{cases} \overline{w}_H\left[1 - \left(1 - \dfrac{z}{H_w}\right)^{n_w}\right], & z/H_w \le 1 \\ \overline{w}_H, & z/H_w > 1 \end{cases}
\tag{B21}
$$

Appendix C

Reynolds averaged equations

(References: André et al., 1976a,b, 1978, 1981)

C1. First-order moment equations

$$
\frac{\partial\overline{u}}{\partial t} + \overline{w}\frac{\partial\overline{u}}{\partial z} = -\frac{\partial\overline{w'u'}}{\partial z} + f_c(\overline{v} - v_g)
\tag{C1}
$$

$$
\frac{\partial\overline{v}}{\partial t} + \overline{w}\frac{\partial\overline{v}}{\partial z} = -\frac{\partial\overline{w'v'}}{\partial z} - f_c(\overline{u} - u_g)
\tag{C2}
$$

$$
\frac{\partial\overline{\theta}}{\partial t} + \overline{w}\frac{\partial\overline{\theta}}{\partial z} = -\frac{\partial\overline{w'\theta'}}{\partial z} + \left(\frac{\partial\overline{\theta}}{\partial t}\right)_{\mathrm{rad}}
\tag{C3}
$$

$$
\frac{\partial\overline{q}}{\partial t} + \overline{w}\frac{\partial\overline{q}}{\partial z} = -\frac{\partial\overline{w'q'}}{\partial z}
\tag{C4}
$$

$$
\begin{aligned}
&\frac{\partial\overline{\chi}_\alpha}{\partial t} + \overline{w}\frac{\partial\overline{\chi}_\alpha}{\partial z} = -\frac{\partial\overline{w'\chi'_\alpha}}{\partial z} + \overline{R}_\alpha + \overline{Q}_\alpha\ , \\
&\qquad\overline{R}_\alpha = \sum_{\mathrm{m}=1}^{\mathrm{N}}\sum_{\mathrm{n}=\mathrm{m}}^{\mathrm{N}} \overline{k}_{\mathrm{mn}}^{\alpha}\left(\overline{\chi}_{\mathrm{m}}\overline{\chi}_{\mathrm{n}} + \overline{\chi'_{\mathrm{m}}\chi'_{\mathrm{n}}}\right)\ , \\
&\qquad\alpha = 1, \ldots, \mathrm{N}
\end{aligned}
\tag{C5}
$$

C2. Second-order moment equations

C2.1 The six velocity correlations ($\overline{u'u'}$, $\overline{u'v'}$, $\overline{u'w'}$, $\overline{v'v'}$, $\overline{v'w'}$, $\overline{w'w'}$)

$$
\begin{aligned}
&\frac{\partial\overline{u'_{\mathrm{i}}u'_{\mathrm{j}}}}{\partial t} + \overline{w}\frac{\partial\overline{u'_{\mathrm{i}}u'_{\mathrm{j}}}}{\partial z} = \\
&\quad -\frac{\partial\overline{u'_{\mathrm{i}}u'_{\mathrm{j}}w'}}{\partial z} - \left(\overline{u'_{\mathrm{i}}w'}\frac{\partial\overline{u}_{\mathrm{j}}}{\partial z} + \overline{u'_{\mathrm{j}}w'}\frac{\partial\overline{u}_{\mathrm{i}}}{\partial z}\right) \\
&\quad + \beta_{\mathrm{buo}}\left(\delta_{3\mathrm{j}}\overline{u'_{\mathrm{i}}\theta'_v} + \delta_{3\mathrm{i}}\overline{u'_{\mathrm{j}}\theta'_v}\right) \\
&\quad + f_c\left(\epsilon_{\mathrm{ik3}}\overline{u'_{\mathrm{j}}u'_{\mathrm{k}}} + \epsilon_{\mathrm{jk3}}\overline{u'_{\mathrm{i}}u'_{\mathrm{k}}}\right) \\
&\quad - \frac{1}{\rho_0}\left(\overline{u'_{\mathrm{i}}\frac{\partial p'}{\partial x_{\mathrm{j}}} + u'_{\mathrm{j}}\frac{\partial p'}{\partial x_{\mathrm{i}}}}\right) - \frac{2}{3}\delta_{\mathrm{ij}}\varepsilon
\end{aligned}
\tag{C6}
$$

$$
\begin{aligned}
-\frac{1}{\rho_0}\left(\overline{u'_{\mathrm{i}}\frac{\partial p'}{\partial x_{\mathrm{j}}}+u'_{\mathrm{j}}\frac{\partial p'}{\partial x_{\mathrm{i}}}}\right) = & \\
& -C_4\frac{\varepsilon}{\overline{e}}\left(\overline{u'_{\mathrm{i}}u'_{\mathrm{j}}}-\frac{2}{3}\delta_{\mathrm{ij}}\overline{e}\right)-C_5\left(P_{\mathrm{ij}}-\frac{2}{3}\delta_{\mathrm{ij}}P\right) \\
P_{\mathrm{ij}} & =\beta_{\mathrm{buo}}\left(\delta_{3\mathrm{j}}\overline{u'_{\mathrm{i}}\theta'_v}+\delta_{3\mathrm{i}}\overline{u'_{\mathrm{j}}\theta'_v}\right) \\
& -\left(\overline{u'_{\mathrm{i}}w'}\frac{\partial\overline{u}_{\mathrm{j}}}{\partial z}+\overline{u'_{\mathrm{j}}w'}\frac{\partial\overline{u}_{\mathrm{i}}}{\partial z}\right) \\
P & =\beta_{\mathrm{buo}}\overline{w'\theta'_v}-\overline{u'w'}\frac{\partial\overline{u}}{\partial z}-\overline{v'w'}\frac{\partial\overline{v}}{\partial z}
\end{aligned}
\tag{C7}
$$

$$
\begin{aligned}
\overline{e} &= \frac{1}{2}\overline{u'_{\mathrm{k}}u'_{\mathrm{k}}} \\
\varepsilon &= C_1(L_{\mathrm{turb}})\frac{\overline{e}^{3/2}}{L_{\mathrm{turb}}}
\end{aligned}
\tag{C8}
$$

C2.2 Scalar fluxes ($\overline{u'_{\mathrm{i}}a'}$, $(u_{\mathrm{i}})=(u,v,w)$, $a=(\theta,q,\chi_\alpha)$, $\alpha=1,\ldots,\mathrm{N}$)

$$
\begin{aligned}
\frac{\partial\overline{u'_{\mathrm{i}}a'}}{\partial t}+\overline{w}\frac{\partial\overline{u'_{\mathrm{i}}a'}}{\partial z} = & \\
& -\frac{\partial\overline{u'_{\mathrm{i}}w'a'}}{\partial z}-\left(\overline{u'_{\mathrm{i}}w'}\frac{\partial\overline{a}}{\partial z}+\overline{w'a'}\frac{\partial\overline{u}_{\mathrm{i}}}{\partial z}\right) \\
& +\delta_{3\mathrm{i}}\beta_{\mathrm{buo}}\overline{\theta'_v a'}+\epsilon_{\mathrm{ik3}}f_c\overline{u'_{\mathrm{k}}a'}-\frac{1}{\rho_0}\overline{a'\frac{\partial p'}{\partial x_{\mathrm{i}}}} \\
& +\left.\frac{\partial\overline{u'_{\mathrm{i}}a'}}{\partial t}\right|_{\mathrm{reac}}
\end{aligned}
\tag{C9}
$$

$$
\begin{aligned}
-\frac{1}{\rho_0}\overline{a'\frac{\partial p'}{\partial x_{\mathrm{i}}}} &= -C_6\frac{\varepsilon}{\overline{e}}\overline{u'_{\mathrm{i}}a'}-C_7P_{\mathrm{ia}} \\
P_{\mathrm{ia}} &= \delta_{3\mathrm{i}}\beta_{\mathrm{buo}}\overline{\theta'_v a'}-\overline{w'a'}\frac{\partial\overline{u}_{\mathrm{i}}}{\partial z}
\end{aligned}
\tag{C10}
$$

The reaction term in the tracer flux equation ($a=\chi_\alpha$) follows from Eq. (C20), i.e.,

$$
\begin{aligned}
\left.\frac{\partial\overline{u'_{\mathrm{i}}\chi'_\alpha}}{\partial t}\right|_{\mathrm{reac}} &= \overline{R}_{u_{\mathrm{i}}\chi_\alpha} \\
=\sum_{\mathrm{m}=1}^{\mathrm{N}}\sum_{\mathrm{n}=\mathrm{m}}^{\mathrm{N}}\overline{k}^{\alpha}_{\mathrm{mn}}&\left(\overline{\chi}_{\mathrm{m}}\overline{u'_{\mathrm{i}}\chi'_{\mathrm{n}}}+\overline{\chi}_{\mathrm{n}}\overline{u'_{\mathrm{i}}\chi'_{\mathrm{m}}}+\overline{u'_{\mathrm{i}}\chi'_{\mathrm{m}}\chi'_{\mathrm{n}}}\right)
\end{aligned}
\tag{C11}
$$

C2.3 Scalar correlations ($\overline{a'b'}$, $(a,b)=(\theta,q,\chi_\alpha,\chi_\beta)$, $(\alpha,\beta)=1,\ldots,\mathrm{N}$)

$$
\begin{aligned}
\frac{\partial\overline{a'b'}}{\partial t}+\overline{w}\frac{\partial\overline{a'b'}}{\partial z} = & \\
& -\frac{\partial\overline{w'a'b'}}{\partial z}-\left(\overline{w'a'}\frac{\partial\overline{b}}{\partial z}+\overline{w'b'}\frac{\partial\overline{a}}{\partial z}\right) \\
& -\varepsilon_{ab}-\varepsilon_R+\left.\frac{\partial\overline{a'b'}}{\partial t}\right|_{\mathrm{reac}}
\end{aligned}
\tag{C12}
$$

$$
\varepsilon_{ab} = C_2\frac{\varepsilon}{\overline{e}}\overline{a'b'} \tag{C13}
$$

The radiative destruction rate ε_R appears only in the temperature variance equation. It is parameterised according to Stull (1997, p. 132, see references therein):

$$
\begin{aligned}
\varepsilon_R &= c_R\overline{\theta'\theta'} \\
c_R &\approx \left(0.036\frac{\mathrm{m}}{\mathrm{s}}\right)\frac{\varepsilon}{\overline{e}^{3/2}}\,, \quad c_R=\left[\frac{1}{\mathrm{s}}\right]
\end{aligned}
\tag{C14}
$$

The interaction term between passive and reactive scalar ($a=(\theta,q)$, $b=\chi_\alpha$) follows from Eq. (C20), i.e.,

$$
\begin{aligned}
\left.\frac{\partial\overline{a'\chi'_\alpha}}{\partial t}\right|_{\mathrm{reac}} &= \overline{R}_{a\chi_\alpha} \\
=\sum_{\mathrm{m}=1}^{\mathrm{N}}\sum_{\mathrm{n}=\mathrm{m}}^{\mathrm{N}}\overline{k}^{\alpha}_{\mathrm{mn}}&\left(\overline{\chi}_{\mathrm{m}}\overline{a'\chi'_{\mathrm{n}}}+\overline{\chi}_{\mathrm{n}}\overline{a'\chi'_{\mathrm{m}}}+\overline{a'\chi'_{\mathrm{m}}\chi'_{\mathrm{n}}}\right)
\end{aligned}
\tag{C15}
$$

The interaction between two reactive scalars ($(a,b)=(\chi_\alpha,\chi_\beta)$), results from Eq. (C25), i.e.,

$$
\left.\frac{\partial\overline{\chi'_\alpha\chi'_\beta}}{\partial t}\right|_{\mathrm{reac}} = \overline{R}_{\chi_\alpha\chi_\beta}\,. \tag{C16}
$$

C2.4 Interaction of a reactive tracer χ_α with a nonreactive scalar $A=(u_{\mathrm{i}},\theta,q)$

$$
\begin{aligned}
\left.\frac{\partial\chi_\alpha}{\partial t}\right|_{\mathrm{reac}} &= \sum_{\mathrm{m}=1}^{\mathrm{N}}\sum_{\mathrm{n}=\mathrm{m}}^{\mathrm{N}}k^{\alpha}_{\mathrm{mn}}\chi_{\mathrm{m}}\chi_{\mathrm{n}} && |\times A \\
+\left.\frac{\partial A}{\partial t}\right|_{\mathrm{reac}} &= 0 && |\times\chi_\alpha \\
\hline
\left.\frac{\partial A\chi_\alpha}{\partial t}\right|_{\mathrm{reac}} &= \sum_{\mathrm{m}=1}^{\mathrm{N}}\sum_{\mathrm{n}=\mathrm{m}}^{\mathrm{N}}k^{\alpha}_{\mathrm{mn}}A\chi_{\mathrm{m}}\chi_{\mathrm{n}} && |\,\overline{(\ )}
\end{aligned}
\tag{C17}
$$

$$
\begin{aligned}
\frac{\partial}{\partial t}&\left(\overline{A}\overline{\chi}_\alpha+\overline{A'\chi'_\alpha}\right)\Big|_{\mathrm{reac}} = \\
&\sum_{\mathrm{m}=1}^{\mathrm{N}}\sum_{\mathrm{n}=\mathrm{m}}^{\mathrm{N}}\overline{k}^{\alpha}_{\mathrm{mn}}\overline{A}\left(\overline{\chi}_{\mathrm{m}}\overline{\chi}_{\mathrm{n}}+\overline{\chi'_{\mathrm{m}}\chi'_{\mathrm{n}}}\right) \\
+&\sum_{\mathrm{m}=1}^{\mathrm{N}}\sum_{\mathrm{n}=\mathrm{m}}^{\mathrm{N}}\overline{k}^{\alpha}_{\mathrm{mn}}\left(\overline{\chi}_{\mathrm{m}}\overline{A'\chi'_{\mathrm{n}}}+\overline{\chi}_{\mathrm{n}}\overline{A'\chi'_{\mathrm{m}}}+\overline{A'\chi'_{\mathrm{m}}\chi'_{\mathrm{n}}}\right)
\end{aligned}
\tag{C18}
$$

$$
\begin{aligned}
\left.\frac{\partial\overline{\chi}_\alpha}{\partial t}\right|_{\mathrm{reac}} &= \sum_{\mathrm{m}=1}^{\mathrm{N}}\sum_{\mathrm{n}=\mathrm{m}}^{\mathrm{N}}\overline{k}^{\alpha}_{\mathrm{mn}}\left(\overline{\chi}_{\mathrm{m}}\overline{\chi}_{\mathrm{n}}+\overline{\chi'_{\mathrm{m}}\chi'_{\mathrm{n}}}\right) && |\times\overline{A} \\
+\frac{\partial\overline{A}}{\partial t} &= 0 && |\times\overline{\chi}_\alpha \\
\hline
\left.\frac{\partial\overline{A}\overline{\chi}_\alpha}{\partial t}\right|_{\mathrm{reac}} &= \sum_{\mathrm{m}=1}^{\mathrm{N}}\sum_{\mathrm{n}=\mathrm{m}}^{\mathrm{N}}\overline{k}^{\alpha}_{\mathrm{mn}}\overline{A}\left(\overline{\chi}_{\mathrm{m}}\overline{\chi}_{\mathrm{n}}+\overline{\chi'_{\mathrm{m}}\chi'_{\mathrm{n}}}\right) && |\,\overline{(\ )}
\end{aligned}
\tag{C19}
$$

Subtracting Eq. (C19) from Eq. (C18):

$$\overline{R}_{A\chi_\alpha} = \left.\frac{\partial \overline{A'\chi'_\alpha}}{\partial t}\right|_{\text{reac}} = \sum_{m=1}^{N}\sum_{n=m}^{N} \overline{k}^{\alpha}_{mn}\left(\overline{\chi}_m \overline{A'\chi'_n} + \overline{\chi}_n \overline{A'\chi'_m} + \overline{A'\chi'_m\chi'_n}\right) \quad \text{(C20)}$$

C2.5 Interaction of reactive tracers χ_α and χ_β

$$\left.\frac{\partial \chi_\alpha}{\partial t}\right|_{\text{reac}} = \sum_{m=1}^{N}\sum_{n=m}^{N} k^{\alpha}_{mn}\chi_m\chi_n \quad |\times \chi_\beta \quad \text{(C21)}$$

$$+\left.\frac{\partial \chi_\beta}{\partial t}\right|_{\text{reac}} = \sum_{m=1}^{N}\sum_{n=m}^{N} k^{\beta}_{mn}\chi_m\chi_n \quad |\times \chi_\alpha$$

$$\left.\frac{\partial \chi_\alpha\chi_\beta}{\partial t}\right|_{\text{reac}} = \sum_{m=1}^{N}\sum_{n=m}^{N} k^{\alpha}_{mn}\chi_\beta\chi_m\chi_n + \sum_{m=1}^{N}\sum_{n=m}^{N} k^{\beta}_{mn}\chi_\alpha\chi_m\chi_n \quad |\overline{(\ )}$$

$$\left.\frac{\partial \overline{\chi_\alpha\chi_\beta}}{\partial t}\right|_{\text{reac}} = \sum_{m=1}^{N}\sum_{n=m}^{N} \overline{k}^{\alpha}_{mn}\overline{\chi_\beta\chi_m\chi_n} + \sum_{m=1}^{N}\sum_{n=m}^{N} \overline{k}^{\beta}_{mn}\overline{\chi_\alpha\chi_m\chi_n}$$

Expanding the last equation using:

$$\begin{aligned}
\overline{ABC} &= \overline{(\overline{A}+A')(\overline{B}+B')(\overline{C}+C')} \\
&= \overline{A}\,\overline{B}\,\overline{C} + \overline{A}\,\overline{B'C'} + \overline{B}\,\overline{A'C'} + \overline{C}\,\overline{A'B'} + \overline{A'B'C'} \\
\overline{\chi_\alpha\chi_m\chi_n} &= \overline{\chi}_\alpha\overline{\chi}_m\overline{\chi}_n + \overline{\chi}_\alpha\overline{\chi'_m\chi'_n} + \overline{\chi}_m\overline{\chi'_\alpha\chi'_n} + \overline{\chi}_n\overline{\chi'_\alpha\chi'_m} + \overline{\chi'_\alpha\chi'_m\chi'_n} \\
\overline{\chi_\beta\chi_m\chi_n} &= \overline{\chi}_\beta\overline{\chi}_m\overline{\chi}_n + \overline{\chi}_\beta\overline{\chi'_m\chi'_n} + \overline{\chi}_m\overline{\chi'_\beta\chi'_n} + \overline{\chi}_n\overline{\chi'_\beta\chi'_m} + \overline{\chi'_\beta\chi'_m\chi'_n}
\end{aligned} \quad \text{(C22)}$$

$$\begin{aligned}
&\left.\frac{\partial}{\partial t}\left(\overline{\chi}_\alpha\overline{\chi}_\beta + \overline{\chi'_\alpha\chi'_\beta}\right)\right|_{\text{reac}} \\
&= \sum_{m=1}^{N}\sum_{n=m}^{N} \overline{k}^{\alpha}_{mn}\left(\overline{\chi}_\beta\overline{\chi}_m\overline{\chi}_n + \overline{\chi}_\beta\overline{\chi'_m\chi'_n} + \overline{\chi}_m\overline{\chi'_\beta\chi'_n} + \overline{\chi}_n\overline{\chi'_\beta\chi'_m} + \overline{\chi'_\beta\chi'_m\chi'_n}\right) \\
&+ \sum_{m=1}^{N}\sum_{n=m}^{N} \overline{k}^{\beta}_{mn}\left(\overline{\chi}_\alpha\overline{\chi}_m\overline{\chi}_n + \overline{\chi}_\alpha\overline{\chi'_m\chi'_n} + \overline{\chi}_m\overline{\chi'_\alpha\chi'_n} + \overline{\chi}_n\overline{\chi'_\alpha\chi'_m} + \overline{\chi'_\alpha\chi'_m\chi'_n}\right)
\end{aligned} \quad \text{(C23)}$$

Contribution of the mean values to the total change rate:

$$\left.\frac{\partial \overline{\chi}_\alpha}{\partial t}\right|_{\text{reac}} = \sum_{m=1}^{N}\sum_{n=m}^{N} \overline{k}^{\alpha}_{mn}\left(\overline{\chi}_m\overline{\chi}_n + \overline{\chi'_m\chi'_n}\right) \quad |\times \overline{\chi}_\beta \quad \text{(C24)}$$

$$+\left.\frac{\partial \overline{\chi}_\beta}{\partial t}\right|_{\text{reac}} = \sum_{m=1}^{N}\sum_{n=m}^{N} \overline{k}^{\beta}_{mn}\left(\overline{\chi}_m\overline{\chi}_n + \overline{\chi'_m\chi'_n}\right) \quad |\times \overline{\chi}_\alpha$$

$$\left.\frac{\partial \overline{\chi}_\alpha\overline{\chi}_\beta}{\partial t}\right|_{\text{reac}} = \sum_{m=1}^{N}\sum_{n=m}^{N} \overline{k}^{\alpha}_{mn}\overline{\chi}_\beta\left(\overline{\chi}_m\overline{\chi}_n + \overline{\chi'_m\chi'_n}\right) + \sum_{m=1}^{N}\sum_{n=m}^{N} \overline{k}^{\beta}_{mn}\overline{\chi}_\alpha\left(\overline{\chi}_m\overline{\chi}_n + \overline{\chi'_m\chi'_n}\right)$$

Subtraction of Eq. (C24) from Eq. (C23) to extract the contribution of the tracer co-variance to the total change rate:

$$\begin{aligned}
\overline{R}_{\chi_\alpha\chi_\beta} &= \left.\frac{\partial \overline{\chi'_\alpha\chi'_\beta}}{\partial t}\right|_{\text{reac}} \\
&= \sum_{m=1}^{N}\sum_{n=m}^{N} \overline{k}^{\alpha}_{mn}\left(\overline{\chi}_m\overline{\chi'_\beta\chi'_n} + \overline{\chi}_n\overline{\chi'_\beta\chi'_m} + \overline{\chi'_\beta\chi'_m\chi'_n}\right) \\
&+ \sum_{m=1}^{N}\sum_{n=m}^{N} \overline{k}^{\beta}_{mn}\left(\overline{\chi}_m\overline{\chi'_\alpha\chi'_n} + \overline{\chi}_n\overline{\chi'_\alpha\chi'_m} + \overline{\chi'_\alpha\chi'_m\chi'_n}\right)
\end{aligned} \quad \text{(C25)}$$

C3. Third-order moment equations

C3.1 Turbulent transport of momentum fluxes ($\overline{u'u'w'}$, $\overline{u'v'w'}$, $\overline{u'w'w'}$, $\overline{v'v'w'}$, $\overline{v'w'w'}$, $\overline{w'w'w'}$)

$$\begin{aligned}
&\frac{\partial \overline{u'_i u'_j w'}}{\partial t} + \overline{w}\frac{\partial \overline{u'_i u'_j w'}}{\partial z} = \\
&\quad - \left(\overline{u'_i w' w'}\frac{\partial \overline{u}_j}{\partial z} + \overline{u'_j w' w'}\frac{\partial \overline{u}_i}{\partial z}\right) \\
&\quad - \overline{w'w'}\frac{\partial \overline{u'_i u'_j}}{\partial z} \\
&\quad - \left(\overline{u'_i w'}\frac{\partial \overline{u'_j w'}}{\partial z} + \overline{u'_j w'}\frac{\partial \overline{u'_i w'}}{\partial z}\right) \\
&\quad + \beta_{buo}\left(\overline{u'_i u'_j \theta'_v} + \delta_{3j}\overline{u'_i w'\theta'_v} + \delta_{3i}\overline{u'_j w'\theta'_v}\right) \\
&\quad - \frac{1}{\rho_0}\left(\overline{u'_i}\frac{\partial \overline{p'}}{\partial z} + \overline{u'_i w'}\frac{\partial \overline{p'}}{\partial x_j} + \overline{u'_j w'}\frac{\partial \overline{p'}}{\partial x_i}\right) \\
&\quad - \varepsilon_{uuu}
\end{aligned} \quad \text{(C26)}$$

$$-\frac{1}{\rho_0}\left(\overline{u'_i u'_j}\frac{\partial \overline{p'}}{\partial z} + \overline{u'_i w'}\frac{\partial \overline{p'}}{\partial x_j} + \overline{u'_j w'}\frac{\partial \overline{p'}}{\partial x_i}\right) = \underbrace{P_{\text{relax}}}_{\text{Andre et al., 1978}} + \underbrace{P_{\text{rapid}}}_{\text{Andre et al., 1981}} \quad \text{(C27)}$$

$$P_{\text{relax}} = -C_8 \frac{\varepsilon}{e} \overline{u_\text{i}' u_\text{j}' w'}$$

$$P_{\text{rapid}} = -C_{11} \beta_{\text{buo}} \left(\overline{u_\text{i}' u_\text{j}' \theta_v'} + \delta_{3\text{j}} \overline{u_\text{i}' w' \theta_v'} + \delta_{3\text{i}} \overline{u_\text{j}' w' \theta_v'} \right)$$

$$\varepsilon_{uuu} = 0$$

$$\left| \overline{u_\text{i}' u_\text{j}' w'} \right| \le \text{Min} \left\{ \begin{array}{l} \sqrt{\overline{u_\text{i}'^2} \left(\overline{u_\text{j}'^2}\ \overline{w'^2} + \overline{u_\text{j}' w'}^2 \right)} \\ \sqrt{\overline{u_\text{j}'^2} \left(\overline{u_\text{i}'^2}\ \overline{w'^2} + \overline{u_\text{i}' w'}^2 \right)} \\ \sqrt{\overline{w'^2} \left(\overline{u_\text{i}'^2}\ \overline{u_\text{j}'^2} + \overline{u_\text{i}' u_\text{j}'}^2 \right)} \end{array} \right\} \tag{C28}$$

C3.2 Turbulent transport of scalar fluxes ("fluxes of fluxes")
($\overline{u_\text{i}' u_\text{j}' a'}$, $a=(\theta, q, \chi_\alpha)$, $\alpha=1, \ldots, \text{N}$)

$$\begin{aligned} &\frac{\partial \overline{u_\text{i}' u_\text{j}' a'}}{\partial t} + \overline{w} \frac{\partial \overline{u_\text{i}' u_\text{j}' a'}}{\partial z} = \\ &\quad - \left(\overline{u_\text{i}' u_\text{j}' w'} \frac{\partial \overline{a}}{\partial z} + \overline{u_\text{i}' w' a'} \frac{\partial \overline{u}_\text{j}}{\partial z} + \overline{u_\text{j}' w' a'} \frac{\partial \overline{u}_\text{i}}{\partial z} \right) \\ &\quad - \left(\overline{w' a'} \frac{\partial \overline{u_\text{i}' u_\text{j}'}}{\partial z} + \overline{u_\text{i}' w'} \frac{\partial \overline{u_\text{j}' a'}}{\partial z} + \overline{u_\text{j}' w'} \frac{\partial \overline{u_\text{i}' a'}}{\partial z} \right) \\ &\quad + \beta_{\text{buo}} \left(\delta_{3\text{j}} \overline{u_\text{i}' \theta_v' a'} + \delta_{3\text{i}} \overline{u_\text{j}' \theta_v' a'} \right) \\ &\quad - \frac{1}{\rho_0} \left(\overline{u_\text{i}' a' \frac{\partial p'}{\partial x_\text{j}}} + \overline{u_\text{j}' a' \frac{\partial p'}{\partial x_\text{i}}} \right) \\ &\quad - \varepsilon_{uua} \end{aligned} \tag{C29}$$

$$\begin{aligned} &-\frac{1}{\rho_0} \left(\overline{u_\text{i}' a' \frac{\partial p'}{\partial x_\text{j}}} + \overline{u_\text{j}' a' \frac{\partial p'}{\partial x_\text{i}}} \right) \\ &\quad = \underbrace{P_{\text{relax}} + P_{\text{diagonal}}}_{\text{Andre et al., 1978}} + \underbrace{P_{\text{rapid}}}_{\text{Andre et al., 1981}} \end{aligned} \tag{C30}$$

$$\begin{aligned} P_{\text{relax}} &= -C_8 \frac{\varepsilon}{e} \left(\overline{u_\text{i}' u_\text{j}' a'} - \frac{1}{3} \delta_{\text{ij}} \overline{u_\text{k}' u_\text{k}' a'} \right) \\ P_{\text{diagonal}} &= \delta_{\text{ij}} C_9 \frac{\varepsilon}{e} \overline{u_\text{k}' u_\text{k}' a'} \\ P_{\text{rapid}} &= -C_{11} \beta_{\text{buo}} \big(\delta_{3\text{j}} \overline{u_\text{i}' \theta_v' a'} \\ &\quad + \delta_{3\text{i}} \overline{u_\text{j}' \theta_v' a'} - \frac{2}{3} \delta_{\text{ij}} \overline{w' \theta_v' a'} \big) \\ \varepsilon_{uua} &= \delta_{\text{ij}} C_{10} \frac{\varepsilon}{e} \frac{\overline{u_\text{k}' u_\text{k}' a'}}{3} \end{aligned}$$

$$\left| \overline{u_\text{i}' u_\text{j}' a'} \right| \le \text{Min} \left\{ \begin{array}{l} \sqrt{\overline{u_\text{i}'^2} \left(\overline{u_\text{j}'^2}\ \overline{a'^2} + \overline{u_\text{j}' a'}^2 \right)} \\ \sqrt{\overline{u_\text{j}'^2} \left(\overline{u_\text{i}'^2}\ \overline{a'^2} + \overline{u_\text{i}' a'}^2 \right)} \\ \sqrt{\overline{a'^2} \left(\overline{u_\text{i}'^2}\ \overline{u_\text{j}'^2} + \overline{u_\text{i}' u_\text{j}'}^2 \right)} \end{array} \right\} \tag{C31}$$

C3.3 Turbulent transport of scalar correlations ("fluxes of correlations")
($\overline{u_\text{i}' a' b'}$, $(a, b)=(\theta, q, \chi_\alpha, \chi_\beta)$, $(\alpha, \beta)=1, \ldots, \text{N}$)

$$\begin{aligned} &\frac{\partial \overline{u_\text{i}' a' b'}}{\partial t} + \overline{w} \frac{\partial \overline{u_\text{i}' a' b'}}{\partial z} = \\ &\quad - \left(\overline{w' a' b'} \frac{\partial \overline{u}_\text{i}}{\partial z} + \overline{u_\text{i}' w' a'} \frac{\partial \overline{b}}{\partial z} + \overline{u_\text{i}' w' b'} \frac{\partial \overline{a}}{\partial z} \right) \\ &\quad - \left(\overline{u_\text{i}' w'} \frac{\partial \overline{a' b'}}{\partial z} + \overline{w' a'} \frac{\partial \overline{u_\text{i}' b'}}{\partial z} + \overline{w' b'} \frac{\partial \overline{u_\text{i}' a'}}{\partial z} \right) \\ &\quad + \delta_{3\text{i}} \beta_{\text{buo}} \overline{\theta_v' a' b'} - \frac{1}{\rho_0} \left(\overline{a' b' \frac{\partial p'}{\partial x_\text{i}}} \right) - \varepsilon_{uab} \end{aligned} \tag{C32}$$

$$-\frac{1}{\rho_0} \left(\overline{a' b' \frac{\partial p'}{\partial x_\text{i}}} \right) = \underbrace{P_{\text{relax}}}_{\text{Andre et al., 1978}} + \underbrace{P_{\text{rapid}}}_{\text{Andre et al., 1981}} \tag{C33}$$

$$\begin{aligned} P_{\text{relax}} &= -C_8 \frac{\varepsilon}{e} \overline{u_\text{i}' a' b'} \\ P_{\text{rapid}} &= -\delta_{3\text{i}} C_{11} \beta_{\text{buo}} \overline{a' b' \theta_v'} \\ \varepsilon_{uab} &= 0 \end{aligned}$$

$$\left| \overline{u_\text{i}' a' b'} \right| \le \text{Min} \left\{ \begin{array}{l} \sqrt{\overline{u_\text{i}'^2} \left(\overline{a'^2}\ \overline{b'^2} + \overline{a' b'}^2 \right)} \\ \sqrt{\overline{a'^2} \left(\overline{u_\text{i}'^2}\ \overline{b'^2} + \overline{u_\text{i}' b'}^2 \right)} \\ \sqrt{\overline{b'^2} \left(\overline{u_\text{i}'^2}\ \overline{a'^2} + \overline{u_\text{i}' a'}^2 \right)} \end{array} \right\} \tag{C34}$$

C3.4 Turbulent transport of scalar correlations
($\overline{a' b' c'}$, $(a, b, c)=(\theta, q, \chi_\alpha, \chi_\beta, \chi_\gamma)$, $(\alpha, \beta, \gamma)=1, \ldots, \text{N}$)

$$\begin{aligned} &\frac{\partial \overline{a' b' c'}}{\partial t} + \overline{w} \frac{\partial \overline{a' b' c'}}{\partial z} = \\ &\quad - \left(\overline{w' a' b'} \frac{\partial \overline{c}}{\partial z} + \overline{w' a' c'} \frac{\partial \overline{b}}{\partial z} + \overline{w' b' c'} \frac{\partial \overline{a}}{\partial z} \right) \\ &\quad - \left(\overline{w' a'} \frac{\partial \overline{b' c'}}{\partial z} + \overline{w' b'} \frac{\partial \overline{a' c'}}{\partial z} + \overline{w' c'} \frac{\partial \overline{a' b'}}{\partial z} \right) \\ &\quad - \varepsilon_{abc} \end{aligned} \tag{C35}$$

$$\varepsilon_{abc} = C_{10} \frac{\varepsilon}{e} \overline{a' b' c'} \tag{C36}$$

$$\left| \overline{a' b' c'} \right| \le \text{Min} \left\{ \begin{array}{l} \sqrt{\overline{a'^2} \left(\overline{b'^2}\ \overline{c'^2} + \overline{b' c'}^2 \right)} \\ \sqrt{\overline{b'^2} \left(\overline{a'^2}\ \overline{c'^2} + \overline{a' c'}^2 \right)} \\ \sqrt{\overline{c'^2} \left(\overline{a'^2}\ \overline{b'^2} + \overline{a' b'}^2 \right)} \end{array} \right\} \tag{C37}$$

C4. Buoyancy fluxes

$$\begin{aligned}
\theta_v &= \theta\,(1+0.61q) = \theta + C_{T_0}\,q \\
C_{T_0} &\approx 0.61\,T_0 \\
\overline{a'\theta'_v} &= \overline{a'\theta'} + C_{T_0}\,\overline{a'q'} \\
\overline{a'b'\theta'_v} &= \overline{a'b'\theta'} + C_{T_0}\,\overline{a'b'q'}
\end{aligned} \tag{C38}$$

Appendix D

Initial and boundary conditions

D1. First-order moments

D1.1 Initial conditions

(References: Liu et al., 2001, for chemical variables)

Initial profiles of meteorological variables, i.e.,

$$\overline{u}(z,t_0)\ , \quad \overline{v}(z,t_0)\ , \quad \overline{\theta}(z,t_0)\ , \quad \overline{q}(z,t_0) \tag{D1}$$

can be either derived from observations or synthetically prescribed. The geostrophic wind components u_g, v_g and the large-scale subsidence velocity $\overline{w}_H$ are prescribed.
The first-order moments of physicochemical variables are initialised as follows:

$$\begin{aligned}
\overline{[\mathrm{OH}]}(z,t_0) &= \overline{[\mathrm{OH}]}_{\min} + \overline{[\mathrm{OH}]}_{\max} \exp\left(-\frac{z}{H_{\mathrm{OH}}}\right) \\
&\quad \times \left[\sin\left(\frac{\pi}{24\times 3600}t_0\right)\right]^{n_{\mathrm{OH}}} \\
\overline{[\mathrm{SO_2}]}(z,t_0) &= \overline{[\mathrm{SO_2}]}_{\mathrm{sfc}} \exp\left(-\frac{z}{H_{\mathrm{SO_2}}}\right) \\
\overline{[\mathrm{NH_3}]}_{\mathrm{tot}}(z,t_0) &= \overline{[\mathrm{NH_3}]}_{\mathrm{tot,sfc}} \exp\left(-\frac{z}{H_{\mathrm{NH_3}}}\right) \\
\overline{[\mathrm{H_2SO_4}]}(z,t_0) &= \overline{[\mathrm{H_2SO_4}]}_{\min} + \overline{[\mathrm{H_2SO_4}]}_{\max} \\
&\quad \times \exp\left(-\frac{z}{H_{\mathrm{H_2SO_4}}}\right) \\
&\quad \times \sin\left(\frac{\pi}{24\times 3600}t_0\right) \\
\overline{N}_{\mathrm{i}}(z,t_0) &= \overline{N}_{\mathrm{i,sfc}} \exp\left(-\frac{z}{H_{N_{\mathrm{i}}}}\right)\ ,\ \mathrm{i}=1,\ldots,3 \\
\overline{M}_{\mathrm{i}}(z,t_0) &= \overline{M}_{\mathrm{i,sfc}} \exp\left(-\frac{z}{H_{M_{\mathrm{i}}}}\right)\ ,\ \mathrm{i}=1,\ldots,3
\end{aligned} \tag{D2}$$

D1.2 Lower boundary conditions ("constant-flux layer" hypothesis)

$$\begin{aligned}
\left(\overline{u'w'}\right)_{z_s} &\approx \left(\overline{u'w'}\right)_{z_p} \approx -K_m \left.\frac{\partial\overline{u}}{\partial z}\right|_{z_p} \\
\left(\overline{v'w'}\right)_{z_s} &\approx \left(\overline{v'w'}\right)_{z_p} \approx -K_m \left.\frac{\partial\overline{v}}{\partial z}\right|_{z_p} \\
\left(\overline{w'\theta'}\right)_{z_s} &\approx \left(\overline{w'\theta'}\right)_{z_p} \approx -K_h \left.\frac{\partial\overline{\theta}}{\partial z}\right|_{z_p} \\
\left(\overline{w'q'}\right)_{z_s} &\approx \left(\overline{w'q'}\right)_{z_p} \approx -K_h \left.\frac{\partial\overline{q}}{\partial z}\right|_{z_p} \\
\left(\overline{w'\chi'_\alpha}\right)_{z_s} &\approx \left(\overline{w'\chi'_\alpha}\right)_{z_p} \approx -K_h \left.\frac{\partial\overline{\chi_\alpha}}{\partial z}\right|_{z_p}\ ,\ \alpha=1,\ldots,\mathrm{N}
\end{aligned} \tag{D3}$$

$$\begin{aligned}
K_m &= \frac{c_m u_\star z}{\phi_m(\zeta)} \\
K_h &= \frac{c_h u_\star z}{\phi_h(\zeta)}
\end{aligned} \tag{D4}$$

$$\begin{aligned}
\left.\frac{\partial\overline{u}}{\partial z}\right|_{z_p} &= \left[\frac{\overline{u}(z_{\mathrm{k}=1})}{\overline{U}(z_{\mathrm{k}=1})}\right]\frac{u_\star}{c_m z_p}\phi_m(\zeta) \\
\left.\frac{\partial\overline{v}}{\partial z}\right|_{z_p} &= \left[\frac{\overline{v}(z_{\mathrm{k}=1})}{\overline{U}(z_{\mathrm{k}=1})}\right]\frac{u_\star}{c_m z_p}\phi_m(\zeta) \\
\left.\frac{\partial\overline{\theta}}{\partial z}\right|_{z_p} &= \frac{\theta_\star}{c_h z_p}\phi_h(\zeta) \\
\left.\frac{\partial\overline{q}}{\partial z}\right|_{z_p} &= \frac{q_\star}{c_h z_p}\phi_h(\zeta) \\
\left.\frac{\partial\overline{\chi}_\alpha}{\partial z}\right|_{z_p} &= \frac{\chi_{\alpha\star}}{c_h z_p}\phi_h(\zeta)\ ,\ \alpha=1,\ldots,\mathrm{N}
\end{aligned} \tag{D5}$$

D1.3 Similarity functions

(References: Dyer and Hicks, 1970)

$$\begin{aligned}
\phi_m &= \begin{cases} (1-16\zeta)^{-1/4}\ , & \zeta<0 \\ (1+5\zeta)\ , & \zeta\geq 0 \end{cases} \\
\phi_h &= \begin{cases} (1-16\zeta)^{-1/2}\ , & \zeta<0 \\ (1+5\zeta)\ , & \zeta\geq 0 \end{cases}
\end{aligned} \tag{D6}$$

D1.4 Skin properties

(References: Holtslag, 1987, p. 55–56, 70)

$$
\begin{aligned}
\theta_\star &= -\frac{\left(\overline{w'\theta'}\right)_{z_s}}{u_\star} \\
&= \kappa \Delta\overline{\theta} \left[\ln\left(\frac{z_p}{z_s}\right) - \Psi_H\left(\frac{z_p}{L}\right) + \Psi_H\left(\frac{z_s}{L}\right) \right]^{-1} \\
q_\star &= -\frac{\left(\overline{w'q'}\right)_{z_s}}{u_\star} \\
&= \kappa \Delta\overline{q} \left[\ln\left(\frac{z_p}{z_s}\right) - \Psi_H\left(\frac{z_p}{L}\right) + \Psi_H\left(\frac{z_s}{L}\right) \right]^{-1} \\
\Delta\overline{\theta} &= \overline{\theta}(z_p) - \overline{\theta}(z_s) \\
\Delta\overline{q} &= \overline{q}(z_p) - \overline{q}(z_s)
\end{aligned}
\tag{D7}
$$

$$
\begin{aligned}
\overline{\theta}(z_s) &= \overline{\theta}(z_p) \\
&\quad - \frac{\theta_\star}{\kappa} \left[\ln\left(\frac{z_p}{z_s}\right) - \Psi_H\left(\frac{z_p}{L}\right) + \Psi_H\left(\frac{z_s}{L}\right) \right]
\end{aligned}
\tag{D8}
$$

$$
\overline{q}(z_s) = \overline{q}(z_p) - \frac{q_\star}{\theta_\star}\left(\overline{\theta}(z_p) - \overline{\theta}(z_s)\right)
$$

$$
\begin{aligned}
\frac{\Delta\overline{\theta}}{\overline{\theta}} &= \frac{\Delta\overline{T}}{\overline{T}} + \frac{g}{c_p}\frac{\Delta z}{\overline{T}} \\
\Delta\overline{T} &\approx \Delta\overline{\theta} - \Gamma_d(z_p - z_s)
\end{aligned}
\tag{D9}
$$

D1.5 Stability functions

(References: Paulson, 1970, unstable case; Carson and Richards, 1978, stable case; Holtslag, 1987, p. 56, 71, 101)

$$
\Psi_M = \begin{cases} 2\ln\left(\frac{1+x}{2}\right) + \ln\left(\frac{1+x^2}{2}\right) & \\ -2\arctan(x) + \frac{\pi}{2}\,, & L < 0 \\ -\left[a\zeta + b\left(\zeta - \frac{c}{d}\right)\exp(-d\zeta) + \frac{bc}{d}\right]\,, & L > 0 \end{cases}
\tag{D10}
$$

$$
\Psi_H = \begin{cases} 2\ln\left(\frac{1+x^2}{2}\right)\,, & L < 0 \\ \Psi_M\,, & L > 0 \end{cases}
$$

$$
x = (1-16\zeta)^{1/4}\,, \quad a{=}0.7,\, b{=}0.75,\, c{=}5,\, d{=}0.35
$$

D1.6 Upper boundary conditions

$$
\left.\frac{\partial\overline{u}}{\partial z}\right|_{\text{top}} = 0\,,\ \left.\frac{\partial\overline{v}}{\partial z}\right|_{\text{top}} = 0\,,\ \left.\frac{\partial\overline{\theta}}{\partial z}\right|_{\text{top}} = 0\,,\ \left.\frac{\partial\overline{q}}{\partial z}\right|_{\text{top}} = 0
\tag{D11}
$$

$$
\left.\frac{\partial\overline{\chi}_\alpha}{\partial z}\right|_{\text{top}} = 0\,, \quad \alpha = 1, \ldots, \mathrm{N}
$$

D2. Second-order moments

D2.1 Initial conditions

At the starting time, second-order moments are set to zero.

D2.2 Lower boundary conditions

(References: Holtslag, 1987, p. 23–46)

Surface energy budget:

$$
\begin{aligned}
Q^\star &= H_{\text{sfc}} + L_v E_{\text{sfc}} + G_{\text{soil}} \\
Q^\star &= (1-\alpha_{\text{sfc}})K^\downarrow + L^\downarrow - L^\uparrow \\
Q^\star &= \frac{1}{1+c_3}\Big((1-\alpha_{\text{sfc}})K^\downarrow \\
&\qquad + c_1(T_{\text{scr}})^6 - \sigma(T_{\text{scr}})^4 + c_2 N_{\text{cld}} \Big) \\
K^\downarrow &= K^\downarrow_{\text{clear}}\left(1 - b_1(N_{\text{cld}})^{b_2}\right) \\
K^\downarrow_{\text{clear}} &= a_1 \sin\Phi_{\text{sun}} + a_2 \\
G_{\text{soil}} &= c_G Q^\star \\
H_{\text{sfc}} &= \frac{(1-\alpha_{\text{PM}}) + (\gamma_{\text{PM}}/s)}{1 + (\gamma_{\text{PM}}/s)}(Q^\star - G_{\text{soil}}) - \beta_{\text{PM}} \\
L_v E_{\text{sfc}} &= \frac{\alpha_{\text{PM}}}{1 + (\gamma_{\text{PM}}/s)}(Q^\star - G_{\text{soil}}) + \beta_{\text{PM}} \\
\gamma_{\text{PM}} &= \frac{c_p}{L_v} \\
s &= \frac{\partial q_{\text{s}}}{\partial T} \\
L_v &= \left(2.5 - 0.00236(T - 273.15)\right) \times 10^6\,\mathrm{J\,kg^{-1}}
\end{aligned}
\tag{D12}
$$

T [°C]	-5	0	5	10	15	20	25	30	35
γ_{PM}/s	2.01	1.44	1.06	0.79	0.60	0.45	0.35	0.27	0.21

Friction velocity:

(a) For unstable conditions (References: Holtslag, 1987, p. 99–100, 106, 130)

$$
\begin{aligned}
L &= -\frac{u_\star^3}{\kappa \frac{g}{\overline{T}(z_{k=1})}(\overline{w'\theta'})_{z_s}} \\
u_\star &= \kappa\overline{U}(z_{k=1}) \\
&\quad \times \left[\ln\left(\frac{z_p}{z_0}\right) - \Psi_M\left(\frac{z_p}{L}\right) + \Psi_M\left(\frac{z_0}{L}\right) \right]^{-1}
\end{aligned}
\tag{D13}
$$

Given the surface layer heat flux, the computation starts with $u_\star{=}\kappa\overline{U}(z_{k=1})/\ln(z_p/z_0)$ for $\Psi_M{=}0$ ($L{=}\infty$). This way, an estimation of L is obtained. With this estimate, $u_\star$ is recalculated using improved Ψ_M and so on. The iteration stops,

when $u_\star$ differs less than 5% from its anterior value.

(b) For stable conditions (References: Holtslag, 1987, p. 130)

(D14)

$$L = \begin{cases} (L_n - L_0) + [L_n(L_n - 2L_0)]^{1/2}\,, & L_n \geq 2L_0 \\ \left(L_0 \dfrac{L_n}{2}\right)^{1/2} & L_n < 2L_0 \end{cases}$$

$$L_0 = \frac{5 z_p}{\ln(\frac{z_p}{z_0})}$$

$$L_n = \frac{\kappa \overline{U}(z_{k=1})^2 \overline{T}(z_{k=1})}{2 g \theta_\star \left[\ln \frac{z_p}{z_0}\right]^2}$$

$$u_\star = \left(-\kappa \frac{g}{\overline{T}(z_{k=1})} (\overline{w'\theta'})_{z_s} L\right)^{1/3}$$

The computation starts with $\theta_\star \approx 0.09\,\mathrm{K}$ to obtain an estimation of L. With this estimate, $\theta_\star$ is recalculated using improved Ψ_H and so on. The iteration stops, when $\theta_\star$ differs less than 5% from its anterior value.

Surface Reynolds stresses (References: André et al., 1978):

$$\begin{aligned} \left(\overline{w'u'}\right)_{z_s} &= -\left[\frac{\overline{u}(z_{k=1})}{\overline{U}(z_{k=1})}\right] u_\star^2 \\ \left(\overline{w'v'}\right)_{z_s} &= -\left[\frac{\overline{v}(z_{k=1})}{\overline{U}(z_{k=1})}\right] u_\star^2 \\ \left(\overline{u'v'}\right)_{z_s} &= 0 \end{aligned} \quad \text{(D15)}$$

$$\left(\overline{u'u'}\right)_{z_s} = \begin{cases} 4u_\star^2 + 0.3 w_\star^2\,, & \left(\overline{w'\theta'}\right)_{z_s} > 0 \\ 4u_\star^2\,, & \left(\overline{w'\theta'}\right)_{z_s} < 0 \end{cases},$$

$$\left(\overline{v'v'}\right)_{z_s} = \begin{cases} 1.75u_\star^2 + 0.3 w_\star^2\,, & \left(\overline{w'\theta'}\right)_{z_s} > 0 \\ 1.75u_\star^2\,, & \left(\overline{w'\theta'}\right)_{z_s} < 0 \end{cases}, \quad \text{(D16)}$$

$$\left(\overline{w'w'}\right)_{z_s} = \begin{cases} \left[1.75 + 2(-\zeta)^{2/3}\right] u_\star^2\,, & \zeta < 0 \\ 1.75 u_\star^2\,, & \zeta > 0 \end{cases}$$

Kinematic and convective heat fluxes (References: André et al., 1978):

$$\begin{aligned} \left(\overline{u'\theta'}\right)_{z_s} &= \left[\frac{\overline{u}(z_{k=1})}{\overline{U}(z_{k=1})}\right] \left(\overline{w'\theta'}\right)_{z_s} \times \Upsilon_1(\zeta) \\ \left(\overline{v'\theta'}\right)_{z_s} &= \left[\frac{\overline{v}(z_{k=1})}{\overline{U}(z_{k=1})}\right] \left(\overline{w'\theta'}\right)_{z_s} \times \Upsilon_1(\zeta) \\ \left(\overline{w'\theta'}\right)_{z_s} &= \frac{H_{\mathrm{sfc}}}{\rho_{\mathrm{air}} c_p} \end{aligned} \quad \text{(D17)}$$

$$\Upsilon_1(\zeta) = \begin{cases} -3.7(1 - 15\zeta)^{-1/4}(1 - 9\zeta)^{-1/2}\,, & \zeta < 0 \\ -3\,, & \zeta > 0 \end{cases} \quad \text{(D18)}$$

Kinematic and convective humidity fluxes (References: André et al., 1978):

$$\begin{aligned} \left(\overline{u'q'}\right)_{z_s} &= \left[\frac{\overline{u}(z_{k=1})}{\overline{U}(z_{k=1})}\right] \left(\overline{w'q'}\right)_{z_s} \times \Upsilon_1(\zeta) \\ \left(\overline{v'q'}\right)_{z_s} &= \left[\frac{\overline{v}(z_{k=1})}{\overline{U}(z_{k=1})}\right] \left(\overline{w'q'}\right)_{z_s} \times \Upsilon_1(\zeta) \\ \left(\overline{w'q'}\right)_{z_s} &= \frac{E_{\mathrm{sfc}}}{\rho_{\mathrm{air}}} \end{aligned} \quad \text{(D19)}$$

Variances, co-variances of temperature and humidity (References: André et al., 1978):

$$\begin{aligned} \left(\overline{\theta'\theta'}\right)_{z_s} \left[\frac{u_\star^2}{\left(\overline{w'\theta'}\right)_{z_s}^2}\right] &= \Upsilon_2(\zeta) \\ \left(\overline{q'q'}\right)_{z_s} \left[\frac{u_\star^2}{\left(\overline{w'q'}\right)_{z_s}^2}\right] &= \Upsilon_2(\zeta) \\ \left(\overline{\theta'q'}\right)_{z_s} \left[\frac{u_\star^2}{\left(\overline{w'\theta'}\right)_{z_s} \left(\overline{w'q'}\right)_{z_s}}\right] &= \Upsilon_2(\zeta) \end{aligned} \quad \text{(D20)}$$

$$\Upsilon_2(\zeta) = \begin{cases} 4(1 - 8.3\zeta)^{-2/3}\,, & \zeta < 0 \\ 4\,, & \zeta > 0 \end{cases} \quad \text{(D21)}$$

Kinematic and convective tracer fluxes (dry deposition) (References: André et al., 1978; Verver et al., 1997):

$$\begin{aligned} \left(\overline{u'\chi'_\alpha}\right)_{z_s} &= \left[\frac{\overline{u}(z_{k=1})}{\overline{U}(z_{k=1})}\right] \left(\overline{w'\chi'_\alpha}\right)_{z_s} \times \Upsilon_1(\zeta) \\ \left(\overline{v'\chi'_\alpha}\right)_{z_s} &= \left[\frac{\overline{v}(z_{k=1})}{\overline{U}(z_{k=1})}\right] \left(\overline{w'\chi'_\alpha}\right)_{z_s} \times \Upsilon_1(\zeta) \\ \left(\overline{w'\chi'_\alpha}\right)_{z_s} &= -V_{\chi_\alpha} \overline{\chi}_\alpha(z_{k=1}) \end{aligned} \quad \text{(D22)}$$

Variances, co-variances of temperature, water vapour mixing ratio and tracer concentration (References: André et al., 1978; Verver et al., 1997):

$$\begin{aligned} \left(\overline{\theta'\chi'_\alpha}\right)_{z_s} \left[\frac{u_\star^2}{\left(\overline{w'\theta'}\right)_{z_s} \left(\overline{w'\chi'_\alpha}\right)_{z_s}}\right] &= \Upsilon_2(\zeta) \\ \left(\overline{q'\chi'_\alpha}\right)_{z_s} \left[\frac{u_\star^2}{\left(\overline{w'q'}\right)_{z_s} \left(\overline{w'\chi'_\alpha}\right)_{z_s}}\right] &= \Upsilon_2(\zeta) \\ \left(\overline{\chi'_\alpha\chi'_\beta}\right)_{z_s} \left[\frac{u_\star^2}{\left(\overline{w'\chi'_\alpha}\right)_{z_s} \left(\overline{w'\chi'_\beta}\right)_{z_s}}\right] &= \Upsilon_2(\zeta) \end{aligned} \quad \text{(D23)}$$

D2.3 Upper boundary conditions

$$\left.\frac{\partial\overline{u_\mathrm{i}'u_\mathrm{j}'}}{\partial z}\right|_{\mathrm{top}}(t)=0$$
$$\left.\frac{\partial\overline{u_\mathrm{i}'a'}}{\partial z}\right|_{\mathrm{top}}(t)=0 \qquad \text{(D24)}$$
$$\left.\frac{\partial\overline{a'b'}}{\partial z}\right|_{\mathrm{top}}(t)=0$$

D3. Third-order moments

D3.1 Initial conditions

At the starting time, third-order moments are set to zero.

D3.2 Upper boundary conditions

$$\left.\frac{\partial\overline{u_\mathrm{i}'u_\mathrm{j}'w'}}{\partial z}\right|_{\mathrm{top}}(t)=0$$
$$\left.\frac{\partial\overline{u_\mathrm{i}'u_\mathrm{j}'a'}}{\partial z}\right|_{\mathrm{top}}(t)=0 \qquad \text{(D25)}$$
$$\left.\frac{\partial\overline{u_\mathrm{i}'a'b'}}{\partial z}\right|_{\mathrm{top}}(t)=0$$
$$\left.\frac{\partial\overline{a'b'c'}}{\partial z}\right|_{\mathrm{top}}(t)=0$$

Appendix E

Numerics

E1. Adams–Bashforth time differencing scheme

(References: Durran, 1999, p. 68, Table 2.1)

$$\begin{aligned}\frac{d\Psi}{dt} &= F(\Psi)\\ \Phi^{\mathrm{n}} &= \Psi(\mathrm{n}\,\Delta t)\\ \Phi^{\mathrm{n+1}} &= \Phi^{\mathrm{n}}+\frac{h}{12}\Big[23\,F(\Phi^{\mathrm{n}})\\ &\quad -16\,F(\Phi^{\mathrm{n-1}})+5\,F(\Phi^{\mathrm{n-2}})\Big]\end{aligned} \qquad \text{(E1)}$$

E2. Vertical finite-differencing scheme

(References: André et al., 1976a,b; Bougeault, 1985)

E2.1 Grid structure

A staggered grid is used with first- and third-order correlations calculated at main levels and second-order ones calculated at half levels.

E2.2 Standard differencing scheme

$$\begin{aligned}\left.\frac{\partial\Phi}{\partial z}\right|_{\mathrm{k}} &= \frac{1}{2}\left(\widetilde{D}_{\mathrm{up}}+\widetilde{D}_{\mathrm{down}}\right)\\ \widetilde{D}_{\mathrm{up}} &= \frac{\Phi_{\mathrm{k+1}}-\Phi_{\mathrm{k}}}{z_{\mathrm{k+1}}-z_{\mathrm{k}}}\\ \widetilde{D}_{\mathrm{down}} &= \frac{\Phi_{\mathrm{k}}-\Phi_{\mathrm{k-1}}}{z_{\mathrm{k}}-z_{\mathrm{k-1}}}\end{aligned} \qquad \text{(E2)}$$

E2.3 Derivatives of mean variables in third-order moment equations

A geometric approximation is used to determine the derivatives of the mean variables in the third-order moment equations to avoid the appearance of negative values of variances just below the inversion:

$$\left.\frac{\partial\Phi}{\partial z}\right|_{\mathrm{k}} \approx 2\,\left|\widetilde{D}_{\mathrm{up}}\right|\,\left|\widetilde{D}_{\mathrm{down}}\right|\,\frac{\widetilde{D}_{\mathrm{up}}+\widetilde{D}_{\mathrm{down}}}{\left(\left|\widetilde{D}_{\mathrm{up}}\right|+\left|\widetilde{D}_{\mathrm{down}}\right|\right)^2} \qquad \text{(E3)}$$

Acknowledgements. The work was realised at the IfT Modelling Department, headed by E. Renner, within the framework of IfT main research direction 1 “Evolution, transport and spatio-temporal distribution of the tropospheric aerosol”. Special thanks go to the following people for the use of their Fortran source codes: A. Nenes (inorganic aerosol thermodynamical equilibrium model ISORROPIA), M. Wilck (exact binary nucleation model), I. Napari (parameterisation of the ternary nucleation rate) and L. Zhang (parameterisation of the particle dry deposition velocity). For the motivation and numerous discussions on the subject of the present Paper I am very indebted to D. Mironov, E. Renner, K. Bernhardt, E. Schaller, M. Kulmala, A. A. Lushnikov, M. Boy, R. Wolke, F. Stratmann, H. Siebert, T. Berndt and J. W. P. Schmelzer. Sincerest thanks are given to M. Kulmala and M. Boy for the opportunity to present and discuss previous results at the Department of Physics at the University of Helsinki as well as to J. W. P. Schmelzer for the chance to discuss selected aspects of cluster formation under atmospheric conditions, generalisation of classical Gibbs theory and phase transformations in multicomponent systems during the X$^{\mathrm{th}}$ Research Workshop on Nucleation Theory and Applications at the Bogoliubov Laboratory of Theoretical Physics of the Joint Institute for Nuclear Research (JINR), Dubna. In this context, I want to express special thanks also to A. K. Shchekin, A. S. Abyzov, H. Heinrich and I. S. Gutzow. Many thanks go to the editor and to the three reviewers for their helpful comments, additional references and suggestions to improve the manuscript. Special thanks go also to N. Otto and N. Deisel for their strong support during the technical processing as well as to M. Reichelt for the proofreading of the manuscript. Last but not least, it should be mentioned, that the pioneering works of J. C. André, P. Bougeault, G. H. L. Verver and their co-workers served as the conditio sine qua non for the approach presented here.

Edited by: M. Kulmala

References

Aalto, P., Hämeri, K., Becker, E., Weber, R., Salm, J., Mäkelä, J. M., Hoell, C., O'Dowd, C. D., Karlsson, H., Hansson, H.-C., Väkevä, M., Koponen, I. K., Buzorius, G., and Kulmala, M.: Physical characterization of aerosol particles during nucleation events, Tellus, 53B, 344–358, 2001.

Abdella, K. and McFarlane, N.: A new second-order turbulence closure scheme for the planetary boundary layer, J. Atmos. Sci., 54, 1850–1867, 1997.

Abdella, K. and McFarlane, N.: Reply, J. Atmos. Sci., 56, 3482–3483, 1999.

Abdella, K. and McFarlane, N.: Modelling boundary-layer clouds with a statistical cloud scheme and a second-order turbulence closure, Boundary-Layer Meteorol., 98, 387–410, 2001.

André, J. C. and Lacarrère, P.: Mean and turbulent structures of the oceanic surface layer as determined from one-dimensional, third-order simulations, J. Phys. Oceanography, 15, 121–132, 1985.

André, J. C., De Moor, G., Lacarrère, P., and Du Vachat, R.: Turbulence approximation for inhomogeneous flows: Part I. The clipping approximation, J. Atmos. Sci., 33, 476–481, 1976a.

André, J. C., De Moor, G., Lacarrère, P., and Du Vachat, R.: Turbulence approximation for inhomogeneous flows: Part II. The numerical simulation of a penetrative convection experiment, J. Atmos. Sci., 33, 482–491, 1976b.

André, J. C., De Moor, G., Lacarrère, P., Therry, G., and Du Vachat, R.: Modeling the 24-hour evolution of the mean and turbulent structures of the planetary boundary layer, J. Atmos. Sci., 35, 1861–1883, 1978.

André, J. C., Lacarrère, P., and Traoré, K.: Pressure effects on triple correlations in turbulent convective flows, Turbulent Shear Flows, Springer Verlag, 3, 243–252, 1981.

Andronache, C., Chameides, W. L., Davis, D. D., Anderson, B. E., Pueschel, R. F., Bandy, A. R., Thornton, D. C., Talbot, R. W., Kasibhatla, P., and Kiang, C. S.: Gas-to-particle conversion of tropospheric sulfur as estimated from observations in the western North Pacific during PEM-West B, J. Geophys. Res., 102(D23), 28 511–28 538, 1997.

Ansari, A. S. and Pandis, S. N.: Prediction of multicomponent inorganic atmospheric aerosol behavior, Atmos. Environ., 33, 745–757, 1999.

Atkinson, R., Baulch, D. L., Cox, R. A., Hampson, R. F., Kerr, J. A., Rossi, M. J., and Troe, J.: Evaluated kinetic and photochemical data for atmospheric chemistry: Supplement VI. IU-PAC subcommittee on gas kinetic data evaluation for atmospheric chemistry, J. Phys. Chem. Ref. Data, 26, 1329–1499, 1997.

Ayotte, K. W., Sullivan, P. P., Andrén, A., Doney, S. C., Holtslag, A. A. M., Large, W. G., McWilliams, J. C., Moeng, C.-H., Otte, M. J., Tribbia, J. J., and Wyngaard, J. C.: An evaluation of neutral and convective planetary boundary-layer parameterizations relative to large eddy simulations, Boundary-Layer Meteorol., 79, 131–175, 1996.

Berndt, T., Böge, O., Stratmann, F., Heintzenberg, J., and Kulmala, M.: Rapid formation of sulfuric acid particles at near-atmospheric conditions, Science, 307, 698–700, 2005.

Bernhardt, K.: Zur Definition der turbulenzbedingten Austauschströme, insbesondere des Turbulenzwärmestroms, Z. Meteorol., 17(3/4), 95–108, 1964.

Bernhardt, K.: Nochmals zur Definition des Turbulenzwärmestroms in der Wärmehaushaltsgleichung der Atmosphäre, Z. Meteorol., 23(3/4), 65–75, 1972.

Bernhardt, K. and Piazena, H.: Zum Einfluß der turbulenzbedingten Dichteschwankungen auf die Bestimmung turbulenter Austauschströme in der Bodenschicht, Z. Meteorol., 38(4), 234–245, 1988.

Bigg, E. K.: A mechanism for the formation of new particles in the atmosphere, Atmos. Res., 43, 129–137, 1997.

Birmili, W.: On the formation and growth of new atmospheric particles in continental atmospheres, in: Abstracts of the European Aerosol Conference 2001, vol. 32, suppl. 1 of J. Aerosol Sci., pp. S321–S322, Pergamon, 2001.

Birmili, W. and Wiedensohler, A.: New particle formation in the continental boundary layer: Meteorological and gas phase parameter influence, Geophys. Res. Lett., 27(20), 3325–3328, 2000.

Birmili, W., Wiedensohler, A., Plass-Dülmer, C., and Berresheim, H.: Evolution of newly formed aerosol particles in the continental boundary layer: A case study including OH and H_2SO_4 measurements, Geophys. Res. Lett., 27(15), 2205–2208, 2000.

Birmili, W., Berresheim, H., Plass-Dülmer, C., Elste, T., Gilge, S., Wiedensohler, A., and Uhrner, U.: The Hohenpeissenberg aerosol formation experiment (HAFEX): A long-term study including size-resolved aerosol, H_2SO_4, OH, and monoterpenes measurements, Atmos. Chem. Phys., 3, 361–376, 2003, http://www.atmos-chem-phys.net/3/361/2003/.

Bohren, C. F. and Albrecht, B. A.: Atmospheric Thermodynamics, Oxford University Press, New York, 1998.

Bougeault, P.: Modeling the trade-wind cumulus boundary layer. Part I: Testing the ensemble cloud relations against numerical data, J. Atmos. Sci., 38, 2414–2428, 1981a.

Bougeault, P.: Modeling the trade-wind cumulus boundary layer. Part II: A high-order one-dimensional model, J. Atmos. Sci., 38, 2429–2439, 1981b.

Bougeault, P.: The diurnal cycle of the marine stratocumulus layer: A high-order model study, J. Atmos. Sci., 42, 2826–2843, 1985.

Bougeault, P. and André, J. C.: On the stability of the third-order turbulence closure for the modeling of the stratocumulus-topped boundary layer, J. Atmos. Sci., 43, 1574–1581, 1986.

Bougeault, P. and Lacarrère, P.: Parameterization of orography-induced turbulence in a mesobeta-scale model, Mon. Wea. Rev., 117, 1872–1890, 1989.

Boy, M. and Kulmala, M.: Nucleation events in the continental boundary layer: Influence of physical and meteorological parameters, Atmos. Chem. Phys., 2, 1–16, 2002, http://www.atmos-chem-phys.net/2/1/2002/.

Boy, M., Nilsson, D., and Kulmala, M.: BLMARC - A 1-dimensional model for the prediction of the aerosol evolution in the continental boundary layer, in: Abstracts of the European Aerosol Conference 2003, vol. 34, suppl. 2 of J. Aerosol Sci., pp. S821–S822, Pergamon, 2003a.

Boy, M., Rannik, Ü., Lehtinen, K. E. J., Tarvainen, V., Hakola, H., and Kulmala, M.: Nucleation events in the continental boundary layer: Long-term statistical analyses of aerosol relevant characteristics, J. Geophys. Res., 108(D21), 4667, doi:10.1029/2003JD003838, 2003b.

Boy, M., Petäjä, T., Dal Maso, M., Rannik, Ü., Rinne, J., Aalto,

P., Laaksonen, A., Vaattovaara, P., Joutsensaari, J., Hoffmann, T., Warnke, J., Apostolaki, M., Stephanou, E. G., Tsapakis, M., Kouvarakis, A., Pio, C., Carvalho, A., Römpp, A., Moortgat, G., Spirig, C., Guenther, A., Greenberg, J., Ciccioli, P., and Kulmala, M.: Overview of the field measurement campaign in Hyytiälä, August 2001 in the framework of the EU project OSOA, Atmos. Chem. Phys., 4, 657–678, 2004, http://www.atmos-chem-phys.net/4/657/2004/.

Boy, M., Kulmala, M., Ruuskanen, T. M., Pihlatie, M., Reissell, A., Aalto, P. P., Keronen, P., Dal Maso, M., Hellen, H., Hakola, H., Jansson, R., Hanke, M., and Arnold, F.: Sulphuric acid closure and contribution to nucleation mode particle growth, Atmos. Chem. Phys., 5, 863–878, 2005, http://www.atmos-chem-phys.net/5/863/2005/.

Brasseur, G. P., Prinn, R. G., and Pszenny, A. A. P., eds.: Atmospheric Chemistry in a Changing World, Springer-Verlag, Berlin, 2003.

Brown, A. R.: Evaluation of parametrization schemes for the convective boundary layer using large-eddy simulation results, Boundary-Layer Meteorol., 81, 167–200, 1996.

Brown, A. R. and Grant, A. L. M.: Non-local mixing of momentum in the convective boundary layer, Boundary-Layer Meteorol., 84, 1–22, 1997.

Buzorius, G., Rannik, Ü., Nilsson, D., and Kulmala, M.: Vertical fluxes and micrometeorology during aerosol particle formation events, Tellus, 53B, 394–405, 2001.

Buzorius, G., Rannik, Ü., Aalto, P., dal Maso, M., Nilsson, E. D., Lehtinen, K. E. J., and Kulmala, M.: On particle formation prediction in continental boreal forest using micrometeorological parameters, J. Geophys. Res., 108(D13), 4377, doi:10.1029/2002JD002850, 2003.

Carlson, M. A. and Stull, R. B.: Subsidence in the nocturnal boundary layer, J. Appl. Meteorol., 25, 1088–1099, 1986.

Carson, D. J. and Richards, P. J. R.: Modelling surface turbulent fluxes in stable conditions, Boundary-Layer Meteorol., 14, 67–81, 1978.

Charlson, R. J., Lovelock, J. E., Andreae, M. O., and Warren, S. G.: Oceanic phytoplankton, atmospheric sulphur, cloud albedo and climate, Nature, 326, 655–661, 1987.

Cheng, A., Xu, K.-M., and Golaz, J.-C.: The liquid water oscillation in modeling boundary layer cumuli with third-order turbulence closure models, J. Atmos. Sci., 61, 1621–1629, 2004.

Clarke, A. D., Eisele, F., Kapustin, V. N., Moore, K., Tanner, D., Mauldin, L., Litchy, M., Lienert, B., Carroll, M. A., and Albercook, G.: Nucleation in the equatorial free troposphere: Favorable environments during PEM-Tropics, J. Geophys. Res., 104(D5), 5735–5744, 1999.

Clement, C. F. and Ford, I. J.: Gas-to-particle conversion in the atmosphere: I. Evidence from empirical atmospheric aerosols, Atmos. Environ., 33, 475–487, 1999a.

Clement, C. F. and Ford, I. J.: Gas-to-particle conversion in the atmosphere: II. Analytical models of nucleation bursts, Atmos. Environ., 33, 489–499, 1999b.

Clement, C. F., Kulmala, M., and Vesala, T.: Theoretical consideration on sticking probabilities, J. Aerosol Sci., 27, 869–882, 1996.

Clement, C. F., Pirjola, L., dal Maso, M., Mäkelä, J. M., and Kulmala, M.: Analysis of particle formation bursts observed in Finland, J. Aerosol Sci., 32, 217–236, 2001.

Coe, H., Williams, P. I., McFiggans, G., Gallagher, M. W., Beswick, K. M., Bower, K. N., and Choularton, T. W.: Behavior of ultrafine particles in continental and marine air masses at a rural site in the United Kingdom, J. Geophys. Res., 105(D22), 26 891–26 905, 2000.

Dal Maso, M., Kulmala, M., Lehtinen, K. E. J., Mäkelä, J. M., Aalto, P., and O'Dowd, C. D.: Condensation and coagulation sinks and formation of nucleation mode particles in coastal and boreal forest boundary layers, J. Geophys. Res., 107(D19), 8097, doi:10.1029/2001JD001053, 2002.

Dal Maso, M., Kulmala, M., Riipinen, I., Wagner, R., Hussein, T., Aalto, P. P., and Lehtinen, K. E. J.: Formation and growth of fresh atmospheric aerosols: Eight years of aerosol size distribution data from SMEAR II, Hyytiälä, Finland, Boreal Environ. Res., 10, 323–336, 2005.

Davidovits, P., Hu, J. H., Worsnop, D. R., Zahniser, M. S., and Kolb, C. E.: Entry of gas molecules into liquids, Faraday Discuss., 100, 65–81, 1995.

de Reus, M., Ström, J., Kulmala, M., Pirjola, L., Lelieveld, J., Schiller, C., and Zöger, M.: Airborne aerosol measurements in the tropopause region and the dependence of new particle formation on preexisting particle number concentration, J. Geophys. Res., 103(D23), 31 255–31 263, 1998.

de Reus, M., Ström, J., Hoor, P., Lelieveld, J., and Schiller, C.: Particle production in the lowermost stratosphere by convective lifting of the tropopause, J. Geophys. Res., 104(D19), 23 935–23 940, 1999.

Degrazia, G. A., Campos Velho, H. F., and Carvalho, J. C.: Nonlocal exchange coefficients for the convective boundary layer derived from spectral properties, Beitr. Phys. Atmosph., 70, 57–64, 1997a.

Degrazia, G. A., Rizza, U., Mangia, C., and Tirabassi, T.: Validation of a new turbulent parameterization for dispersion models in convective conditions, Boundary-Layer Meteorol., 85, 243–254, 1997b.

Degrazia, G. A., Mangia, C., and Rizza, U.: A comparison between different methods to estimate the lateral dispersion parameter under convective conditions, J. Appl. Meteorol., 37, 227–231, 1998.

Degrazia, G. A., Moreira, D. M., and Vilhena, M. T.: Derivation of an eddy diffusivity depending on source distance for vertically inhomogeneous turbulence in a convective boundary layer, J. Appl. Meteorol., 40, 1233–1240, 2001.

DeMore, W. B., Sander, S. P., Golden, D. M., Hampson, R. F., Huie, R. E., Kurylo, M. J., Howard, C. J., Ravishankara, A. R., Kolb, C. J., and Molina, M. J.: Chemical kinetics and photochemical data for use in stratospheric modeling, evaluation number 11, JPL Publication, 94-26, 1994.

DeMore, W. B., Sander, S. P., Golden, D. M., Hampson, R. F., Kurylo, M. J., Howard, C. J., Ravishankara, A. R., Kolb, C. E., and Molina, M. J.: Chemical kinetics and photochemical data for use in stratospheric modeling, evaluation number 12, JPL Publication, 97-4, 1997.

Donaldson, C.: Construction of a dynamic model of the production of atmospheric turbulence and the dispersal of atmospheric pollutants, in: Workshop on Micrometeorology, edited by Haugen, D. A., pp. 313–392, American Meteorological Society, Boston, 1973.

Durran, D. R.: Numerical Methods for Wave Equations in Geo-

physical Fluid Dynamics, Texts in Applied Mathematics, 32, Springer-Verlag, New York, 1999.

Dyer, A. J. and Hicks, B. B.: Flux-gradient relationships in the constant flux layer, Quart. J. Roy. Meteorol. Soc., 96, 715–721, 1970.

Easter, R. C. and Peters, L. K.: Binary homogeneous nucleation: Temperature and relative humidity fluctuations, nonlinearity, and aspects of new particle production in the atmosphere, J. Appl. Meteorol., 33, 775–784, 1994.

Ebert, E. E., Schumann, U., and Stull, R. B.: Nonlocal turbulent mixing in the convective boundary layer evaluated from large-eddy simulation, J. Atmos. Sci., 46, 2178–2207, 1989.

Eichkorn, S., Wilhelm, S., Aufmhoff, H., Wohlfrom, K. H., and Arnold, F.: Cosmic ray-induced aerosol-formation: First observational evidence from aircraft-based ion mass spectrometer measurements in the upper troposphere, Geophys. Res. Lett., 29(14), 1698, doi:10.1029/2002GL015044, 2002.

Elperin, T., Kleeorin, N., and Rogachevskii, I.: Mechanisms of formation of aerosol and gaseous inhomogeneities in the turbulent atmosphere, Atmos. Res., 53, 117–129, 2000.

Ervens, B.: Troposphärische Multiphasenchemie: Modellrechnungen und kinetische Untersuchungen von Reaktionen des OH-Radikals in wäßriger Lösung, Ph.D. thesis, Universität Leipzig, Fakultät für Chemie und Mineralogie, 232 pp., 2001.

Ervens, B., George, C., Williams, J. E., Buxton, G. V., Salmon, G. A., Bydder, M., Wilkinson, F., Dentener, F., Mirabel, P., Wolke, R., and Herrmann, H.: CAPRAM 2.4 (MODAC mechanism): An extended and condensed tropospheric aqueous phase mechanism and its application, J. Geophys. Res., 108(D14), 4426, doi:10.1029/2002JD002202, 2003.

Ferrero, E. and Racca, M.: The role of the nonlocal transport in modeling the shear-driven atmospheric boundary layer, J. Atmos. Sci., 61, 1434–1445, 2004.

Foken, T.: Anmerkungen zur Problematik möglicher Fehler bei der Bestimmung turbulenter Austauschströme nach der Flux-Methode, Z. Meteorol., 39(2), 112–113, 1989.

Frech, M. and Mahrt, L.: A two-scale mixing formulation for the atmospheric boundary layer, Boundary-Layer Meteorol., 73, 91–104, 1995.

Fuchs, N. A. and Sutugin, A. G.: Highly dispersed aerosols, in: Topics in Current Aerosol Research, edited by Hidy, G. M. and Brock, J. R., pp. 1–60, Pergamon Press, Oxford, 1971.

Galmarini, S., Vilà-Guerau De Arellano, J., and Duynkerke, P. G.: Scaling the turbulent transport of chemical compounds in the surface layer under neutral and stratified conditions, Quart. J. Roy. Meteorol. Soc., 123, 223–242, 1997.

Gaydos, T. M., Stanier, C. O., and Pandis, S. N.: Modeling of in situ ultrafine atmospheric particle formation in the eastern United States, J. Geophys. Res., 110, D07S12, doi:10.1029/2004JD004683, 2005.

Hämeri, K. and Laaksonen, A., eds.: Quantification of aerosol nucleation in the European boundary layer (QUEST 2002-2004), ACP - Special Issue, Copernicus Gesellschaft mbH, 2004.

Held, A., Nowak, A., Birmili, W., Wiedensohler, A., Forkel, R., and Klemm, O.: Observations of particle formation and growth in a mountainous forest region in central Europe, J. Geophys. Res., 109, D23204, doi:10.1029/2004JD005346, 2004.

Hellmuth, O. and Helmert, J.: Parameterization of turbulence-enhanced nucleation in large scale models: Conceptual study, in: Air Pollution Modeling and Its Application XV, edited by Borrego, C. and Schayes, G., pp. 295–304, Kluwer Academic/Plenum Publishers, New York, 2002.

Hermann, M., Heintzenberg, J., Wiedensohler, A., Zahn, A., Heinrich, G., and Brenninkmeijer, C. A. M.: Meridional distributions of aerosol particle number concentrations in the upper and lower stratosphere obtained by civil aircraft for regular investigation of the atmosphere based on an instrument container (CARIBIC) flights, J. Geophys. Res., 108(D3), 4114, doi:10.1029/2001JD001077, 2003.

Holtslag, A. A. M.: Surface fluxes and boundary layer scaling, Scientific Report WR 87-2(FM), Koninklijk Nederlands Meteorologisch Instituut, De Bilt, 1987.

Holtslag, A. A. M. and Moeng, C.-H.: Eddy diffusivity and countergradient transport in the convective atmospheric boundary layer, J. Atmos. Sci., 48, 1690–1698, 1991.

Holtslag, A. A. M., van Meijgaard, E., and de Rooy, W. C.: A comparison of boundary layer diffusion schemes in unstable conditions over land, Boundary-Layer Meteorol., 76, 69–95, 1995.

Hõrrak, U., Salm, J., and Tammet, H.: Bursts of intermediate ions in atmospheric air, J. Geophys. Res., 103(D12), 13 909–13 915, 1998.

Housiadas, C., Drossinos, Y., and Lazaridis, M.: Effect of small-scale turbulent fluctuations on rates of particle formation, J. Aerosol Sci., 35, 545–559, 2004.

Hyvönen, S., Junninen, H., Laakso, L., Dal Maso, M., Grönholm, T., Bonn, B., Keronen, P., Aalto, P., Hiltunen, V., Pohja, T., Launiainen, S., Hari, P., Mannila, H., and Kulmala, M.: A look at aerosol formation using data mining techniques, Atmos. Chem. Phys., 5, 3345–3356, 2005, http://www.atmos-chem-phys.net/5/3345/2005/.

IPCC: IPCC Third Assessment Report. Climate Change 2001: The Scientific Basis, Tech. rep., Intergovernmental Panel on Climate Change, 2001.

Itoh, M.: Theoretical prediction of sticking probability of H_2O and H_2SO_4 systems by free angle ratio, in: Aerosols: Science, Industry, Health and Environment, edited by Masuda, S. and Takahashi, K., vol. I of *Proceedings of the 3rd International Conference, Kyoto, Japan*, pp. 197–200, Pergamon Press, Oxford, 1990.

Jaecker-Voirol, A. and Mirabel, P.: Nucleation rate in a binary mixture of sulfuric acid and water vapor, J. Phys. Chem., 92, 3518–3521, 1988.

Jaecker-Voirol, A. and Mirabel, P.: Heteromolecular nucleation in the sulfuric acid–water system, Atmos. Environ., 23, 2053–2057, 1989.

Jaecker-Voirol, A., Mirabel, P., and Reiss, H.: Hydrates in supersaturated binary sulfuric acid–water vapor: A reexamination, J. Chem. Phys., 87, 4849–4852, 1987.

Jaenisch, V., Stratman, F., Nilsson, D., and Austin, P. H.: Influence of turbulent mixing processes on new particle formation, in: Abstracts of the 5th International Aerosol Conference 1998, vol. 29, suppl. 1, part 2 of J. Aerosol Sci., pp. S1063–S1064, Pergamon, 1998a.

Jaenisch, V., Stratman, F., and Wilck, M.: Particle nucleation and condensational growth during turbulent mixing processes, in: Abstracts of the 5th International Aerosol Conference 1998, vol. 29, suppl. 1, part 2 of J. Aerosol Sci., pp. S1161–S1162, Pergamon, 1998b.

Jefferson, A., Eisele, F. L., Ziemann, P. J., Weber, R. J., Marti, J. J.,

and McMurry, P. H.: Measurements of the H_2SO_4 mass accommodation coefficient onto polydisperse aerosol, J. Geophys. Res., 102(D15), 19 021–19 028, 1997.

Katoshevski, D., Nenes, A., and Seinfeld, J. H.: A study of processes that govern the maintenance of aerosols in the marine boundary layer, J. Aerosol Sci., 30, 503–532, 1999.

Kerminen, V.-M. and Kulmala, M.: Analytical formulae connecting the "real" and the "apparent" nucleation rate and the nuclei number concentration for atmospheric nucleation events, J. Aerosol Sci., 33, 609–622, 2002.

Kerminen, V.-M. and Wexler, A. S.: Enhanced formation and development of sulfate particles due to marine boundary layer circulation, J. Geophys. Res., 100(D11), 23 051–23 062, 1995.

Kerminen, V.-M. and Wexler, A. S.: Growth behavior of the marine submicron boundary layer aerosol, J. Geophys. Res., 102(D15), 18 813–18 825, 1997.

Khosrawi, F. and Konopka, P.: Enhanced particle formation and growth due to mixing processes in the tropopause region, Atmos. Environ., 37, 903–910, 2003.

Köhler, H.: The nucleus in and the growth of hygroscopic droplets, Trans. Faraday Soc., 32, 1152–1161, 1936.

Komppula, M., Dal Maso, M., Lihavainen, H., Aalto, P. P., Kulmala, M., and Viisanen, Y.: Comparison of new particle formation events at two locations in northern Finland, Boreal Environ. Res., 8, 395–404, 2003a.

Komppula, M., Lihavainen, H., Hatakka, J., Paatero, J., Aalto, P., Kulmala, M., and Viisanen, Y.: Observations of new particle formation and size distributions at two different heights and surroundings in subarctic area in northern Finland, J. Geophys. Res., 108(D9), 4295, doi:10.1029/2002JD002939, 2003b.

Korhonen, H., Lehtinen, K. E. J., and Kulmala, M.: Multicomponent aerosol dynamics model UHMA: Model development and validation, Atmos. Chem. Phys., 4, 757–771, 2004, http://www.atmos-chem-phys.net/4/757/2004/.

Korhonen, P., Kulmala, M., Laaksonen, A., Viisanen, Y., McGraw, R., and Seinfeld, J. H.: Ternary nucleation of H_2SO_4, NH_3, and H_2O in the atmosphere, J. Geophys. Res., 104(D21), 26 349–26 353, 1999.

Krejci, R., Ström, J., de Reus, M., Hoor, P., Williams, J., Fischer, H., and Hansson, H.-C.: Evolution of aerosol properties over the rain forest in Surinam, South America, observed from aircraft during the LBA-CLAIRE 98 experiment, J. Geophys. Res., 108(D18), 4561, doi:10.1029/2001JD001375, 2003.

Krishnamurti, T. N. and Bounoua, L.: An Introduction to Numerical Weather Prediction Techniques, CRC Press LLC, Boca Raton, 1996.

Kulmala, M.: How particles nucleate and grow, Science, 302, 1000–1001, 2003.

Kulmala, M. and Laaksonen, A.: Binary nucleation of water–sulfuric acid system: Comparison of classical theories with different H_2SO_4 saturation vapor pressures, J. Chem. Phys., 93, 696–701, 1990.

Kulmala, M., Kerminen, V.-M., and Laaksonen, A.: Simulations on the effect of sulphuric acid formation on atmospheric aerosol concentrations, Atmos. Environ., 29, 377–382, 1995.

Kulmala, M., Laaksonen, A., and Pirjola, L.: Parameterizations for sulfuric acid/water nucleation rates, J. Geophys. Res., 103(D7), 8301–8307, 1998a.

Kulmala, M., Toivonen, A., Mäkelä, J. M., and Laaksonen, A.: Analysis of the growth of nucleation mode particles observed in Boreal forest, Tellus, 50B, 449–462, 1998b.

Kulmala, M., Pirjola, L., and Mäkelä, J. M.: Stable sulphate clusters as a source a new atmospheric particles, Nature, 404, 66–69, 2000.

Kulmala, M., Dal Maso, M., Mäkelä, J. M., Pirjola, L., Väkevä, M., Aalto, P., Miikkulainen, P., Hämeri, K., and O'Dowd, C. D.: On the formation, growth and composition of nucleation mode particles, Tellus, 53B, 479–490, 2001a.

Kulmala, M., Hämeri, K., Aalto, P. P., Mäkelä, J. M., Pirjola, L., Nilsson, E. D., Buzorius, G., Rannik, Ü., Dal Maso, M., Seidl, W., Hoffman, T., Janson, R., Hansson, H.-C., Viisanen, Y., Laaksonen, A., and O'Dowd, C. D.: Overview of the international project on biogenic aerosol formation in the boreal forest (BIOFOR), Tellus, 53B, 324–343, 2001b.

Kulmala, M., Napari, I., Merikanto, J., Vehkamäki, H., Laakso, L., Lehtinen, K. E. J., Noppel, M., and Laaksonen, A.: Homogeneous and ion induced nucleation: Kinetic and thermodynamic nucleation regimes, in: Abstracts of the European Aerosol Conference 2003, vol. 34, suppl. 2 of J. Aerosol Sci., pp. S1393–S1394, Pergamon, 2003.

Kulmala, M., Kerminen, V.-M., Anttila, T., Laaksonen, A., and O'Dowd, C. D.: Organic aerosol formation via sulphate cluster activation, J. Geophys. Res., 109, D04205, doi:10.1029/2003JD003961, 2004a.

Kulmala, M., Laakso, L., Lehtinen, K. E. J., Riipinen, I., Dal Maso, M., Anttila, T., Kerminen, V.-M., Hõrrak, U., Vana, M., and Tammet, H.: Initial steps of aerosol growth, Atmos. Chem. Phys., 4, 2553–2560, 2004b.

Kulmala, M., Suni, T., Lehtinen, K. E. J., Dal Maso, M., Boy, M., Reissell, A., Rannik, Ü., Aalto, P., Keronen, P., Hakola, H., Bäck, J., Hoffmann, T., Vesala, T., and Hari, P.: A new feedback mechanism linking forests, aerosols, and climate, Atmos. Chem. Phys., 4, 557–562, 2004c.

Kulmala, M., Vehkamäki, H., Petäjä, T., Dal Maso, M., Lauri, A., Kerminen, V.-M., Birmili, W., and McMurry, P. H.: Formation and growth rates of ultrafine atmospheric particles: A review of observations, J. Aerosol Sci., 35, 143–176, 2004d.

Kulmala, M., Lehtinen, K. E. J., Laakso, L., Mordas, G., and Hämeri, K.: On the existence of neutral atmospheric clusters, Boreal Environ. Res., 10, 79–87, 2005.

Kulmala, M., Lehtinen, K. E. J., and Laaksonen, A.: Cluster activation theory as an explanation of the linear dependence between formation rate of 3 nm particles and sulphuric acid concentration, Atmos. Chem. Phys., 6, 787–793, 2006, http://www.atmos-chem-phys.net/6/787/2006/.

Kuni, F. M., Shchekin, A. K., and Grinin, A. P.: Kinetics of condensation on macroscopic solid nuclei at low dynamic vapor supersaturations, in: Nucleation Theory and Applications, edited by Schmelzer, J. W. P., Röpke, G., and Priezzhev, V. B., pp. 208–236, JINR Joint Institute for Nuclear Research, Bogoliubov Laboratory of Theoretical Physics, Dubna, 1999.

Laakso, L., Mäkelä, J. M., Pirjola, L., and Kulmala, M.: Model studies on ion-induced nucleation in the atmosphere, J. Geophys. Res., 107(D20), 4427, doi:10.1029/2002JD002140, 2002.

Laakso, L., Kulmala, M., and Lehtinen, K. E. J.: Effect of condensation rate enhancement factor on 3-nm (diameter) particle formation in binary ion-induced and homogeneous nucleation, J. Geophys. Res., 108(D18), 4574, doi:10.1029/2003JD003432,

2003.

Laaksonen, A. and Kulmala, M.: Homogeneous heteromolecular nucleation of sulphuric acid and water vapours in stratospheric conditions: A theoretical study of the effect of hydrate interaction, J. Aerosol Sci., 22, 779–787, 1991.

Larson, V. E.: Prognostic equations for cloud fraction and liquid water, and their relation to filtered density functions, J. Atmos. Sci., 61, 338–351, 2004.

Lauros, J., Nilsson, E. D., Vehkamäki, H., and Kulmala, M.: Effect of variability in temperature and humidity on binary water–sulfuric acid nucleation rate, in: Nucleation and Atmospheric Aerosols 2004: 16th International Conference, Kyoto, pp. 73–76, 2004.

Lauros, J., Nilsson, E. D., Vehkamäki, H., and Kulmala, M.: Atmospheric variability and binary homogeneous nucleation: A parametrisation and conditions required for a significant effect, Atmos. Res., in press, 2006.

Lesniewski, T. and Friedlander, S. K.: The effect of turbulence on rates of particle formation by homogeneous nucleation, Aerosol Sci. Tech., 23, 174–182, 1995.

Lewellen, D. C. and Lewellen, W. S.: Buoyancy flux modeling for cloudy boundary layers, J. Atmos. Sci., 61, 1147–1160, 2004.

Liu, X., Hegg, D. A., and Stoelinga, M. T.: Numerical simulation of new particle formation over the northwest Atlantic using the MM5 mesoscale model coupled with sulfur chemistry, J. Geophys. Res., 106(D9), 9697–9715, 2001.

Lovejoy, E. R., Curtius, J., and Froyd, K. D.: Atmospheric ion-induced nucleation of sulfuric acid and water, J. Geophys. Res., 109, D08204, doi:10.1029/2003JD004460, 2004.

Lovelock, J.: Das Gaia-Prinzip. Die Biographie unseres Planeten, Insel Taschenbuch 1542, Insel Verlag, Frankfurt am Main und Leipzig, 1993.

Mäkelä, J. M., Aalto, P., Jokinen, V., Pohja, T., Nissinen, A., Palmroth, S., Markkanen, T., Seitsonen, K., Lihavainen, H., and Kulmala, M.: Observations of ultrafine aerosol particle formation and growth in boreal forest, Geophys. Res. Lett., 24(10), 1219–1222, 1997.

Marti, J. J., Weber, R. J., McMurry, P. H., Eisele, F., Tanner, D., and Jefferson, A.: New particle formation at a remote continental site: Assessing the contributions of SO_2 and organic precursors, J. Geophys. Res., 102(D5), 6331–6339, 1997.

Mellor, G. L. and Yamada, T.: A hierarchy of turbulence closure models for planetary boundary layers, J. Atmos. Sci., 31, 1791–1806, 1974.

Mironov, D. V., Gryanik, V. M., Lykossov, V. N., and Zilitinkevich, S. S.: Comments on "A new second-order turbulence closure scheme for the planetary boundary layer", J. Atmos. Sci., 56, 3478–3481, 1999.

Moeng, C.-H. and Randall, D. A.: Problems in simulating the stratocumulus-topped boundary layer with a third-order closure model, J. Atmos. Sci., 41, 1588–1600, 1984.

Monteith, J. L.: Evaporation and surface temperature, Quart. J. Roy. Meteorol. Soc., 107, 1–27, 1981.

Müller, K.: A 3 year study of the aerosol in northwest Saxony (Germany), Atmos. Environ., 33, 1679–1685, 1999.

Nadykto, A. B. and Yu, F.: Uptake of neutral polar vapor molecules by charged clusters/particles: Enhancement due to dipole-charge interaction, J. Geophys. Res., 108(D23), 4717, doi:10.1029/2003JD003664, 2003.

Napari, I., Noppel, M., Vehkamäki, H., and Kulmala, M.: An improved model for ternary nucleation of sulfuric acid–ammonia–water, J. Chem. Phys., 116, 4221–4227, 2002a.

Napari, I., Noppel, M., Vehkamäki, H., and Kulmala, M.: Parametrization of ternary nucleation rates for H_2SO_4–NH_3–H_2O vapors, J. Geophys. Res., 107(D19), 4381, doi:10.1029/2002JD002132, 2002b.

Nenes, A., Pandis, S., and Pilinis, C.: ISORROPIA v1.5 Reference Manual, University of Miami, Carnegie Mellon University, 2000.

Nilsson, E. D. and Kulmala, M.: The potential for atmospheric mixing processes to enhance the binary nucleation rate, J. Geophys. Res., 103(D1), 1381–1389, 1998.

Nilsson, E. D., Pirjola, L., and Kulmala, M.: The effect of atmospheric waves on aerosol nucleation and size distribution, J. Geophys. Res., 105(D15), 19 917–19 926, 2000a.

Nilsson, E. D., Rannik, Ü., Paatero, J., Boy, M., O'Dowd, C. D., Buzorius, G., Laakso, L., and Kulmala, M.: Effects of synoptic weather and boundary layer dynamics on aerosol formation in the continental boundary layer, in: Abstracts of the European Aerosol Conference 2000, vol. 31, suppl. 1 of J. Aerosol Sci., pp. S600–S601, Pergamon, 2000b.

Nilsson, E. D., Paatero, J., and Boy, M.: Effects of air masses and synoptic weather on aerosol formation in the continental boundary layer, Tellus, 53B, 462–478, 2001a.

Nilsson, E. D., Rannik, Ü., Kulmala, M., Buzorius, G., and O'Dowd, C. D.: Effects of continental boundary layer evolution, convection, turbulence and entrainment, on aerosol formation, Tellus, 53B, 441–461, 2001b.

Noppel, M., Vehkamäki, H., and Kulmala, M.: An improved model for hydrate formation in sulfuric acid–water nucleation, J. Chem. Phys., 116, 218–228, 2002.

Nyeki, S., Kalberer, M., Lugauer, M., Weingartner, E., Petzold, A., Schröder, F., Colbeck, I., and Baltensperger, U.: Condensation nuclei (CN) and ultrafine CN in the free troposphere to 12 km: A case study over the Jungfraujoch high-alpine research station, Geophys. Res. Lett., 26(14), 2195–2198, 1999.

O'Brien, J. J.: A note on the vertical structure of the eddy exchange coefficient in the planetary boundary layer, J. Atmos. Sci., 27, 1213–1215, 1970.

O'Dowd, C. D., Hämeri, K., Mäkelä, J. M., Pirjola, L., Kulmala, M., Jennings, S. G., Berresheim, H., Hansson, H.-C., de Leeuw, G., Kunz, G. J., Allen, A. G., Hewitt, C. N., Jackson, A., Viisanen, Y., and Hoffmann, T.: A dedicated study of new particle formation and fate in the coastal environment (PARFORCE): Overview of objectives and achievements, J. Geophys. Res., 107(D19), 8108, doi:10.1029/2001JD000555, 2002.

O'Dowd, C. D., Aalto, P. P., Yoon, Y. J., and Hämeri, K.: The use of the pulse height analyser ultrafine condensation particle counter (PHA-UCPC) technique applied to sizing of nucleation mode particles of differing chemical composition, J. Aerosol Sci., 35, 205–216, 2004.

Pandis, S. N., Russell, L. M., and Seinfeld, J. H.: The relationship between DMS flux and CCN concentration in remote marine regions, J. Geophys. Res., 99(D8), 16 945–16 957, 1994.

Pandis, S. N., Wexler, A. S., and Seinfeld, J. H.: Dynamics of tropospheric aerosols, J. Phys. Chem., 99, 9646–9659, 1995.

Paulson, C. A.: The mathematical representation of wind speed and temperature profiles in the unstable atmospheric surface layer, J. Appl. Meteorol., 9, 857–861, 1970.

Pirjola, L.: Effects of the increased UV radiation and biogenic VOC emissions on ultrafine sulphate aerosol formation, J. Aerosol Sci., 30, 355–367, 1999.

Pirjola, L. and Kulmala, M.: Modelling the formation of H_2SO_4–H_2O particles in rural, urban and marine marine conditions, Atmos. Res., 46, 321–347, 1998.

Pirjola, L., Kulmala, M., Wilck, M., Bischoff, A., Stratmann, F., and Otto, E.: Formation of sulphuric acid aerosols and cloud condensation nuclei: An expression for significant nucleation and model comparison, J. Aerosol Sci., 30, 1079–1094, 1999.

Pirjola, L., O'Dowd, C. D., Brooks, I. M., and Kulmala, M.: Can new particle formation occur in the clean marine boundary layer?, J. Geophys. Res., 105(D21), 26 531–26 546, 2000.

Pirjola, L., Tsyro, S., Tarrason, L., and Kulmala, M.: A monodisperse aerosol dynamics module, a promising candidate for use in long-range transport models: Box model tests, J. Geophys. Res., 108(D9), 4258, doi:10.1029/2002JD002867, 2003.

Plauskaite, K., Gaman, A. I., Aalto, P., Mordas, G., Ulevicius, V., Lehtinen, K. E. J., and Kulmala, M.: Characterisation of nucleation events at Preila and Hyytiälä stations, in: Abstracts of the European Aerosol Conference 2003, vol. 34, suppl. 1 of J. Aerosol Sci., pp. S731–S732, Pergamon, 2003.

Pleim, J. E. and Chang, J. S.: A non-local closure model for vertical mixing in the convective boundary layer, Atmos. Environ., 26A, 965–981, 1992.

Press, W. H., Teukolsky, S. A., Vetterling, W. T., and Flannery, B. P.: Numerical Recipes in Fortran 77. The Art of Scientific Computing. Second Edition. Volume 1 of Fortran Numerical Recipes, Cambridge University Press, New York, 1996.

Raes, F. and Janssens, A.: Ion-induced aerosol formation in a H_2O-H_2SO_4 system – II. Numerical calculations and conclusions, J. Aerosol Sci., 17, 715–722, 1986.

Russell, L. M., Lenschow, D. H., Laursen, K. K., Krummel, P. B., Siems, S. T., Bandy, A. R., Thornton, D. C., and Bates, T. S.: Bidirectional mixing in an ACE 1 marine boundary layer overlain by a second turbulent layer, J. Geophys. Res., 103(D13), 16 411–16 432, 1998.

Schmelzer, J. W. P. and Abyzov, A. S.: Generalized Gibbs' approach to the thermodynamics of heterogeneous systems and the kinetics of first-order phase transitions, in: Nucleation Theory and Applications, edited by Schmelzer, J. W. P., Röpke, G., and Priezzhev, V. B., pp. 3–21, JINR Joint Institute for Nuclear Research, Bogoliubov Laboratory of Theoretical Physics, Dubna, 2005.

Schmelzer, J. W. P. and Schmelzer Jr., J.: Kinetics of bubble formation and the tensile strength of liquids, in: Nucleation Theory and Applications, edited by Schmelzer, J. W. P., Röpke, G., and Priezzhev, V. B., pp. 88–119, JINR Joint Institute for Nuclear Research, Bogoliubov Laboratory of Theoretical Physics, Dubna, 2002.

Schmelzer, J. W. P., Schmelzer jn., J., and Gutzow, I. S.: Reconciling Gibbs and van der Waals: A new approach to nucleation theory, in: Nucleation Theory and Applications, edited by Schmelzer, J. W. P., Röpke, G., and Priezzhev, V. B., pp. 237–267, JINR Joint Institute for Nuclear Research, Bogoliubov Laboratory of Theoretical Physics, Dubna, 1999.

Schmelzer, J. W. P., Baidakov, V. G., and Boltachev, G. S.: Kinetics of boiling in binary liquid–gas solutions: A new approach, in: Nucleation Theory and Applications, edited by Schmelzer, J. W. P., Röpke, G., and Priezzhev, V. B., pp. 120–145, JINR Joint Institute for Nuclear Research, Bogoliubov Laboratory of Theoretical Physics, Dubna, 2002.

Schmelzer, J. W. P., Baidakov, V. G., and Boltachev, G. S.: Kinetics of boiling in binary liquid–gas solutions: Comparison of different approaches, J. Chem. Phys., 119, 6166–6183, 2003.

Schmelzer, J. W. P., Abyzov, A. S., and Möller, J.: Nucleation versus spinodal decomposition in phase formation processes in multicomponent solutions, J. Chem. Phys., 121, 6900–6917, 2004a.

Schmelzer, J. W. P., Gokhman, A. R., and Fokin, V. M.: Dynamics of first-order phase transitions in multicomponent systems: A new theoretical approach, J. Coll. Interf. Sci., 272, 109–133, 2004b.

Schmelzer, J. W. P., Boltachev, G. S., and Baidakov, V. G.: Is Gibbs' thermodynamic theory of heterogeneous systems really perfect?, in: Nucleation Theory and Applications, edited by Schmelzer, J. W. P., pp. 418–446, Wiley-VCH Verlag GmbH & Co. KGaA, Weinheim, 2005.

Schröder, F. and Ström, J.: Aircraft measurements of sub micrometer aerosol particles (> 7 nm) in the midlatitude free troposphere and tropopause region, Atmos. Res., 44, 333–356, 1997.

Schröder, F., Kärcher, B., Fiebig, M., and Petzold, A.: Aerosol states in the free troposphere at northern midlatitudes, J. Geophys. Res., 107(D21), 8126, doi:10.1029/2000JD000194, 2002.

Schwartz, S. E.: Mass-transport considerations pertinent to aqueous phase reactions of gases in liquid-water clouds, in: Chemistry of Multiphase Atmospheric Systems, edited by Jaeschke, W., vol. G6 of *NATO ASI Series*, pp. 415–471, Springer-Verlag, Berlin, 1986.

Seinfeld, J. H. and Pandis, S. N.: Atmospheric Chemistry and Physics. From Air Pollution to Climate Change, John Wiley & Sons, Inc., New York, 1998.

Shaw, B. D.: Asymptotic evaluation of probability density functions for mean aerosol particle formation rates by homogeneous nucleation in turbulent gas jets, J. Aerosol Sci., 35, 177–184, 2004.

Shchekin, A. K. and Shabaev, I. V.: Thermodynamics and kinetics of deliquescence of small soluble particles, in: Nucleation Theory and Applications, edited by Schmelzer, J. W. P., Röpke, G., and Priezzhev, V. B., pp. 267–291, JINR Joint Institute for Nuclear Research, Bogoliubov Laboratory of Theoretical Physics, Dubna, 2005.

Shchekin, A. K., Tatianenko, D. V., and Kuni, F. M.: Towards thermodynamics of uniform film formation on solid insoluble particles, in: Nucleation Theory and Applications, edited by Schmelzer, J. W. P., Röpke, G., and Priezzhev, V. B., pp. 320–340, JINR Joint Institute for Nuclear Research, Bogoliubov Laboratory of Theoretical Physics, Dubna, 1999.

Siebert, H., Stratmann, F., and Wehner, B.: First observations of increased ultrafine particle number concentrations near the inversion of a continental planetary boundary layer and its relation to ground-based measurements, Geophys. Res. Lett., 31, L09102, doi:10.1029/2003GL019086, 2004.

Siebesma, A. P. and Holtslag, A. A. M.: Model impacts of entrainment and detrainment rates in shallow cumulus convection, J. Atmos. Sci., 53, 2354–2364, 1996.

Sorbjan, Z.: Numerical study of penetrative and "solid lid" nonpenetrative convective boundary layer, J. Atmos. Sci., 53, 101–112, 1996.

Stanier, C. O., Khlystov, A. Y., Zhang, Q., Jimenez, J. L., Cara-

garatna, M., Worsnop, D., and Pandis, S. N.: Examining sulfuric acid nucleation events in the Northeast United States, in: Abstracts of the European Aerosol Conference 2003, vol. 34, suppl. 2 of J. Aerosol Sci., pp. S1343–S1344, Pergamon, 2003.

Stauffer, D.: Kinetic theory of two-component ("heteromolecular") nucleation and condensation, J. Aerosol Sci., 7, 319–333, 1976.

Steinbrecher, R. and BEWA2000-Team: Regional biogenic emissions of reactive volatile organic compounds (BVOC) from forests: Process studies, modelling and validation experiments (BEWA2000), AFO2000 Newsletter, 8(9-2004), 7–10, 2004.

Stratmann, F., Siebert, H., Spindler, G., Wehner, B., Althausen, D., Heintzenberg, J., Hellmuth, O., Rinke, R., Schmieder, U., Seidel, C., Tuch, T., Uhrner, U., Wiedensohler, A., Wandinger, U., Wendisch, M., Schell, D., and Stohl, A.: New-particle formation events in a continental boundary layer: First results from the SATURN experiment, Atmos. Chem. Phys., 3, 1445–1459, 2003,
http://www.atmos-chem-phys.net/3/1445/2003/.

Stull, R. B.: An Introduction to Boundary Layer Meteorology, Kluwer Academic Publishers, Dordrecht/Boston/London, 1997.

Sullivan, P. P., Moeng, C.-H., Stevens, B., Lenschow, D. H., and Mayor, S. D.: Structure of the entrainment zone capping the convective atmospheric boundary layer, J. Atmos. Sci., 55, 3042–3064, 1998.

Thuburn, J. and Tan, D. G. H.: A parameterization of mixdown time for atmospheric chemicals, J. Geophys. Res., 102(D11), 13 037–13 049, 1997.

Twomey, S.: Pollution and the planetary albedo, Atmos. Environ., 8, 1251–1256, 1974.

Uhrner, U., Birmili, W., Stratmann, F., Wilck, M., Ackermann, I. J., and Berresheim, H.: Particle formation at a continental background site: Comparison of model results with observations, Atmos. Chem. Phys., 3, 347–359, 2003,
http://www.atmos-chem-phys.net/3/347/2003/.

Van Dingenen, R. and Raes, F.: Determination of the condensation accommodation coefficient of sulfuric acid on water–sulfuric acid aerosol, Aerosol Sci. Tech., 15, 93–106, 1991.

van Dop, H.: Discussion: The parametrization of the vertical dispersion of a scalar in the atmospheric boundary layer, Atmos. Environ., 32, 257–258, 1998.

Vana, M., Kulmala, M., Dal Maso, M., Hõrrak, U., and Tamm, E.: Comparative study of nucleation mode aerosol particles and intermediate air ions formation events at three sites, J. Geophys. Res., 109, D17201, doi:10.1029/2003JD004413, 2004.

Vehkamäki, H., Kulmala, M., Napari, I., Lehtinen, K. E. J., Timmreck, C., Noppel, M., and Laaksonen, A.: An improved parameterization for sulfuric acid–water nucleation rates for tropospheric and stratospheric conditions, J. Geophys. Res., 107(D22), 4622, doi:10.1029/2002JD002184, 2002.

Venkatram, A.: The parameterization of the vertical dispersion of a scalar in the atmospheric boundary layer, Atmos. Environ., 27A, 1963–1966, 1993.

Verver, G. H. L., van Dop, H., and Holtslag, A. A. M.: Turbulent mixing of reactive gases in the convective boundary layer, Boundary-Layer Meteorol., 85, 197–222, 1997.

Vinuesa, J.-F. and Vilà-Guerau de Arellano, J.: Introducing effective reaction rates to account for the inefficient mixing of the convective boundary layer, Atmos. Environ., 39, 445–461, 2005.

Weber, R. J., Marti, J. J., McMurry, P. H., Eisele, F. L., Tanner, D. J., and Jefferson, A.: Measured atmospheric new particle formation rates: Implications for nucleation mechanisms, Chem. Eng. Comm., 151, 53–64, 1996.

Weber, R. J., Marti, J. J., McMurry, P. H., Eisele, F. L., Tanner, D. J., and Jefferson, A.: Measurements of new particle formation and ultrafine particle growth rates at a clean continental site, J. Geophys. Res., 102(D4), 4375–4385, 1997.

Wehner, B. and Wiedensohler, A.: Long term measurements of submicrometer urban aerosols: Statistical analysis for correlations with meteorological conditions and trace gases, Atmos. Chem. Phys., 3, 867–879, 2003,
http://www.atmos-chem-phys.net/3/867/2003/.

Wehner, B., Schmieder, U., Siebert, H., Stratmann, F., Spindler, G., Tuch, T., and Wiedensohler, A.: Horizontal variability of new particle formation during SATURN, in: Abstracts of the European Aerosol Conference 2003, vol. 34, suppl. 1 of J. Aerosol Sci., pp. S725–S726, Pergamon, 2003.

Whitby, E. R. and McMurry, P. H.: Modal aerosol dynamics modeling, Aerosol Sci. Tech., 27, 673–688, 1997.

Wichmann, M. and Schaller, E.: Comments on "Problems in simulating the stratocumulus-topped boundary layer with a third-order closure model", J. Atmos. Sci., 42, 1559–1561, 1985.

Wichmann, M. and Schaller, E.: On the determination of the closure parameters in high-order closure models, Boundary-Layer Meteorol., 37, 323–341, 1986.

Wilck, M.: Modal modelling of multicomponent aerosols, Ph.D. thesis, Universität Leipzig, Leipzig, doctoral thesis, 1998.

Wilck, M. and Stratmann, F.: A 2-D multicomponent modal aerosol model and its application to laminar flow reactors, J. Aerosol Sci., 28, 959–972, 1997.

Wilhelm, S., Eichkorn, S., Wiedner, D., Pirjola, L., and Arnold, F.: Ion-induced aerosol formation: New insights from laboratory measurements of mixed cluster ions $H_2SO_4^-(H_2SO_4)_a(H_2O)_w$ and $H^+(H_2SO_4)_a(H_2O)_w$, Atmos. Environ., 38, 1735–1744, 2004.

Worsnop, D. R., Zahniser, M. S., Kolb, C. E., Gardner, J. A., Watson, L. R., Van Doren, J. M., Jayne, J. T., and Davidovits, P.: Temperature dependence of mass accommodation of SO_2 and H_2O_2 on aqueous surfaces, J. Phys. Chem., 93, 1159–1172, 1989.

Yu, F.: Nucleation rate of particles in the lower atmosphere: Estimated time needed to reach pseudo-steady state and sensitivity to H_2SO_4 gas concentration, Geophys. Res. Lett., 30(10), 1526, doi:10.1029/2003GL017084, 2003.

Yu, F. and Turco, R. P.: Ultrafine aerosol formation via ion-mediated nucleation, Geophys. Res. Lett., 27(6), 883–886, 2000.

Yu, F. and Turco, R. P.: On the contribution of lightning to ultrafine aerosol formation, Geophys. Res. Lett., 28(1), 155–158, 2001a.

Yu, F. and Turco, R. P.: From molecular clusters to nanoparticles: Role of ambient ionization in tropospheric aerosol formation, J. Geophys. Res., 106(D5), 4797–4814, 2001b.

Zhang, L., Gong, S., Padro, J., and Barrie, L.: A size-segregated particle dry deposition scheme for an atmospheric aerosol module, Atmos. Environ., 35, 549–560, 2001.

Zilitinkevich, S., Gryanik, V. M., Lykossov, V. N., and Mironov, D. V.: Third-order transport and nonlocal turbulence closures for convective boundary layers, J. Atmos. Sci., 56, 3463–3477, 1999.